

**POLYKETIDE-BASED ANTI-AGING
THERAPEUTIC DEVELOPMENT VIA SYNTHETIC
ENZYMOLGY**

LIM YAN PING

(B.Sc.(Hons.), NUS)

**A THESIS SUBMITTED
FOR THE DEGREE OF
DOCTOR OF PHILOSOPHY**

**DEPARTMENT OF BIOCHEMISTRY
NATIONAL UNIVERSITY OF SINGAPORE**

2016

DECLARATION

I hereby declare that this thesis is my original work and it has been written by me in its entirety. I have duly acknowledged all the sources of information which have been used in the thesis.

This thesis has also not been submitted for any degree in any university previously.



Lim Yan Ping

1st July 2016

ACKNOWLEDGEMENTS

I would like to express my most sincere gratitude to my supervisor A/P Yew Wen Shan and co-supervisor A/P Markus Wenk, for their guidance and support throughout the course of my Ph.D. studies. I also want to show appreciation to A/P Yew Wen Shan for taking care of me over the past six years and encouraging me to reach my full potential. I am grateful for the pleasant research environment that I had worked in, and I will definitely remember your teaching as it has sparked more interest and broadened my perspectives in science.

I would also like to express thanks to the members of my Thesis Advisory Committee, Dr. Takao Inoue and Dr. Chng Shu Sin, for spending their time to understand my project and providing me with invaluable suggestions. I also wish to thank Dr. Takao Inoue for kindly providing me with *Caenorhabditis elegans* strains, and useful advice with regards to handling them. I am grateful to NUS for providing me with financial support throughout the past four years, and the group of collaborators whom I had worked with. Without their assistance, many experiments described in this thesis would not have been possible. These include Dr. Manfred Raida, Dr. Shareef Mohideen Ismail, Dr. Yap Lai Lai, and Ms. Shen Yanqing.

Lastly, I would like to thank all my past and present laboratory mates, for all their advice and support given to me throughout my studies. Their presence had made my research journey even more enjoyable and memorable.

TABLE OF CONTENTS

SUMMARY	v
LIST OF PUBLICATIONS	vi
LIST OF CONFERENCE PRESENTATIONS (POSTER)	vii
LIST OF TABLES	viii
LIST OF FIGURES	ix
LIST OF ABBREVIATIONS	xiii
 CHAPTER 1: INTRODUCTION	 1
1.1 Metabolic networks of longevity	1
1.2 Caloric restriction and its role in anti-aging	4
1.3 <i>Caenorhabditis elegans</i> as a model organism	7
1.4 Polyketides and their potential in the development of caloric restriction mimetics	10
1.4.1 Synthesis of polyketides by type I, type II, and type III polyketide synthases	10
1.4.2 Chalcone synthase superfamily of type III polyketide synthases	13
1.4.3 Stilbene synthase superfamily of type III polyketide synthases	16
1.4.4 Precursor-directed combinatorial biosynthesis of unnatural polyketides	19
1.5 Alkaloids as potential caloric restriction mimetics	22
1.5.1 Biosynthesis of alkaloids in nature	23
1.5.2 Precursor-directed combinatorial biosynthesis as a novel means to produce alkaloids	26
1.6 Anti-aging therapeutic development	27

CHAPTER 2: TOWARDS THE DEVELOPMENT OF NOVEL ANTI-AGING POLYKETIDES USING PRECURSOR-DIRECTED COMBINATORIAL BIOSYNTHESIS

2.1	Introduction	29
2.2	Materials and methods	31
2.2.1	Establishing a combinatorial biosynthetic route in <i>Escherichia coli</i>	32
2.2.2	<i>In vivo</i> precursor-directed combinatorial biosynthesis of polyketides and HPLC analysis	34
2.2.3	Expression and purification of CoA ligases and CHS18	36
2.2.4	<i>In vitro</i> precursor-directed combinatorial biosynthesis of polyketides and HPLC analysis	37
2.2.5	Mass spectrometry profiling of novel polyketides	38
2.2.6	Life span assays using resveratrol or novel polyketides	39
2.3	Results and discussion	42
2.3.1	Establishing a combinatorial biosynthetic route in <i>Escherichia coli</i>	42
2.3.2	Starter acyl-CoA substrate preference of CHS18	46
2.3.3	Extender acyl-CoA substrate preference of CHS18	50
2.3.4	Mass spectrometry profiling of novel polyketides	52
2.3.5	Life span assays using resveratrol or novel polyketides	60

CHAPTER 3: TOWARDS THE DEVELOPMENT OF NOVEL ANTI-AGING ALKALOIDS USING PRECURSOR-DIRECTED COMBINATORIAL BIOSYNTHESIS

3.1	Introduction	66
3.2	Materials and methods	69
3.2.1	Cloning, expression and purification of novel acid-CoA ligases Cg2, Sc1, Sc3, and Ec1	69
3.2.2	<i>In vitro</i> biosynthesis of nitrogen-containing acyl-CoA esters	70
3.2.3	Kinetic assays of acid-CoA ligase activity	72
3.2.4	<i>In vitro</i> precursor-directed combinatorial biosynthesis of alkaloids and HPLC analysis	74
3.2.5	Mass spectrometry profiling of novel nitrogen-containing acyl-CoA esters and alkaloids	75

3.3	Results and discussion	76
3.3.1	Catalytic functions of Cg2, Sc1, Sc3, and Ec1	76
3.3.2	Precursor-directed combinatorial biosynthesis is a novel means to produce alkaloids	83

CHAPTER 4: MITOCHONDRIAL FUNCTION ASSAY AS A NOVEL MEANS TO SCREEN FOR CALORIC RESTRICTION MIMETICS

4.1	Introduction	91
4.2	Materials and methods	95
4.2.1	Optimization of mitochondrial function assays in <i>Caenorhabditis elegans</i>	95
4.2.2	Screening for more potent caloric restriction mimetics	96
4.3	Results and discussion	98
4.3.1	Optimization of mitochondrial function assays in <i>Caenorhabditis elegans</i>	98
4.3.2	Establishing a reference mitochondrial function profile using resveratrol as a caloric restriction mimetic	103
4.3.3	Screening for more potent caloric restriction mimetics	109

CHAPTER 5: FUTURE DIRECTIONS IN ANTI-AGING NUTRACEUTICAL DEVELOPMENT AND CONCLUSION

REFERENCES	120
------------------	------------

APPENDIX	132
----------------	------------

SUMMARY

An intervention that consistently extends maximal life span is caloric restriction (CR), but its application in humans is not practical. A more feasible approach is to develop a CR mimetic that targets biochemical pathways affected by CR, and thus achieve life span extension. Polyketides and alkaloids are structurally diverse secondary metabolites produced by microorganisms and plants. Some of these compounds have important clinical uses, while others are known to have bioactive properties that range from anti-oxidant, anti-microbial to anti-aging activities. By establishing a combinatorial biosynthetic route in *Escherichia coli* and exploring the substrate promiscuity of a mutant polyketide synthase (PKS) from alfalfa, many potential anti-aging polyketides and alkaloids can be biosynthesized. In this approach, novel acyl-CoA precursors including nitrogen-containing precursors generated by various promiscuous acid-CoA ligases will be delivered to the mutant PKS, and the polyketides and alkaloids thus generated will be introduced to *Caenorhabditis elegans* when they feed on the engineered *E. coli*. A molecular screening platform where compound libraries are screened in *C. elegans*-based life span assays can thus be developed. Mitochondrial function assays were also adopted to look at the mitochondrial activity of *C. elegans* when they were exposed to potential CR mimetics. It was found that CR mimetics like resveratrol can counter the age-associated decline in mitochondrial function. This study highlights the utility of synthetic enzymology in anti-aging studies, and its potential in the development of novel anti-aging nutraceuticals.

LIST OF PUBLICATIONS

Go MK, Chow JY, Cheung VWN, **Lim YP**, Yew WS. (2012). Establishing a toolkit for precursor-directed polyketide biosynthesis: exploring substrate promiscuities of acid-CoA ligases. Biochemistry 51(22), 4568-4579.

Lim YP, Go MK, Yew WS. (2016). Exploiting the biosynthetic potential of type III polyketide synthases. Molecules. 21(6), 806.

Lim YP, Go MK, Raida M, Wenk MR, Yew WS. (2016). Synthetic enzymology and the fountain of youth: repurposing biology for longevity. ACS Synthetic Biology.

(In preparation)

LIST OF CONFERENCE PRESENTATIONS (POSTER)

Lim YP, Yew WS. (2013). Polyketide-Based Anti-Aging Therapeutic Development *via* Synthetic Enzymology. 23rd Enzyme Mechanisms Conference. Coronado, California, USA.

Lim YP, Yew WS. (2015). Developing Anti-Ageing Therapeutics *via* Synthetic Polyketide Enzymology. 24th Enzyme Mechanisms Conference. Galveston, Texas, USA.

Lim YP, Yew WS. (2015). Developing Anti-Ageing Therapeutics *via* Synthetic Polyketide Enzymology. Biosystems Design 1.0. Singapore.

Lim YP, Yew WS. (2015). Polyketide-Based Anti-Aging Therapeutic Development *via* Synthetic Enzymology. Biology of Aging Conference. Singapore.

Lim YP, Yew WS. (2016). Anti-Aging Therapeutic Development *via* Synthetic Enzymology. Biosystems Design 2.0. Singapore.

LIST OF TABLES

Table 2.1	Substrate profile of CHS18 using 69 starter CoA thioesters and 12 extender CoA thioesters	45
Table 2.2	Potential polyketides biosynthesized by CHS18.....	53
Table 2.3	Assessing the anti-aging properties of novel polyketides	63
Table 3.1	Low-resolution MS analysis and kinetic parameters for the biosynthesis of new nitrogen-containing acyl-CoA esters....	77
Table 3.2	Potential alkaloids biosynthesized by CHS18	88

LIST OF FIGURES

Figure 1.1	Aging is a very complex process that is characterized by nine hallmarks	3
Figure 1.2	Overview of the insulin/IGF-1 signaling pathway and its relationship to CR and aging	6
Figure 1.3	Domain organization of the different PKSs	12
Figure 1.4	Crystal structure of a monomer of a modified CHS from alfalfa (PDB ID: 1U0W)	14
Figure 1.5	Chalcone and naringenin synthesis catalyzed by <i>M. sativa</i> CHS using <i>p</i> -coumaroyl-CoA as the starter with malonyl-CoA as the extender	16
Figure 1.6	The hydrogen bonding network involving Glu192, Thr132, H ₂ O and Ser338	18
Figure 1.7	Precursor-directed combinatorial biosynthesis of novel polyketides	22
Figure 1.8	Diverse alkaloid scaffolds and their precursors	25
Figure 1.9	Precursor-directed combinatorial biosynthesis of novel alkaloids	27
Figure 2.1	<i>E. coli</i> constructs generated for <i>in vivo</i> precursor-directed combinatorial biosynthesis of polyketides	34
Figure 2.2	Malonic acid and <i>p</i> -coumaric acid were supplemented to the <i>E. coli</i> constructs	43
Figure 2.3	MS analysis of purified resveratrol fraction after <i>in vivo</i> precursor-directed combinatorial biosynthesis	43
Figure 2.4	Overlay of NMR analyses of purified resveratrol fraction after <i>in vitro</i> precursor-directed combinatorial biosynthesis (red), and a commercially available resveratrol standard (blue) ...	44
Figure 2.5	Biosynthesized products in spent minimal medium containing either <i>E. coli</i> with CoA ligases + CHS18 or <i>E. coli</i> with CoA ligases only	45
Figure 2.6	Unfavorable steric effects due to bulky extenders like 3-thiophenemalonyl-CoA (substituent group highlighted in pink) resulted in a strong preference for smaller starters like benzoyl-CoA	49

Figure 2.7	Structural mimicry of bicyclic aromatic CoA thioesters	50
Figure 2.8	Stabilization of the carbanion intermediate after decarboxylation of the extender acyl-CoA	51
Figure 2.9	Resonance structures depicting the stabilization of the carbanion of 3-thiophenemalonyl-CoA	51
Figure 2.10	Potential polyketide formed from one unit of <i>p</i> -coumaroyl-CoA and butylmalonyl-CoA without cyclization occurring	57
Figure 2.11	Novel polyketides formed via (A) lactonization, (B) Claisen condensation, (C) aldol condensation	58
Figure 2.12	Survival plots of N2 <i>C. elegans</i> fed with 5 μ M, 20 μ M, 40 μ M, or 50 μ M commercially available resveratrol	61
Figure 2.13	Survival plots of N2 <i>C. elegans</i> fed with either 50 μ M purified biosynthesized resveratrol (green) or DMSO (blue).....	61
Figure 2.14	Survival plots of N2 <i>C. elegans</i> fed with either CHS18 <i>E. coli</i> strain (green) or control <i>E. coli</i> strain (blue) supplemented with 3-chlorocinnamic acid + malonic acid (left) or 3-(3'-chloro-4'-methoxy)phenylpropanoic acid + methylmalonic acid (right)	62
Figure 2.15	Survival plots of N2 <i>C. elegans</i> fed with either CHS18 <i>E. coli</i> strain (green) or control <i>E. coli</i> strain (blue) supplemented with <i>p</i> -coumaric acid and malonic acid	65
Figure 3.1	Chemical synthesis of nitrogen-containing acyl-CoA thioesters such as 2-carbamoylbenzoyl-CoA from the respective carboxylic acid precursors	67
Figure 3.2	A continuous spectrophotometric coupled-enzyme assay was used to monitor the activities of acid-CoA ligases	73
Figure 3.3	HPLC chromatogram showing the detection of a new acyl-CoA thioester peak at an R_t of 26.8 min	82
Figure 3.4	Precursor-directed combinatorial biosynthesis of novel alkaloids by supplying nitrogen-containing starter acyl-CoA esters and malonyl-CoA to CHS18	84
Figure 3.5	<i>In vitro</i> precursor-directed combinatorial biosynthesis involving 3-aminobenzoyl-CoA and malonyl-CoA produced by Ec1 and MCS respectively	84

Figure 3.6	<i>In vitro</i> precursor-directed combinatorial biosynthesis involving 3-aminobenzoyl-CoA and malonyl-CoA produced by Cg2 and MCS respectively 85
Figure 3.7	<i>In vitro</i> precursor-directed combinatorial biosynthesis involving 3-quinolinecarboxyl-CoA and malonyl-CoA produced by Ec1 and MCS respectively 86
Figure 3.8	<i>In vitro</i> precursor-directed combinatorial biosynthesis involving pyridine-2-carboxyl-CoA and malonyl-CoA produced by Cg2 and MCS respectively 87
Figure 3.9	Nitrogen-containing derivatives of malonyl-CoA 89
Figure 4.1	Four parameters of <i>C. elegans</i> mitochondrial respiration can be acquired by using mitochondrial inhibitors 94
Figure 4.2	Average basal OCR readings of <i>C. elegans</i> exposed to (A) 6 days, (B) 7 days, (C) 8 days, and (D) 14 days of FUDR + 50 μ M resveratrol 99
Figure 4.3	Average maximal OCR readings of <i>C. elegans</i> exposed to (A) 6 days, (B) 7 days, (C) 8 days, and (D) 14 days of FUDR + 50 μ M resveratrol 100
Figure 4.4	Average spare respiratory capacity of <i>C. elegans</i> exposed to (A) 6 days, (B) 7 days, (C) 8 days, and (D) 14 days of FUDR + 50 μ M resveratrol 101
Figure 4.5	Average basal OCR, maximal OCR, and spare respiratory capacity of <i>C. elegans</i> exposed to 8 days of FUDR + varying concentrations of resveratrol 104
Figure 4.6	The mean life span of <i>C. elegans eat-2</i> mutants (17.6 days) was significantly longer than the mean life span of wild-type worms (14.3 days) 105
Figure 4.7	Consistent with results using the CR mimetic resveratrol, <i>eat-2</i> mutants undergo chronic CR and have a higher basal respiration, maximal respiration, and spare respiratory capacity compared to wild-type <i>C. elegans</i> 106
Figure 4.8	The mean life span of <i>C. elegans eat-2</i> mutants subjected to 50 μ M resveratrol treatment (15.9 days) was significantly shorter than the mean life span of <i>C. elegans eat-2</i> mutants subjected to 0.1% DMSO treatment only (20.0 days) 107
Figure 4.9	<i>C. elegans daf-2</i> mutants seem to have a lower basal respiration, maximal respiration, and spare respiratory capacity compared to <i>eat-2</i> and wild-type <i>C. elegans</i> 108

Figure 4.10	Ethylmalonic acid and <i>p</i> -coumaric acid were incorporated into NGM agar together with either the control (Ctrl) or CHS18 <i>E. coli</i> construct	111
Figure 4.11	Butylmalonic acid and <i>p</i> -coumaric acid were incorporated into NGM agar together with either the control (Ctrl) or CHS18 <i>E. coli</i> construct	112
Figure 4.12	Malonic acid and 3-aminobenzoic acid were incorporated into NGM agar together with either the control (Ctrl) or CHS18 <i>E. coli</i> construct	113
Figure 4.13	<i>C. elegans</i> exposed to <i>p</i> -coumaric acid and butylmalonic acid only do not have a higher basal respiration, maximal respiration, and spare respiratory capacity compared to <i>C. elegans</i> exposed to FUdR only	113

LIST OF ABBREVIATIONS

ACP	Acyl Carrier Protein
ADP	5'-Adenosine Diphosphate
AMP	5'-Adenosine Monophosphate
AMPK	5'-Adenosine Monophosphate-activated Protein Kinase
AT	Acyltransferase
ATP	5'-Adenosine Triphosphate
BZL	Benzoate-CoA Ligase
Cg2	Putative long chain fatty acid-CoA ligase from <i>Corynebacterium glutamicum</i>
CHS	Chalcone Synthase
4CL	4-Coumarate-CoA Ligase
CoA	Coenzyme A
COX	Cyclooxygenase
CR	Caloric Restriction
CTAL	<i>p</i> -Coumaroyl Triacetic Acid Lactone
CV	Column Volume
DH	Dehydratase
DMSO	Dimethyl Sulfoxide
DNA	Deoxyribonucleic Acid
DTNB	5,5'-Dithiobis-(2-Nitrobenzoic Acid)
Ec1	Putative crotonobetaine / carnitine-CoA ligase from <i>Escherichia coli</i>
ER	Enoyl reductase
ETC	Electron Transport Chain

FCCP	Carbonyl Cyanide <i>p</i> -(Trifluoromethoxy)Phenylhydrazone
FOXO	Forkhead Box O
FUdR	5-fluoro-2'-deoxyuridine
GH	Growth Hormone
HPLC	High Performance Liquid Chromatography
IGF	Insulin-like Growth Factor
IPTG	Isopropyl β -D-1-Thiogalactopyranoside
KR	Ketoreductase
KS	Ketosynthase
LB	Lysogeny Broth
MCS	Malonyl-CoA Synthetase
MCS1	Multiple Cloning Site 1
MCS2	Multiple Cloning Site 2
MnSOD	Manganese-Dependent Superoxide Dismutase
MS	Mass Spectrometry
MtDNA	Mitochondrial DNA
mTOR	Mechanistic Target of Rapamycin
NAD	Nicotinamide Adenine Dinucleotide
NADH	Nicotinamide Adenine Dinucleotide (reduced)
NGM	Nematode Growth Medium
NMR	Nuclear Magnetic Resonance
OCR	Oxygen consumption rate
OD	Optical Density
PAL	Phenylalanine Ammonia Lyase
PCL	Phenylacetate-CoA Ligase

PCR	Polymerase Chain Reaction
PEP	Phosphoenolpyruvate
PDB	Protein Data Bank
PGC-1 α	Peroxisome Proliferator-activated Receptor Gamma Coactivator-1-alpha
PI3K	Phosphatidylinositol-3-OH Kinase
PKS	Polyketide Synthase
PTEN	Phosphatase and Tensin homolog
RNAi	Ribonucleic Acid Interference
ROS	Reactive Oxygen Species
R _t	Retention Time
Sc1	Putative long chain fatty acid-CoA ligase from <i>Streptomyces coelicolor</i>
Sc3	Putative ligase from <i>Streptomyces coelicolor</i>
Sirt1	Silent Information Regulator T1
STS	Stilbene Synthase
TE	Thioesterase
TFA	Trifluoroacetic Acid

CHAPTER 1: INTRODUCTION

1.1 Metabolic networks of longevity

Aging is a major risk factor for many diseases such as stroke, cancer, and Alzheimer's disease (Martin, 2011). Given existing demographic trends and the associated health care expenditure of aging societies (Olshansky *et al.*, 2009), there is a pressing need to focus biomedical research efforts in the biology of aging. The first biochemical genetic pathway able to modulate the life spans of several organisms was inspired when Johnson and Freidman succeeded in mapping the first "longevity gene", *age-1*, in the 1980s (Friedman and Johnson, 1988).

A mutation in *age-1* in *Caenorhabditis elegans* was found to extend their mean and maximal life span. Further research in the subsequent years led to the finding that *age-1* encoded the catalytic subunit of phosphatidylinositol-3-OH kinase (PI3K) (Morris *et al.*, 1996) which could negatively regulate a downstream forkhead transcription factor, DAF-16 (Dorman *et al.*, 1995). DAF-16 controls the expression of antioxidant scavenger genes such as manganese-dependent superoxide dismutase (MnSOD) in *C. elegans* (Honda and Honda, 2002), explaining why *age-1* mutants are more resistant to free radicals and thus, possibly leading to a longer life span (Martin, 2011). Mutations in DAF-2, an insulin-like growth factor (IGF) receptor homologue that is upstream of *age-1*, also resulted in increased MnSOD levels and life span extension in *C. elegans* (Honda and Honda, 2002). This constitutes the insulin/IGF-1, PI3K pathway, and suppression of this nutrient-sensing pathway brings about increased life span in various model organisms

(Tissenbaum and Ruvkun, 1998; Tatar *et al.*, 2001). In addition, rising interest in the field of aging sparked a series of new discoveries in two other areas, namely the role of telomerase in replicative senescence, and stem cells and regenerative medicine (Martin, 2011).

Though the theories of aging are rather well established, the knowledge regarding how we can prevent or delay aging is still limited. This is due to the fact that none of these theories are considered sufficient to explain the mechanism of aging, as aging is a very complex process that is not likely to be elucidated by a single pathway (Houtkooper *et al.*, 2010; Cesari *et al.*, 2013). Furthermore, aging encompasses diverse changes in various parts of the body, and at different biological levels of organization such as macromolecules, organelles, cells, and tissues (Gems and Partridge, 2013). Currently, nine hallmarks have been proposed to contribute to the aging phenotype, namely genomic instability, telomere attrition, epigenetic alterations, loss of proteostasis, mitochondrial dysfunction, deregulated nutrient sensing, altered intercellular communication, stem cell exhaustion, and cellular senescence (Lopez-Otin *et al.*, 2013) (Figure 1.1).

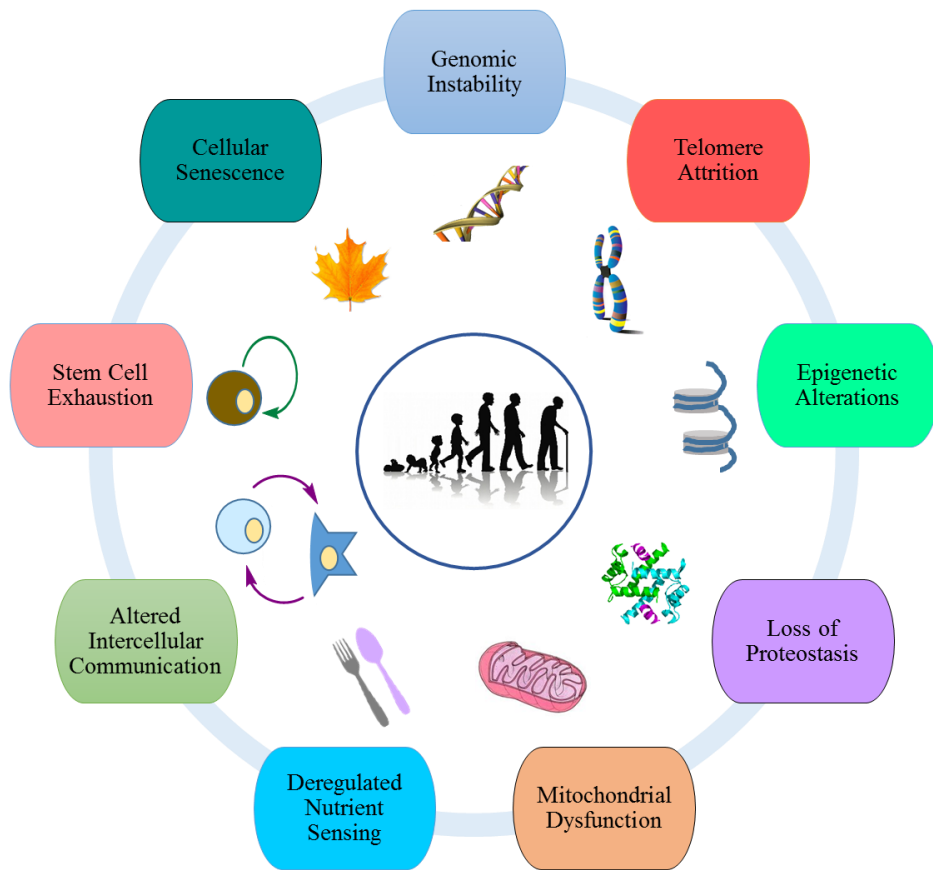


Figure 1.1: Aging is a very complex process that is characterized by nine hallmarks.

The average human life expectancy has increased substantially over the last century, but this increase is attributed to large-scale improvements in human nutrition and environmental factors, and the breakthroughs in preventive and therapeutic medicine (Vendelbo and Nair, 2011). While drug interventions have largely improved the quality of life in numerous patients and effectively extended life span, limited interventions exist which focus on the increase of maximal life span in relatively healthy subjects (Gems and Partridge, 2013). Humans are still relatively helpless with regards to the numerous damaging cellular changes that eventually result in a senescent phenotype, and ultimately death. The only non-genetic intervention that

consistently extended maximal life span in various healthy animals is caloric restriction (CR) (Lanza and Nair, 2010; Cesari *et al.*, 2013). In recent years, many studies have suggested that longevity is intrinsically related to metabolism, and this will be further expounded upon in this thesis.

1.2 Caloric restriction and its role in anti-aging

The anti-aging effects of CR were first discovered in 1935 through experiments on rats (McCay *et al.*, 1935), but research interest in longevity has only gained momentum in recent decades. Currently, CR is defined as a reduction of caloric intake by 30 – 40% of *ad libitum* consumption, without causing malnutrition (Lanza and Nair, 2010). It is thought that CR can cause life span extension in model organisms by triggering a shift from a physiological state of proliferation and growth, to repair and maintenance. In particular, studies have shown that CR can reduce oxidative damage, retard age-related functional decline such as deteriorations in DNA repair capacity, and cause a 30 – 40% increase in maximal life span of mammals (Weindruch *et al.*, 1986; Walford *et al.*, 1987; Sohal and Weindruch, 1996).

Other than the insulin/IGF-1 pathway which is involved in nutrient-sensing, three other interconnected nutrient-sensing systems have been identified to play a role in CR (Kenyon, 2010). The mechanistic target of rapamycin (mTOR) kinase is important for sensing high amino acid concentrations and regulates anabolic metabolism. Reduction of mTOR activity by ribonucleic acid interference (RNAi) was found to increase resistance to environmental stress (Hansen *et al.*, 2007) and prolonged life

span independently of the FOXO (forkhead box O) transcription factor in *C. elegans* (Jia *et al.*, 2004). On the other hand, low energy states can be sensed by 5'-Adenosine Monophosphate-activated Protein Kinase (AMPK) and sirtuins via detection of high 5'-Adenosine Monophosphate (AMP) levels, and high oxidized Nicotinamide Adenine Dinucleotide (NAD⁺) levels respectively, thus playing a role in the regulation of catabolic metabolism such as fatty acid oxidation (Lopez-Otin *et al.*, 2013). Interestingly, supplying the anti-diabetic drug metformin to mice can activate AMPK (Zhou *et al.*, 2001) and lead to life span extension (Anisimov *et al.*, 2008). However, metformin has potential adverse effects such as gastrointestinal problems in humans (Bolen *et al.*, 2007), and more studies are needed to test the anti-aging effects in humans (Anisimov, 2013). Increasing NAD⁺ levels by inhibiting NAD⁺ breakdown or supplying NAD⁺ precursors, can also delay aging in model organisms (Mouchiroud *et al.*, 2013).

A diet low in calories, while maintaining essential nutrient intake, can increase maximal life span by triggering nutrient sensors such as reducing IGF-1 and mTOR signaling, and activating AMPK, sirtuins and other NAD⁺-dependent mechanisms to promote energy production (Moroz *et al.*, 2014) (Figure 1.2). This will in turn activate the transcriptional coactivator PGC-1 α (peroxisome proliferator-activated receptor gamma coactivator-1-alpha) and certain transcription factors like FOXO, which are involved in mitochondrial biogenesis (Finley *et al.*, 2012), promoting fat mobilization from white adipose tissue to blood (Guarente, 2013), and regulating oxidative stress responses (Houtkooper *et al.*, 2010). CR has also been found to maintain longer telomeres due to less telomere shortening caused by DNA damage

(Wang *et al.*, 2015). Short term studies in humans have suggested health benefits like better lipid profiles and insulin sensitivity (Walford *et al.*, 2002), while a 3- to 15-year CR diet in humans showed additional benefits such as lowered levels of inflammation markers, and reduced risk of atherosclerosis and heart disease (Fontana *et al.*, 2004; Stein *et al.*, 2012).

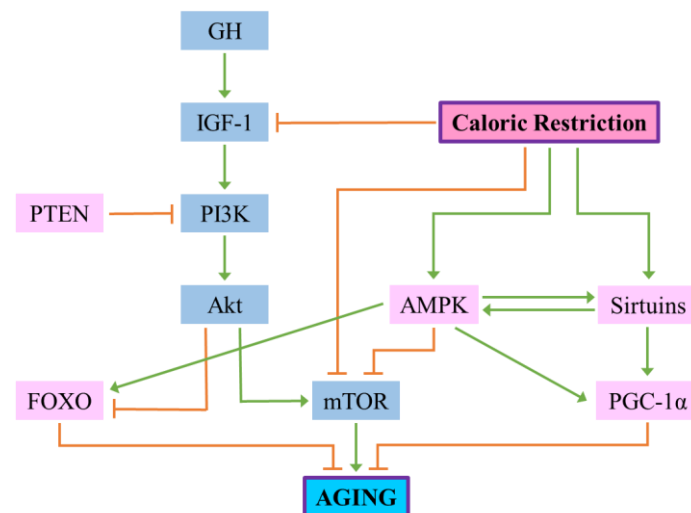


Figure 1.2: Overview of the insulin/IGF-1 signaling pathway and its relationship to CR and aging. Molecules which play a role in anti-aging when activated, are shown in light pink. GH: Growth hormone; PTEN: Phosphatase and tensin homolog.

Some studies have suggested that CR causes an overall effect of slowed metabolic rate and reduced mitochondrial reactive oxygen species (ROS) production on the host organism, thus bringing about life span extension (Sohal and Weindruch, 1996; Heilbronn and Ravussin, 2003). However, there is increasing evidence which supports the view that CR generates ROS, resulting in a small increase in oxidative stress, and yet promoting longer life span. This is because CR reduces caloric intake, which in turn causes metabolism to shift away from glycolysis towards respiration in order to maintain body function (Lin *et al.*, 2002; Moroz *et al.*, 2014). Hence, there is

an elevated electron transport, respiration, and ROS production. This low exposure to a greater oxidative stress triggers a secondary adaptive response in the host's defence system, leading to better stress resistance and life span extension (Houthoofd and Vanfleteren, 2006; Schulz *et al.*, 2007; Kim *et al.*, 2015). This contrary effect to a potentially harmful stressor is termed mitohormesis.

Nevertheless, the regimented use of CR to improve life span in humans has not been conducted for long periods of time due to difficulties in adhering to such a rigorous intervention, and ethical issues (Heilbronn and Ravussin, 2003; Gems and Partridge, 2013). Moreover, there are potential adverse effects such as depression, bone thinning, slowed wound healing, and hypotension (Finkel and Holbrook, 2000; Dirks and Leeuwenburgh, 2006). The amount and duration of CR necessary to extend life span is not practical in humans (Dirks and Leeuwenburgh, 2006). Hence, the key lies in developing a CR mimetic that can directly target biochemical pathways affected by CR, and achieve life span extension (Ingram *et al.*, 2006). Discovery of anti-aging drug leads is a promising and expanding research endeavor warranting more effort from researchers.

1.3 *Caenorhabditis elegans* as a model organism

In the search for an anti-aging compound, various model organisms such as *Escherichia coli*, budding yeast, *C. elegans*, *Drosophila melanogaster*, and mouse, have been used by different researchers. The soil-dwelling nematode *C. elegans* is a small, transparent, free-living roundworm which feeds on bacteria (Brenner, 1974). They are in general self-fertilizing and

hermaphroditic, producing up to 300 clonal progeny during the first week of their adult life. *C. elegans* is a eukaryote simple enough to be studied in great detail because the developmental fate of every single somatic cell (959 in the adult hermaphrodite) has been mapped out (Gruber *et al.*, 2009). Hence, it is a model of choice for many investigators researching on developmental pathways, neurobiology, aging and antioxidant mechanisms. *C. elegans* provides a powerful metazoan model for studying longevity because it has a short life span of approximately three weeks at 20°C, is easily maintained under laboratory conditions, and is amenable to genetic modification of processes that might be essential in mammals. Furthermore, numerous age-associated changes seen in mammals are recapitulated in *C. elegans*, including deteriorations in cellular components like mitochondria, and declines in physiological functions like locomotion and sensory behavior (Maglioni *et al.*, 2014).

As such, many anti-aging studies have been conducted on *C. elegans*, consistently proving that CR extends life span (Klass, 1977; Greer and Brunet, 2009). CR in *C. elegans* has been shown to increase metabolic rate, which is a key element in CR-induced longevity in *C. elegans* (Bishop and Guarente, 2007; Schulz *et al.*, 2007; Greer and Brunet, 2009; Gruber *et al.*, 2009). A study carried out by Yuan and colleagues examined metabolism in *C. elegans* *eat-2* mutants, which have a pharyngeal pumping defect leading to compromised food intake (Lakowski and Hekimi, 1998), allowing mutants to undergo chronic CR and subsequently life span extension. By using a quantitative proteomic analysis of key proteins involved in energy metabolism such as the nematode homologs of mammalian α -enolase, pyruvate kinase,

fructose-1,6-bisphosphatase, short-chain fatty acid-specific acyl-CoA dehydrogenase, and enoyl-CoA hydratase, it was found that carbohydrate metabolism was reduced, while short-chain fatty acids replaced carbohydrates as the main energy source in these mutants (Yuan *et al.*, 2012). In addition, *eat-2* mutants had a 21-fold higher rate of oxidative metabolism of acetate, and had an approximately 30% longer life span compared to the wild-type.

Similarly, reducing glucose metabolism of wild-type *C. elegans* using glycolysis inhibitors or RNAi increased lipid metabolism, resulting in greater mitochondrial respiration and oxygen consumption (Schulz *et al.*, 2007). This suggests that enhanced substrate flux and oxidation of calories is important in life span extension mediated by CR (Yuan *et al.*, 2012). However, further analysis of mitochondrial function is necessary in order to better understand the effects of CR on metabolism.

CR mimetics involve drug interventions which can result in physiological and anti-aging effects similar to CR without reducing caloric intake (Ingram *et al.*, 2006). Hence, a promising anti-aging drug lead will most likely target systems involved in nutrient sensing, regulation, and metabolism, and subsequently shift cells to a physiological state of repair and maintenance. A major limitation in anti-aging therapeutic development lies in the generation of novel and bioactive compound libraries for drug screening. Based on studies on model organisms, polyketides and alkaloids, such as resveratrol and berberine respectively, can direct effects on AMPK (Um *et al.*, 2010; Park *et al.*, 2012; Chow and Sato, 2013) and sirtuin (Lagouge *et al.*, 2006; Gertz *et al.*, 2012; Menzies and Hood, 2012) pathways, and have potential anti-aging

properties (Gruber *et al.*, 2007; Houtkooper *et al.*, 2013; Zhao and Darzynkiewicz, 2014), bringing us a step closer to developing an elixir of life.

1.4 Polyketides and their potential in the development of caloric restriction mimetics

Considerable focus has been awarded to polyketide research since its initial discovery about a century ago (Collie, 1907). Polyketides are structurally and functionally diverse secondary metabolites produced by bacteria, fungi, and plants. Many of these bioactive natural products have significant medical or agricultural applications (Staunton and Weissman, 2001), such as rapamycin (a macrolide immunosuppressant) (Calne *et al.*, 1989), lovastatin (used for the treatment of hypercholesterolemia) (Alberts *et al.*, 1980), actinorhodin (an antibiotic) (Wright and Hopwood, 1976), and resveratrol (reported anti-aging properties in model organisms) (Houtkooper *et al.*, 2013). This highlights the vital role polyketides or their derivatives can play in the development of novel therapeutics (Newman and Cragg, 2012) such as CR mimetics. Although chemical synthesis can be used to generate polyketide analogues (Tatsuta and Hosokawa, 2006), the chemical and structural complexity of polyketides and their derivatives render this means difficult.

1.4.1 Synthesis of polyketides by type I, type II, and type III polyketide synthases

Insights into the biosynthetic mechanisms of polyketides only achieved considerable progress from 1953 when Birch and Donovan hypothesized a

potential biosynthetic pathway analogous to that of fatty acids (Birch and Donovan, 1953). Further advancements in the polyketide field led to the consensus that polyketides are typically biosynthesized via successive decarboxylative condensations of coenzyme A (CoA)-derived units, into a complex polycyclic multi-carbon compound containing hydroxyl or keto groups (Dunn and Khosla, 2013). Recent studies in the engineering and structural characterization of polyketide synthases (PKSs) have facilitated the usage of target enzymes as biocatalysts to generate novel functionally optimized polyketides, which can serve as potential drug leads (Abe, 2012).

In general, PKSs are grouped into three classes: type I, II, or III PKS (Figure 1.3) (Staunton and Weissman, 2001). Type I PKSs are big multi-domain polypeptides which can function in either a modular or iterative manner, shuttling substrates between functional domains through acyl carrier proteins (ACPs). In modular type I PKSs, functional domains are grouped into several modules, with each module being responsible for a distinct decarboxylative condensation step and the associated polyketide backbone modification in polyketide biosynthesis (Staunton and Weissman, 2001; Shen, 2003). Conversely for iterative type I PKSs, the functional domains are clustered in only one module; hence, each domain is used repeatedly during each step of polyketide synthesis (Cox, 2007). Type II PKSs are dissociable multi-enzyme complexes, with each protein in the complex bearing an independent catalytic domain that is used iteratively during polyketide formation (Shen, 2003). Type III PKSs are homodimeric enzymes, which are structurally simpler and mechanistically different from the type I and II PKSs.

The relative simplicity, versatility, and unusually broad substrate specificity of type III PKSs make them ideal candidates for the engineering of biocatalysts, enabling the access of bioactive polyketide compound libraries which can be otherwise not easily available (Stewart *et al.*, 2013).

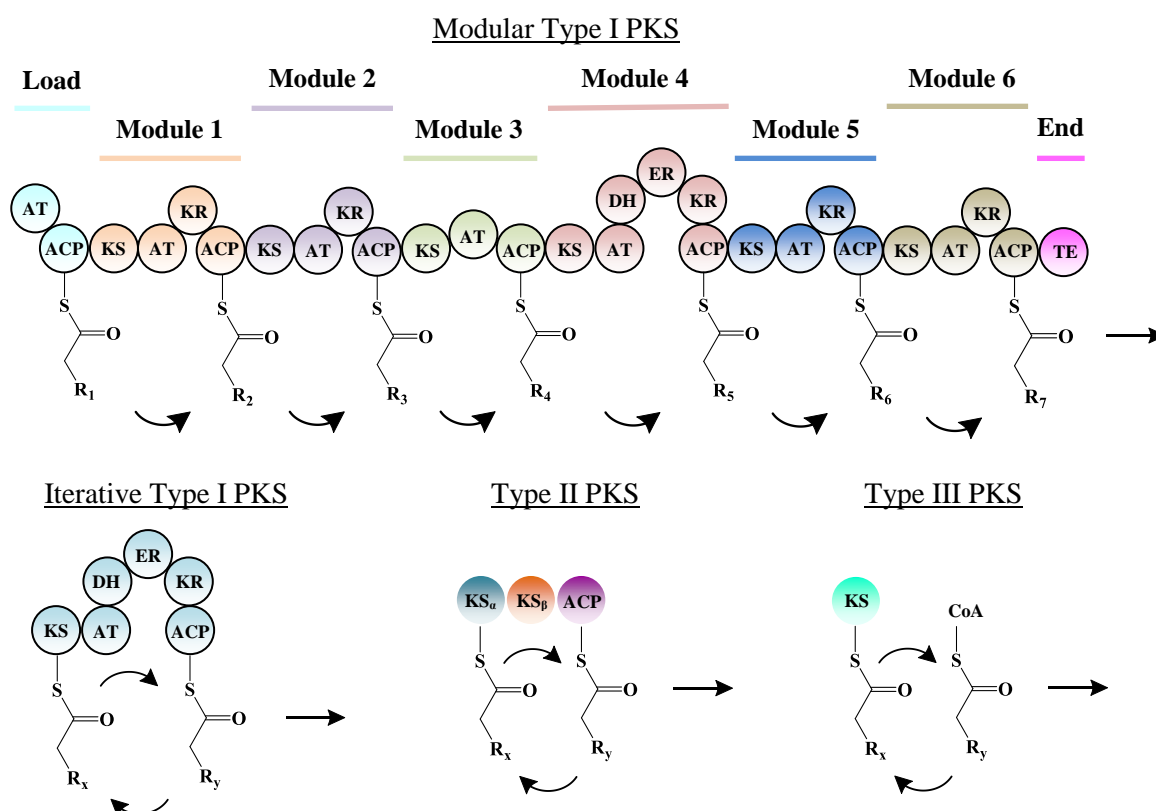


Figure 1.3: Domain organization of the different PKSs. Putative domains are depicted by circles. In modular type I PKSs, functional domains are organized into modules, with each module being responsible for a single decarboxylative condensation step in polyketide formation. For iterative type I PKSs, the functional domains are clustered in a single module, and each domain is used repeatedly during polyketide biosynthesis. Type II PKSs are dissociable multi-enzyme complexes, with each protein bearing one independent catalytic domain that is used iteratively. Type III PKSs are also iterative but do not require ACP to attach to the growing polyketide chain. AT: Acyltransferase; ACP: Acyl carrier protein; KS: Ketosynthase; KR: Ketoreductase; DH: Dehydratase; ER: Enoyl reductase; TE: Thioesterase; CoA: Coenzyme A.

1.4.2 Chalcone synthase superfamily of type III polyketide synthases

Unlike type I and II PKSs, type III PKSs generally employ CoA thioesters as substrates and do not entail the use of ACP domains. In addition, type III PKSs are capable of accomplishing an entire series of decarboxylative condensations and cyclization reactions in only a single active site (Staunton and Weissman, 2001). Its simple architecture enables type III PKSs to be amenable to *in vitro* manipulation and examination. Moreover, the inherent substrate promiscuity of these PKSs also permits them to accept unnatural precursors, thus generating an extensive range of compounds with novel scaffolds (Katsuyama *et al.*, 2007; Go *et al.*, 2015). Even though type III PKSs have been studied since the 1980s (Schuz *et al.*, 1983), structural information on how a single active site can direct the chemistry of several decarboxylative condensations and subsequent cyclization of the polyketide was only made known after the crystal structure of chalcone synthase (CHS) from *Medicago sativa* (alfalfa) was solved (Ferrer *et al.*, 1999). This was the first crystal structure of a PKS and it facilitated a framework for engineering type III PKSs to create novel polyketides.

CHSs are the most well studied type III PKSs as they are ubiquitous in higher plants and crucial for plant metabolism and defense (Stewart *et al.*, 2013). Based on the structure of CHS from alfalfa, it was found that the symmetric dimer encapsulates a CoA-binding tunnel, a coumaroyl-binding pocket, and a cyclization pocket so as to facilitate chalcone biosynthesis (Ferrer *et al.*, 1999). Together with the conserved Cys164-His303-Asn336 catalytic triad, and the ‘gatekeeper’ Phe215 which is hypothesized to assist in the orientation of substrates during polyketide chain elongation, these

connected cavities make up the active site architecture of a typical type III PKS (Figure 1.4) (Jez *et al.*, 2000; Austin and Noel, 2003). Chalcone synthesis by CHS is initiated by the loading of *p*-coumaroyl-CoA onto the sulfhydryl group of the active site cysteine residue. The reaction then continues with three iterative decarboxylative condensations of the extender substrate, malonyl-CoA, with the cysteine-bound starter substrate, aided by the active site asparagine and histidine residues. After chain extension, the linear tetraketide, *p*-coumaroyl triacetyl thioester, undergoes an intramolecular C6 to C1 Claisen condensation and cyclizes into chalcone, which undergoes a further Michael-type ring closure to yield naringenin (Figure 1.5) (Austin and Noel, 2003).

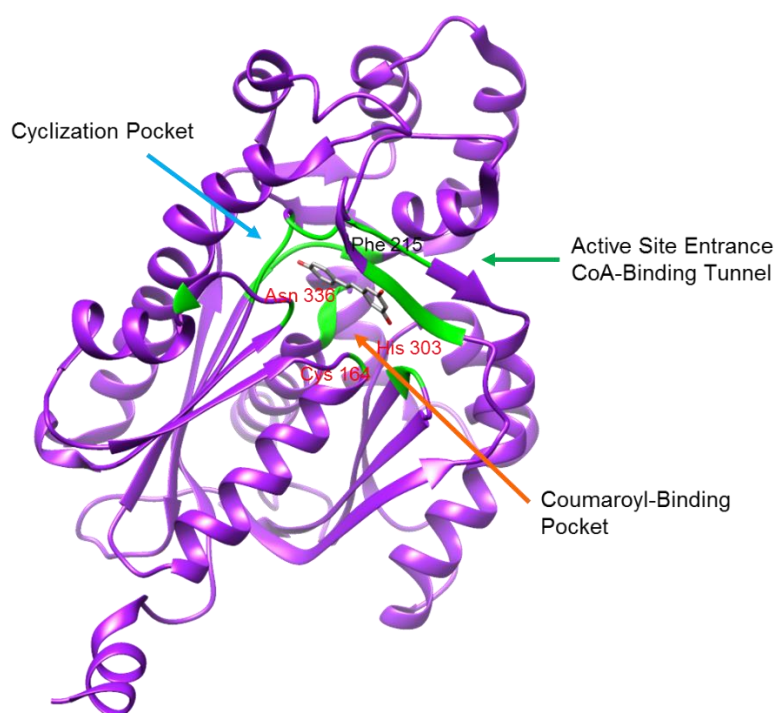


Figure 1.4: Crystal structure of a monomer of a modified CHS from alfalfa (PDB ID: 1U0W) showing the conserved Cys164-His303-Asn336 catalytic triad highlighted in red, and the ‘gatekeeper’ Phe215. A resveratrol molecule is co-crystallized in the active site cavity, and active site residues within 5 Å distance are highlighted in green.

Numerous type III PKSs have been identified till date, and the variety of reactions and product classes discovered is due to differences in intramolecular cyclizations of the linear polyketide intermediate, the choice of starter and extender CoAs used, and the number of polyketide extension steps involved (Austin *et al.*, 2004). The diverse polyketide scaffolds catalyzed by type III PKSs can be classified into different groups, such as chalcone, stilbene, pyrone, stilbenecarboxylate, curcuminoid, acridone, quinolone, phloroglucinol, resorcinol, and naphthalene families, amongst many others that were discovered (Austin and Noel, 2003; Abe and Morita, 2010). By characterizing type III PKSs, we can understand reaction mechanisms better and thus, direct the generation of unnatural polyketide compound libraries using synthetic enzymology.

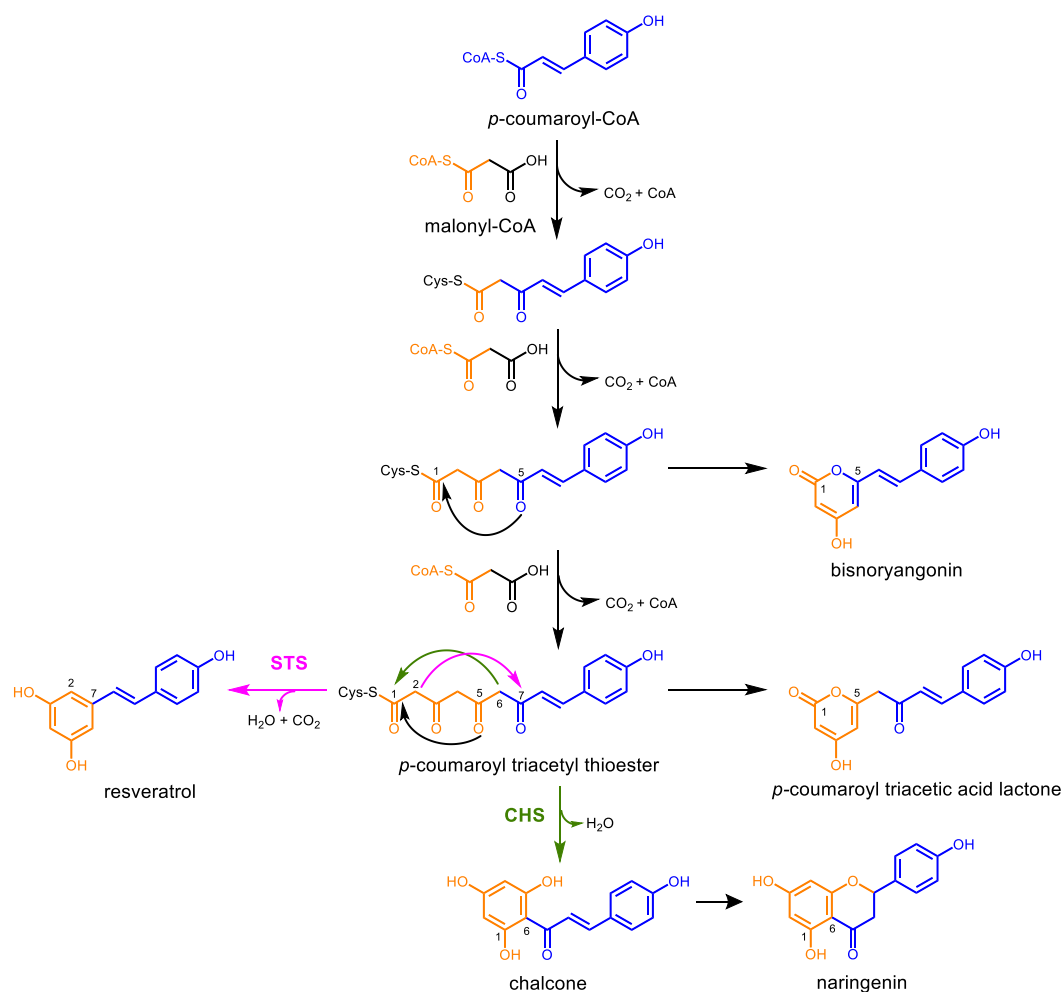


Figure 1.5: Chalcone and naringenin synthesis catalyzed by *M. sativa* CHS using *p*-coumaroyl-CoA as the starter with malonyl-CoA as the extender. Truncation products of CHS undergo a spontaneous C5-oxygen to C1 lactonization to form bisnoryangonin or *p*-coumaroyl triacetic acid lactone (CTAL). Another type III PKS, stilbene synthase (STS), can instead catalyze a C2 to C7 aldol condensation, followed by decarboxylation to yield the anti-aging compound, resveratrol.

1.4.3 Stilbene synthase superfamily of type III polyketide synthases

Stilbene synthases (STSs) are identified in only a small subset of unrelated plants, unlike CHSs which are ubiquitous. STSs and CHSs are structurally related and share approximately 65% amino acid sequence identity (Yamaguchi *et al.*, 1999). These enzymes follow a similar overall reaction

mechanism which encompasses initiation, followed by the iterative decarboxylative condensation of three units of malonyl-CoA to a starter substrate, and lastly cyclization of the linear tetraketide intermediate. Slight variations in active site residues facilitate STSs to catalyze an intramolecular C2 to C7 aldol condensation, followed by decarboxylation and dehydration to create a stilbene scaffold instead of a chalcone backbone (Figure 1.5) (Austin *et al.*, 2004). Previous homology modeling studies have revealed no substantial structural or chemical differences in the STS active site compared to CHS, and no obvious STS or CHS consensus sequence was recognized (Tropf *et al.*, 1994; Austin *et al.*, 2004). With the report of the first STS crystal structure from *Pinus sylvestris* (Scots pine) in 2004, the mechanism of stilbene biosynthesis was finally resolved (Austin *et al.*, 2004; Abe and Morita, 2010).

Structure-based mutagenic transformation of alfalfa CHS into STS showed that the different cyclization specificity of STSs is due to a conformational backbone change in a short, concealed loop between residues 132 and 137 in alfalfa CHS, that spans the dimer interface in the active site. Several amino acid substitutions at buried sites near this loop can lead to a slight displacement of Thr132, a residue that is conserved in both CHS and STS. Consequently, the side chain hydroxyl group of Thr132 is brought within the hydrogen bonding distance of a Ser338-stabilized water molecule adjacent to the catalytic cysteine, and a unique active site hydrogen bonding network comprising Glu192-Thr132-H₂O-Ser338 forms in STS (Figure 1.6) (Austin and Noel, 2003; Austin *et al.*, 2004; Shomura *et al.*, 2005). The nucleophilic water activated by this “aldol-switch” hydrogen bonding network subsequently plays a part in the cleavage of the thioester bond of the cysteine-

bound linear tetraketide intermediate. With the absence of the ester bond at C1, the intermediate is capable of undergoing a C2 to C7 aldol condensation and ultimately produces a stilbene scaffold. Hence in the case of CHS and STS, the functional divergence is caused by electronic factors in the active site cavity.

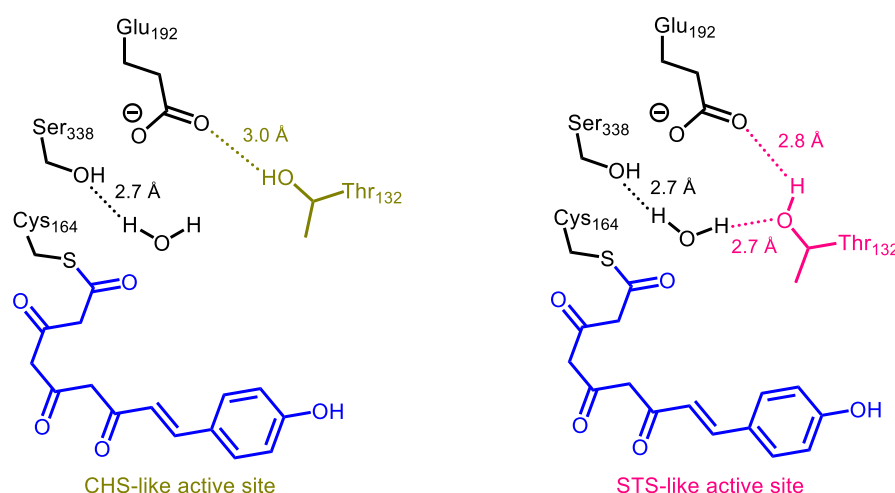


Figure 1.6: The hydrogen bonding network involving Glu192, Thr132, H₂O and Ser338 (numbering in alfalfa CHS). Differences in this network switches the chemistry of the active site of alfalfa CHS or Scots pine STS between chalcone and stilbene biosynthesis.

Resveratrol is a polyphenolic phytoalexin that is commonly found in grapes, pine, nuts and dark chocolate. It is biosynthesized by STSs from *p*-coumaroyl-CoA and malonyl-CoA. Resveratrol is hypothesized to be a CR mimetic (Chung *et al.*, 2012; Gertz *et al.*, 2012) as it increases mitochondrial resistance to oxidative stress and extends the life span of *C. elegans* (Gruber *et al.*, 2007). It has also been found to extend the life span of other model organisms such as yeast and fruit flies (Bass *et al.*, 2007). Resveratrol was found to activate AMPK (Um *et al.*, 2010; Park *et al.*, 2012) and increase Sirt1

expression and activity, bringing about mitochondrial biogenesis and cell survival (Menzies and Hood, 2012), thus mimicking CR and contributing to life span extension. Although resveratrol has some potential health benefits, its application on humans has limitations. One main problem of administering resveratrol in humans is its low solubility and high metabolism, resulting in low bioavailability (Pirola and Frojdo, 2008). A study in human subjects revealed that even after high oral doses, the peak amount of free resveratrol in the plasma only reached less than 2% of the total resveratrol administered, possibly explaining why resveratrol studies in humans have inconclusive results (Goldberg *et al.*, 2003). In addition, some research has suggested that resveratrol may have potential side effects like nephrotoxicity (Crowell *et al.*, 2004; Cottart *et al.*, 2010; Chung *et al.*, 2012). Consequently, there is a need to discover new CR mimetics that are more potent than resveratrol in bringing about life span extension in humans. It will be useful if we can utilize enzymes like resveratrol synthase to conduct precursor-directed biosynthesis of novel polyketides which still retain the phenol moieties for potential biological activities.

1.4.4 Precursor-directed combinatorial biosynthesis of unnatural polyketides

Considerable effort has been spent in exploring the biosynthesis of polyketides, and although there has been good progress, rationally guided combinatorial biosynthesis to produce novel and bioactive polyketides remains difficult. Using *in vitro* assays, when both the starters and the extenders were substituted with non-physiological substrates, CHS from the herb *Scutellaria*

baicalensis was able to catalyze the production of unnatural polyketides (Abe *et al.*, 2003). Other than the preferred substrates of *p*-coumaroyl-CoA and malonyl-CoA, *S. baicalensis* CHS was able to accept benzoyl-CoA as a starter and methylmalonyl-CoA as the extender to produce methylated triketide and tetraketide pyrones. Similar to studies on CHSs, STS from *Arachis hypogaea* (peanut) was also found to accept several unnatural substrates to produce unique stilbene-like products (Morita *et al.*, 2001).

Synthetic enzymology is the use of enzymological principles such as combinatorial biosynthesis, mechanistic enzymology, and enzyme engineering in the intentional design of biological systems for purposeful function (Go *et al.*, 2015). Although synthetic biology and the idea to engineer organisms were first posited in the 1960s, the synthetic biology field only picked up momentum after the year 2000 when technological advancements such as improved computational programs and automated DNA sequencing surfaced (Cameron *et al.*, 2014). By manipulating a number of promiscuous acid-CoA ligases and PKSs together in a microbial host like *Escherichia coli* (Katsuyama *et al.*, 2007; Go *et al.*, 2012; Go *et al.*, 2015), novel acyl-CoA precursors can be delivered to PKSs, thus generating a large library of novel polyketides with therapeutic potential via precursor-directed combinatorial biosynthesis (Figure 1.7A).

A starter acid such as *p*-coumaric acid can be converted to *p*-coumaroyl-CoA via a CoA ligase, while malonic acid can be converted to the extender CoA, malonyl-CoA, by a malonyl-CoA synthetase (MCS). A type III PKS such as resveratrol synthase is then capable of using one unit of starter-CoA and three units of extender-CoA to generate polyketides like resveratrol

(Figure 1.7B). Since the CoA ligases and PKS used are promiscuous in activity, different precursors can be used to direct the biosynthesis of polyketide compound libraries, which can be otherwise difficult to obtain for screening assays. Positions of critical pharmacophoric moieties in polyketides can be manipulated easily by varying the carboxylic acid used in the biosynthesis. Additional diversity also comes from the number of elongation steps in polyketide biosynthesis, and the cyclization mechanisms of the intermediate (Austin *et al.*, 2004). In contrast, modifications done using chemical synthesis are more challenging due to the generation of side products and low yields (Tatsuta and Hosokawa, 2006). Furthermore, precursor-directed combinatorial biosynthesis is believed to be capable of creating compound libraries with sufficient diversity and complexity that is not attainable by chemical synthesis (Katsuyama *et al.*, 2007; Chemler and Koffas, 2008). It is interesting to note that due to a lack of a toolkit to modify drug compounds easily, the chemically synthesized derivatives of resveratrol are currently limited to simple functional group changes in the aromatic rings, such as fluoro, amino, hydroxyl, methyl, methoxy, acetyl, and methyl ester derivatives which are usually produced via the Wittig reaction or Heck reaction (Moran *et al.*, 2009; Aldawsari *et al.*, 2015).

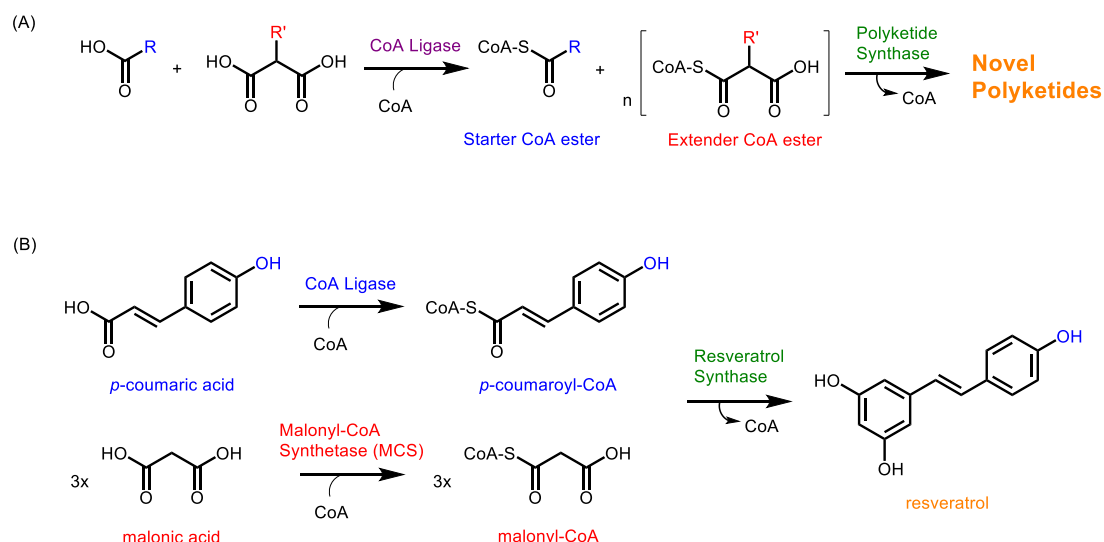


Figure 1.7: Precursor-directed combinatorial biosynthesis of novel polyketides. (A) Promiscuous substrate specificities of choice CoA ligases can deliver unnatural acyl-CoA esters to PKSs, which can in turn generate novel polyketide compound libraries. (B) In one of the combinatorial biosynthetic pathways, resveratrol synthase utilizes one unit of *p*-coumaroyl-CoA and three units of malonyl-CoA, generated by a CoA ligase and malonyl-CoA synthetase respectively, to yield the polyketide resveratrol.

1.5 Alkaloids as potential caloric restriction mimetics

Compared to polyketides and other classes of low molecular weight natural compounds, alkaloids have the highest structural diversity (Cordell *et al.*, 2001). Alkaloids contain the basic nitrogen in addition to carbon and hydrogen, and some may contain oxygen, sulphur, and other elements. They are initially isolated mainly from plants but are now found to be widely distributed in animal (Daly *et al.*, 1987; Laurent *et al.*, 2003) and microbial (Liu *et al.*, 2015; Young *et al.*, 2015) species too.

Like polyketides, alkaloids play an important role in the pharmaceutical industry. The first alkaloid was discovered in 1817 by Sertürner from *Papaver somniferum* (opium poppy) and is known commonly as the analgesic drug, morphine (Dodds, 1946; Lesch, 1981). In addition, berberine is the active

constituent in *Coptis chinensis* Franch extracts, a herb used to treat gastrointestinal disorders and diabetes in traditional Chinese medicine for more than 2000 years (Ko *et al.*, 2005; Wang *et al.*, 2014). Interestingly, berberine is now known to have potential anti-aging properties in fruit flies (Navrotskaya *et al.*, 2012). At least 21,120 alkaloids have been discovered, but only 3.3% of these were evaluated in no more than five bioassays (Cordell *et al.*, 2001). Hence, the untapped potential of alkaloids as therapeutic drug leads is profound.

1.5.1 Biosynthesis of alkaloids in nature

Alkaloids are extremely diverse and can be classified based on their biosynthetic pathways and chemical structures. Depending on the precursors used, and the final structure of the alkaloids, the assorted alkaloid scaffolds can be grouped into different classes such as simple amines, oxazoles, isoquinolines, quinolines, indoles, imidazoles, pyrrolidines, pyrrolizidines, tropanes, polyamines, piperidines, quinolizidines, indolizidines, quinazolines, pyridines, and aminated purines and terpenes (Figure 1.8) (Cordell *et al.*, 2001). The biosynthetic pathway of alkaloids in nature branched out from main metabolic pathways to secondary pathways to yield the different precursors and intermediates of alkaloids. Alkaloids can be derived from L-amino acids such as L-tryptophan, L-phenylalanine, L-tyrosine, L-histidine, L-ornithine, and L-lysine. Other building blocks of alkaloids include anthranilic acid, nicotinic acid, purines, acetate, selected polyterpene units, and polyketide units (Cordell *et al.*, 2001; Cordell, 2013). From a single L-amino acid, step-wise biosynthetic pathways are usually able to produce several types of

alkaloid scaffolds. For instance, L-tryptophan can be converted to indole alkaloids, terpenoid indole alkaloids such as the ergot alkaloids in several fungal species, and quinoline alkaloids. A classic example of an ergot alkaloid is lysergic acid (Young *et al.*, 2015). Given the diversity of bioactive alkaloids, they have a huge potential in therapeutic drug development (Figure 1.8) (Meneses, 1998; Kobayashi *et al.*, 1999; Cordell *et al.*, 2001; Wattanathorn *et al.*, 2008; Karmase *et al.*, 2013; Servillo *et al.*, 2013; Appadurai and Rathinasamy, 2014; Minois, 2014).

1.5.2 Precursor-directed combinatorial biosynthesis as a novel means to produce alkaloids

Alkaloids can be obtained through several methods such as extraction from the source directly, chemical synthesis, and biosynthesis via enzymes. Extraction from the source is difficult and not economically feasible because alkaloids are typically only present in low amounts of 1% to 2% of dried biomass (Cordell *et al.*, 2001). This is due to the fact that alkaloids are secondary metabolites in many organisms, and are generally not essential for the survival of the plants. Chemical synthesis is also challenging and not cost-effective because the extremely diverse structures of alkaloids will pose difficulties in the production of complex alkaloids from simple chemical substrates (Minami *et al.*, 2008). Enzymes on the other hand are optimized for the generation of bioactive compounds, therefore biosynthesis should have better yields of desired target compounds. However, conventional biochemical pathways of synthesizing alkaloids in plants can be lengthy, compartmentalized and localized to different cell types, and tightly regulated, making them difficult to manipulate using molecular biology (Facchini, 2001; Ziegler and Facchini, 2008). By establishing a precursor-directed combinatorial biosynthetic route involving promiscuous acid-CoA ligases and PKSs, and utilizing nitrogen-containing compounds as substrates, a wide range of alkaloids can be biosynthesized (Figure 1.9).

Similar to the precursor-directed combinatorial biosynthesis of polyketide libraries, promiscuous acid-CoA ligases are able to biosynthesize unique nitrogen-containing acyl-CoA esters which can act as the starter and/or extender units for PKSs. Hence, the diversity of alkaloids produced hinges on

the choice of starter and extender CoA esters used. Furthermore, the number of elongation steps catalyzed, and the mode of cyclization of the intermediates, provide a further element of structural diversity (Austin *et al.*, 2004). By manipulating PKSs innovatively, this represents a novel and feasible means to biosynthesize alkaloid compound libraries effectively.

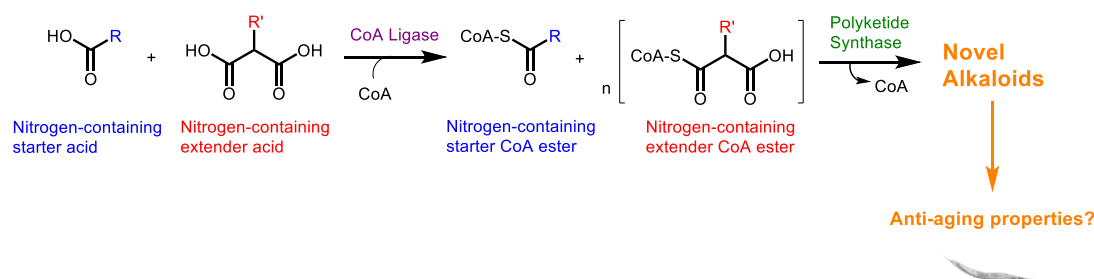


Figure 1.9: Precursor-directed combinatorial biosynthesis of novel alkaloids. Promiscuous substrate specificities of choice CoA ligases can deliver nitrogen-containing acyl-CoA esters to PKSs, which can in turn generate alkaloid compound libraries. These unnatural alkaloids can then be introduced to model organisms like *C. elegans* to test for anti-aging properties.

1.6 Anti-aging therapeutic development

With a bioactive library of polyketides and alkaloids, anti-aging therapeutics can be developed. The conventional way of anti-aging drug screening is via life span assays. However even for the relatively short-lived model organism *C. elegans*, life span assays are time consuming and impractical to screen for a large library of bioactive compounds. This study aims to develop a medium throughput screening methodology by conducting mitochondrial function assays on *C. elegans* exposed to various drugs using an Extracellular Flux Analyzer. By periodically introducing pharmacological agents such as electron transport chain (ETC) inhibitors to manipulate mitochondrial activity and respiratory function, the mitochondrial biology of

C. elegans can be looked into, so as to establish a connection between oxygen consumption rates (OCR), CR mimetics, and life span extension.

Preliminary studies showed that worms subjected to CR had a higher metabolic rate and thus a higher OCR and better mitochondrial function than worms fed on a normal diet (Schulz *et al.*, 2007; Yuan *et al.*, 2012). Consequently, treatment with CR mimetics is likely to have a similar effect on *C. elegans* as reductions in caloric intake. Since resveratrol is a potential CR mimetic, the mitochondrial respiration profile of resveratrol-treated *C. elegans* can be analyzed, which will function as a reference for future screening of potential CR mimetics to narrow down drug hits for subsequent validation studies.

Different dietary interventions and therapeutic drug leads have been studied for their potential to counter age-associated dysfunctions. By looking for polyketides and alkaloids that can alleviate declines in mitochondrial function and aerobic capacity, which is one of the hallmarks of aging, it is believed that the aging process can be modulated. This study serves as a primer towards the development of unique anti-aging nutraceuticals via synthetic enzymology.

CHAPTER 2: TOWARDS THE DEVELOPMENT OF NOVEL ANTI-AGING POLYKETIDES USING PRECURSOR-DIRECTED COMBINATORIAL BIOSYNTHESIS

2.1 Introduction

Several studies have illustrated the feasibility of performing precursor-directed combinatorial biosynthesis using type III PKSs to generate novel polyketides (Katsuyama *et al.*, 2007; Abe and Morita, 2010). Recently, a group of researchers demonstrated the production of novel polyketides via precursor-directed combinatorial biosynthesis and identified some lead compounds with anti-angiogenic or anti-cancer properties (Kim *et al.*, 2009; Kwon *et al.*, 2010). Similar work in synthetic enzymology using a CHS from *Oryza sativa* (rice) led to the development of novel polyketides as antimicrobial drug leads (Go *et al.*, 2015).

Previous substrate specificity studies have demonstrated the production of unnatural polyketides by the promiscuous alfalfa CHS. Alfalfa CHS was reported to utilize 3-phenylpropanoyl, phenylacetyl, benzoyl, several derivatives of cinnamyl, and short to medium-length aliphatic acyl-CoA thioesters to biosynthesize a range of compounds including chalcones and lactones (Jez *et al.*, 2002). These studies were limited mostly to structural derivatives of the cognate substrates from the cinnamyl-CoA and malonyl-CoA families, due to a lack of a means to deliver novel acyl-CoA precursors.

Mutagenesis studies on alfalfa CHS led to the development of a mutant CHS with STS activity (CHS18) (Austin *et al.*, 2004). Eighteen distal amino acid residues in alfalfa CHS spanning from residue 98 to 268 were mutated,

resulting in a new active site hydrogen bonding network comprising Glu192-Thr132-H₂O-Ser338, which caused the PKS (CHS18) to produce resveratrol as the major product and naringenin as the minor product when incubated with *p*-coumaroyl-CoA and malonyl-CoA. An exploration of the substrate specificity of CHS18 across various acyl-CoA classes has not been systematically attempted or reported. Since CHS18 is able to produce the CR mimetic resveratrol, and it originated from the promiscuous alfalfa CHS scaffold (Jez *et al.*, 2002), it provided an excellent platform for the engineered biosynthesis of novel bioactive stilbenes and other polyketides with potential anti-aging activities. In precursor-directed combinatorial biosynthesis, production of unnatural acyl-CoA esters by promiscuous CoA-ligases was coupled to polyketide biosynthesis by CHS18. The whole combinatorial biosynthetic pathway was constructed in *E. coli* so as to make use of its own ATP and CoA for the biosynthesis of our desired products. By establishing the substrate and product profiles of CHS18, we can direct the biosynthesis of polyketide compound libraries, which can be screened for anti-aging properties.

2.2 Materials and methods

The carboxylic acid substrates for acid-CoA ligases were obtained from Sigma-Aldrich Co. (St. Louis, MO, USA), Tokyo Chemical Industry Co. (Tokyo, Japan), Extrasynthese Co. (Genay Cedex, France), and Lier Chemical Co. (Sichuan, People's Republic of China). A total of 81 carboxylic acids were utilized as precursors for acyl-CoA thioester biosynthesis catalyzed by four acid-CoA ligases (Go *et al.*, 2012). The acids were from the malonate, cinnamate, phenylpropanoate, benzoate, phenylacetate, naphthalene, quinoline, saturated aliphatic, and unsaturated aliphatic families. All reagents were of the best quality grade that is available commercially.

A total of 12 malonate-type acids form the extender substrates for precursor-directed combinatorial biosynthesis and include: malonic acid, methylmalonic acid, ethylmalonic acid, isopropylmalonic acid, butylmalonic acid, allylmalonic acid, hydroxymalonic acid, fluoromalonic acid, chloromalonic acid, bromomalonic acid, phenylmalonic acid, and 3-thiophenemalonic acid. The remaining 69 carboxylic acids form the starter substrates and include: **(cinnamate type)** cinnamic acid, 2-fluorocinnamic acid, 3-fluorocinnamic acid, 4-fluorocinnamic acid, α -fluorocinnamic acid, 3-chlorocinnamic acid, 3-chloro-4-methoxycinnamic acid, 4-chlorocinnamic acid, 2-hydroxycinnamic acid, 4-hydroxycinnamic acid (also known as *p*-coumaric acid), 3-methoxy-4-hydroxycinnamic acid, 4-methoxycinnamic acid, 4-methylcinnamic acid, α -methylcinnamic acid; **(phenylpropanoate type)** 3-phenylpropanoic acid, 3-(3'-chloro)phenylpropanoic acid, 3-(3'-chloro-4'-methoxy)phenylpropanoic acid, 3-(3',4'-dihydroxy)phenylpropanoic acid, 3-(3'-methoxy)phenylpropanoic acid, 3-(4'-methoxy)phenylpropanoic acid, 3-

(4'-fluoro)phenylpropanoic acid; **(benzoate type)** benzoic acid, 2-fluorobenzoic acid, 3-fluorobenzoic acid, 4-fluorobenzoic acid, 2,6-difluorobenzoic acid, 2-chlorobenzoic acid, 3-chlorobenzoic acid, 4-chlorobenzoic acid, 2-bromobenzoic acid, 3-bromobenzoic acid, 4-bromobenzoic acid, 2-iodobenzoic acid, 2-hydroxybenzoic acid, 2,3-dihydroxybenzoic acid, 2,4-dihydroxybenzoic acid, 2,5-dihydroxybenzoic acid, 2-methoxybenzoic acid, 2-methylbenzoic acid, 3-aminobenzoic acid, 4-aminobenzoic acid; **(phenylacetate type)** phenylacetic acid, 2-hydroxyphenylacetic acid, 4-hydroxyphenylacetic acid, 4-methoxyphenylacetic acid, phenoxyacetic acid, phenylpyruvic acid; **(naphthalene and quinoline type)** 1-naphthalenecarboxylic acid, 2-naphthalenecarboxylic acid, 2-quinolinecarboxylic acid, 3-quinolinecarboxylic acid; **(saturated aliphatic type)** propanoic acid, butanoic acid, pentanoic acid, hexanoic acid, heptanoic acid, octanoic acid, nonanoic acid, decanoic acid; **(unsaturated aliphatic type)** 2-butenic acid, 2-methyl-2-butenic acid, 3-methyl-2-butenic acid, 3-butenic acid, 2-pentenoic acid, 3-pentenoic acid, 4-pentenoic acid, 3-methyl-4-pentenoic acid, 3-hexenoic acid, 5-hexenoic acid. The chemical structures of all substrates tested are depicted in Table A1 in the Appendix.

2.2.1 Establishing a combinatorial biosynthetic route in *Escherichia coli*

The type III PKS used in this research study is a mutant CHS with STS activity from *M. sativa* that was previously created by Austin *et al.* in 2004. Alfalfa CHS (GI: 166363) was cloned previously in the lab from *M. sativa* cDNA library into a modified pET-15b vector (Tom-15b vector) containing

ten histidine tags at the N-terminus of the protein. PCR-mediated mutagenesis was conducted with reference to the paper published by Austin *et al.* (2004) in order to replicate the same mutations in alfalfa CHS, resulting in CHS18 which has STS activity. In particular, the amino acids Asp98, Val100, Val101, Val102, Thr131, Ser133, Gly134, Val135, Met137, Tyr158, Met159, Met160, Tyr161, Gln163, Leu268, Lys269, Asp270, and Gly273 in alfalfa CHS were mutated to Ala98, Leu100, Ala101, Met102, Ser131, Thr133, Thr134, Pro135, Leu137, Val158, Gly159, Val160, Phe161, His163, Lys268, Gly269, Ala270, and Asp273 in CHS18.

MCS (GI: 3982573) and phenylacetate-CoA ligase (PCL) (GI: 1099823) were cloned previously in the laboratory from *Rhizobium trifolii* genomic DNA (ATCC) and *Streptomyces coelicolor* A3(2) genomic DNA (ATCC) respectively, each into a Tom-15b vector containing 10 histidine tags at the N-terminus of the protein. Benzoate-CoA ligase (BZL) (GI: 1040685) from *Rhodopseudomonas palustri* and 4-coumarate-CoA ligase (4CL) (GI: 12229632) from *Nicotiana tabacum* were kindly provided by E. Pichersky (Beuerle and Pichersky, 2002) in a pCRT7/CT-TOPO vector (Invitrogen) containing six histidine tags at the C-terminus of the protein.

In order to establish a combinatorial biosynthetic route in *E. coli*, three CoA ligases (4CL, PCL and BZL) that are involved in the generation of starter CoA thioesters were subcloned into the multiple cloning site 1 (MCS1) of a pRSFDuet-1 vector (Novagen) separately. To produce the extender CoA thioesters, MCS and PCL were each subcloned into the MCS2 region of the same vector. Thereafter, this pRSFDuet-1 vector was co-transformed with the Tom-15b vector containing CHS18 into *E. coli* Rosetta II (DE3) strain

(Novagen) (Figure 2.1). Depending on the identity of the starter and extender acids, *E. coli* harboring the appropriate combination of CoA ligases was used for the *in vivo* precursor-directed combinatorial biosynthesis of polyketides (see Table A1 in Appendix). An *E. coli* construct without the CHS18 gene was also prepared to serve as a control for the subsequent detection of novel polyketides. A matrix of 69 starter acids with 12 extender acids were separately introduced to the engineered *E. coli* host cells, giving a possible combination of 828 substrate profiles.

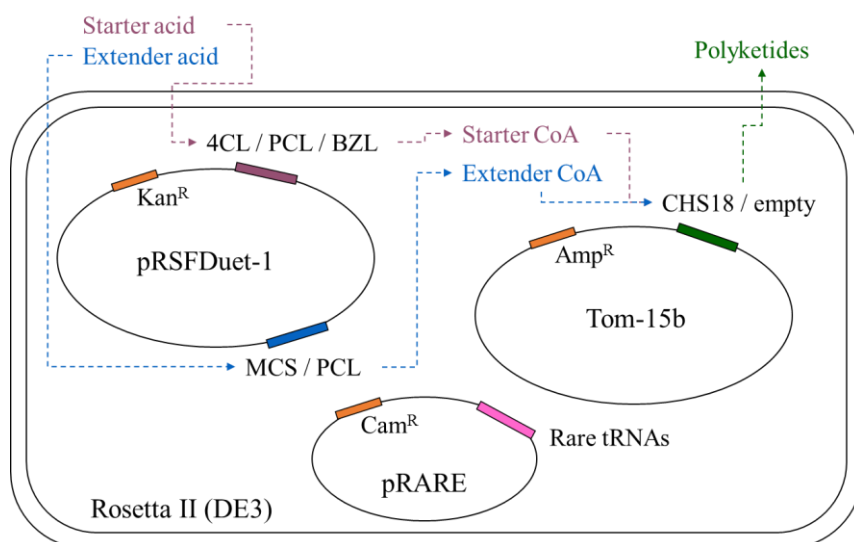


Figure 2.1: *E. coli* constructs generated for *in vivo* precursor-directed combinatorial biosynthesis of polyketides. Constructs containing the CoA ligases with an empty Tom-15b vector served as controls during the subsequent high performance liquid chromatography (HPLC) analyses.

2.2.2 *In vivo* precursor-directed combinatorial biosynthesis of polyketides and HPLC analysis

The *E. coli* host cells harboring the biosynthetic genes were first grown in 10 mL Lysogeny Broth (LB) containing 34 $\mu\text{g/mL}$ chloramphenicol, 100 $\mu\text{g/mL}$ ampicillin, and 30 $\mu\text{g/mL}$ kanamycin at 25°C. When $OD_{600\text{nm}}$ reached 0.6, protein expression was induced by 0.1 mM isopropyl β -D-1-

thiogalactopyranoside (IPTG) for 16 h. The cells were subsequently pelleted and resuspended in 10 mL minimal medium containing antibiotics, 0.1 mM IPTG, 1 mM starter acid and 1 mM extender acid, and incubated at 25°C for a further 72 h. The carboxylic acids were introduced only after the enzymes had been expressed, so that any potential toxicities to the *E. coli* due to the acids, CoA esters, or polyketides formed will have minimal effects on the expression of the enzymes and yields of the products. In addition, the carboxylic acids were introduced at 1 mM so as to ensure the maintenance of the highest possible intracellular concentration of carboxylic acids over 72 h without killing the cells, given that the uptake rates for the starter and extender acids into *E. coli* could have some slight variations. After centrifugation, the supernatant was acidified to pH 3.0 with 6 M HCl and extracted with ethyl acetate thrice. The organic solvent was subsequently removed by a vacuum concentrator, and the residue was dissolved in 100 μ L dimethyl sulfoxide (DMSO) for HPLC analysis.

The Atlantis Analytical C18 reverse-phase column (Waters) was first equilibrated with 10% acetonitrile, 0.1% trifluoroacetic acid (TFA) in water at a flow rate of 1 mL/min for 15 min. 10 μ L of sample was then loaded onto the column and the mobile phase was changed to 50% acetonitrile, 0.1% TFA in water under a linear gradient over a period of 40 min at a flow rate of 1 mL/min. For the next 5 min, a linear gradient to 100% acetonitrile containing 0.1% TFA was conducted. The eluted compounds were detected by measuring the absorbance at 230 nm, 280 nm, 320 nm, and 370 nm. Chromatogram peaks that were present (minimum absorbance of 20 mAU) in the extracts of

constructs containing CHS18 but absent in the extracts of control constructs, indicate the occurrence of polyketide biosynthesis.

2.2.3 Expression and purification of CoA ligases and CHS18

Tom-15b plasmids harboring the genes encoding MCS, PCL, or CHS18, and pCRT7/CT-TOPO vector harboring the gene encoding BZL were transformed individually into *E. coli* BL21(DE3) strain for expression. The pCRT7/CT-TOPO plasmid harboring the gene encoding 4CL was transformed into *E. coli* Rosetta II (DE3) strain for expression. The transformed host cells were grown in LB at 25°C, supplemented with either 100 µg/mL ampicillin (for BL21 (DE3) strains) or 34 µg/mL chloramphenicol and 100 µg/mL ampicillin (for Rosetta II (DE3) strain). When OD_{600nm} reached 0.6, protein expression was induced by 0.1 mM IPTG for 16 h. The cells were subsequently harvested by centrifugation and stored at -20°C.

To purify these enzymes, the cell pellets were resuspended in a binding buffer containing 20 mM Tris-HCl (pH 7.9), 500 mM NaCl, and 5 mM imidazole. The cells were subsequently lysed by sonication, and the cell lysate was centrifuged at 21,000 rpm for 20 min. The supernatant containing His-tagged proteins was passed through a column of chelating Sepharose resin (GE Healthcare Bio-Sciences Corp) charged with Ni²⁺. The column was washed with five column volumes (CV) of binding buffer, followed by five CV of wash buffer containing 20 mM Tris-HCl (pH 7.9), 500 mM NaCl, and 107 mM imidazole. After that, the enzymes were eluted with buffer containing 20 mM Tris-HCl (pH 7.9), 500 mM NaCl, and 100 mM L-histidine. Fractions containing the recombinant proteins were pooled together and dialyzed against

a storage buffer containing 20 mM Tris-HCl (pH 7.9) and 100 mM NaCl. The solutions containing the purified enzymes were concentrated to around 10 – 30 mg/mL using 10 kDa Amicon Ultra centrifugal filter units (Millipore), and stored in aliquots at -80°C.

2.2.4 *In vitro* precursor-directed combinatorial biosynthesis of polyketides and HPLC analysis

In order to obtain a higher yield of polyketides for subsequent mass spectrometry (MS) and nuclear magnetic resonance (NMR) analyses, *in vitro* precursor-directed combinatorial biosynthesis of polyketides was conducted. Initial biosyntheses of the starter and extender CoA thioesters were carried out in 1 mL reaction mixtures containing 100 mM Tris-HCL (pH 8.0), 10 mM MgCl₂, 10 mM 5'-Adenosine Triphosphate (ATP), 0.5 mM CoA, 2.5 mM starter acid, 5 mM extender acid, 2 mg/mL 4CL / PCL / BZL, and 2 mg/mL MCS or PCL. After incubation for 6 h at 25°C, additional cofactors, CoA ligases, and 2 mg/mL CHS18 were added to give a final reaction volume of 2 mL, containing 100 mM Tris (pH 8.0), 10 mM MgCl₂, <10 mM ATP, <0.5 mM CoA, <2.5 mM starter acid, <5 mM extender acid, <0.5 mM starter CoA, <0.5 mM extender CoA, 2 mg/mL 4CL / PCL / BZL, 2 mg/mL MCS or PCL, and 2 mg/mL CHS18. This ensures that there are adequate amounts of ATP, CoA, and ligases for the reactions to be completed. Due to the presence of a CoA regeneration system involving CoA ligases and CHS18, only a low amount of the expensive CoA is needed for the biosynthesis of polyketides to take place. An aliquot of 400 µL of the reaction mixture was immediately pipetted out and centrifuged at 4°C through Amicon Ultra 10kDa Ultracel

membranes (Millipore) to remove all enzymes from the mixture. The filtrate (representing time = 0 h) was collected and stored at -80°C until HPLC analysis. The remaining 1.6 mL reaction mixture was then incubated at 25°C for another 20 h. Subsequently, enzymes were removed via centrifugation through Ultracel membranes, and the filtrate (representing time = 20 h) was collected and stored at -80°C until HPLC analysis.

In order to purify the novel polyketide products from the reaction mixture, HPLC analysis was conducted as in section 2.2.2, with minimal changes. The Atlantis Prep C18 reverse-phase column (Waters) was used instead, and first equilibrated with 10% acetonitrile, 0.1% TFA in water at a flow rate of 5 mL/min for 15 min. Up to 800 µL of sample was loaded and the column was washed with 10% acetonitrile, 0.1% TFA in water at a flow rate of 5 mL/min for 4 min. The novel polyketides were eluted with a linear gradient from 10% acetonitrile, 0.1% TFA in water to 50% acetonitrile, 0.1% TFA in water over a period of 40 min at a flow rate of 5 mL/min. For the next 5 min, a linear gradient to 100% acetonitrile containing 0.1% TFA was conducted. Eluted compounds were detected by measuring the absorbance at 230 nm, 280 nm, and 320 nm. Fractions that were only present in the 20 h time-point samples and absent in the 0 h time-point samples indicate polyketide biosynthesis, and were lyophilized, and sent for MS or NMR analyses. Purified resveratrol fractions were also used for life span assays in *C. elegans*.

2.2.5 Mass spectrometry profiling of novel polyketides

MS analysis was conducted under the assistance of our collaborator, Dr. Manfred Raida, in A/P Markus Wenk's laboratory, National University of

Singapore. HPLC-MS/MS analysis of the purified polyketides was carried out on a QTOF 6550 with iFunnel and turbo ion spray, connected to a UHPLC 1290 (AGILENT, Singapore). The Phenomenex Synergy-Polar C18, 2.1 mm x 50 mm column, with 3 μ m particle size (Phenomenex, US) was first equilibrated with 5% acetonitrile, 0.2% formic acid in water for 1 min at a flow rate of 600 μ L/min. The samples were dissolved in 100 μ L acetonitrile, and 2 μ L was loaded for the analysis. Separation of the polyketides was performed with a gradient from 5% acetonitrile, 0.2% formic acid in water to 90% acetonitrile, 0.2% formic acid in water over 5 min. 90% acetonitrile, 0.2% formic acid in water was then maintained for another 1 min, with the column temperature set at 40°C throughout the run. The mass spectrometer was set to a MS scan range from 100 to 1400 m/z at 1 scan/sec, and the three most intense precursor ions were selected for fragmentation at a fixed collision energy of 35. Electrospray conditions were optimized for the polyketides in previous experiments in their laboratory. Data were recorded with Masshunter Acquisition B6.0 (AGILENT) and analyzed with Masshunter Qualitative Analysis software version 6 (AGILENT). After MS detection, NMR analyses of selected compounds were carried out by the Nuclear Magnetic Resonance Laboratory (Department of Chemistry, National University of Singapore).

2.2.6 Life span assays using resveratrol or novel polyketides

C. elegans were maintained as in Stiernagle (2006) with slight changes. Various concentrations (5 μ M, 20 μ M, 40 μ M, or 50 μ M) of resveratrol (TCI Co.) or DMSO (as a control) were incorporated into 5 cm nematode growth medium (NGM) agar plates by another lab member to ensure blinding of the

assays. NGM plates used for life span assays also contained 90 μ M 5-fluoro-2'-deoxyuridine (FUdR) (Sigma-Aldrich Co.) which is an inhibitor of thymidylate synthase. Hence, DNA synthesis is inhibited and this prevents cell division, growth, and hatching of young *C. elegans* which can complicate results analyses (Mitchell *et al.*, 1979). Adult worms on the other hand, are not affected by FUdR treatment as all adults do not undergo any further cell division after reaching the 959-cell stage. Cultures of *E. coli* OP50 strain (obtained from Dr. Takao Inoue, Department of Biochemistry, National University of Singapore) were grown in LB overnight at 25°C, and concentrated 10-fold by centrifugation and resuspension in a smaller volume of LB. OP50 was then spotted onto these NGM agar plates as the food source for *C. elegans*, and allowed to dry overnight at room temperature. Wild-type *C. elegans* N2 strain (obtained from Dr. Takao Inoue) were cultured at 20°C on the various NGM agar plates containing a lawn of *E. coli* OP50.

Age-synchronized wild-type N2 worms were acquired by first placing adult worms on NGM agar plates without FUdR, and allowing them to lay eggs for 4 h. Hypochlorite treatment (Stiernagle, 2006) was utilized to kill and remove adult worms, and eggs were obtained by centrifugation. Eggs were washed thrice with autoclaved water, transferred onto NGM plates without FUdR, and allowed to hatch and grow to adults at 20°C. A total of 20 – 25 age-synchronized adult N2 worms were transferred randomly to each treatment plate, to begin the life span assay (third day after hatching is equivalent to day one of adult life span at 20°C). Worms were transferred to a fresh treatment plate every day using a sterile platinum wire, for the first week of the life span assay to replenish food supply and avoid complications from

progeny. Additional *E. coli* OP50 was supplemented to the treatment plates at day 12 as worms could be too old to be transferred manually. Worms were scored daily, and scored as dead if no response was observed when they were gently prodded with a platinum wire. *C. elegans* that were lost due to crawling on the walls of the agar plates were omitted from analysis. Survival analysis was conducted using the log rank test in the IBM SPSS Statistics 22 program.

For life span assays using novel polyketides, selected combinations of 0.5 mM starter acids and 1 mM extender acids together with 90 μ M FUdR, 34 μ g/mL chloramphenicol, 100 μ g/mL ampicillin, 30 μ g/mL kanamycin, and 0.1 mM IPTG were incorporated into NGM agar plates. The corresponding CoA ligases + CHS18 *E. coli* constructs, and constructs without CHS18 were grown in LB with antibiotics overnight at 25°C by another lab member to ensure blinding of the life span studies. Protein expression was induced by 0.1 mM IPTG for 3 h at 25°C, and 0.5 mM starter acids and 1 mM extender acids were subsequently introduced to the media. After incubation at 25°C for another 3 h, the *E. coli* culture was concentrated 20-fold as above, seeded onto the respective NGM plates, and allowed to dry overnight at room temperature as the food source which can expose *C. elegans* to the biosynthesized novel polyketides concurrently. The life spans of wild-type N2 *C. elegans* exposed to the CoA thioesters and novel polyketides were compared to the life spans of N2 worms exposed to CoA thioesters only, using the log rank test.

2.3 Results and discussion

2.3.1 Establishing a combinatorial biosynthetic route in *Escherichia coli*

Since most starter and extender CoA thioesters are either too expensive to obtain, or not commercially available, the biosynthesis of CoA thioesters had to be coupled to the PKS, CHS18, in order to generate polyketides. This mutant chalcone synthase (CHS18) was cloned into *E. coli*, together with 4CL from *N. tabacum* and MCS from *R. trifolii*. A control *E. coli* construct containing 4CL, MCS, and an empty Tom-15b vector was also constructed. The CoA ligases had previously been shown to catalyze the biosynthesis of CoA thioesters from their respective carboxylic acid precursors (Go *et al.*, 2012). By supplying *p*-coumaric acid and malonic acid to the *E. coli* constructs, *p*-coumaroyl-CoA and malonyl-CoA were synthesized by 4CL and MCS respectively. CHS18 was validated to have resveratrol synthase activity when incubated with the biosynthesized *p*-coumaroyl-CoA and malonyl-CoA (Figure 2.2). The resveratrol generated by CHS18 was verified to have an experimental mass of 227.0712 in the negative MS mode (theoretical mass of 228.25) (Figure 2.3), and NMR analysis further established the identity of the compound (Figure 2.4). Several minor HPLC peaks were also observed at R_t of 24.4 min, 33.8 min, 35.0 min, and 40.4 min, indicating the potential biosynthesis of bisnoryangonin, CTAL, naringenin, and other polyketides with a different number of extension step or an alternate intramolecular cyclization mode as minor products. This allowed us to set up the platform for precursor-directed combinatorial biosynthesis, which requires the utilization of different combinations of acyl-CoA derivatives for the generation of novel polyketides.

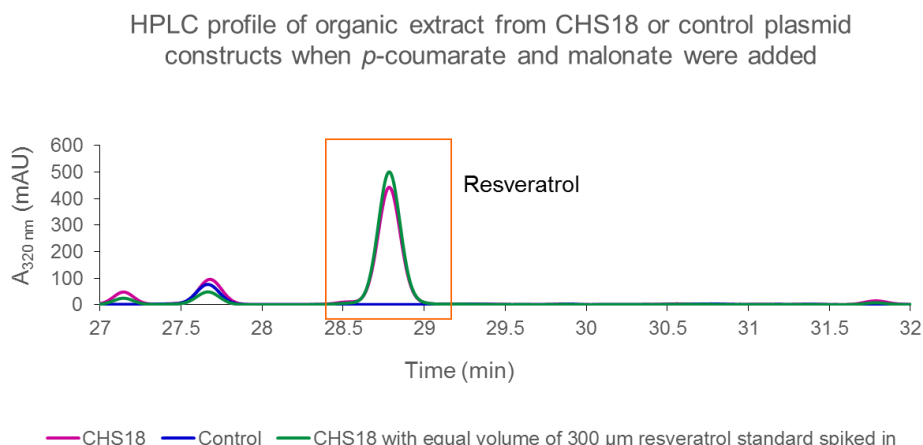


Figure 2.2: Malonic acid and *p*-coumaric acid were supplemented to the *E. coli* constructs. Biosynthesized products in spent minimal medium containing either *E. coli* with CoA ligases + CHS18 or *E. coli* with CoA ligases only (control construct) were extracted and subjected to HPLC analysis using an Atlantis Analytical C18 reverse-phase column. An additional peak corresponding to resveratrol was observed in the extract from the CHS18 construct, but was absent in the extract from the control construct. The retention time (R_t) of the additional peak was found to be identical to the R_t of a commercially available resveratrol standard.

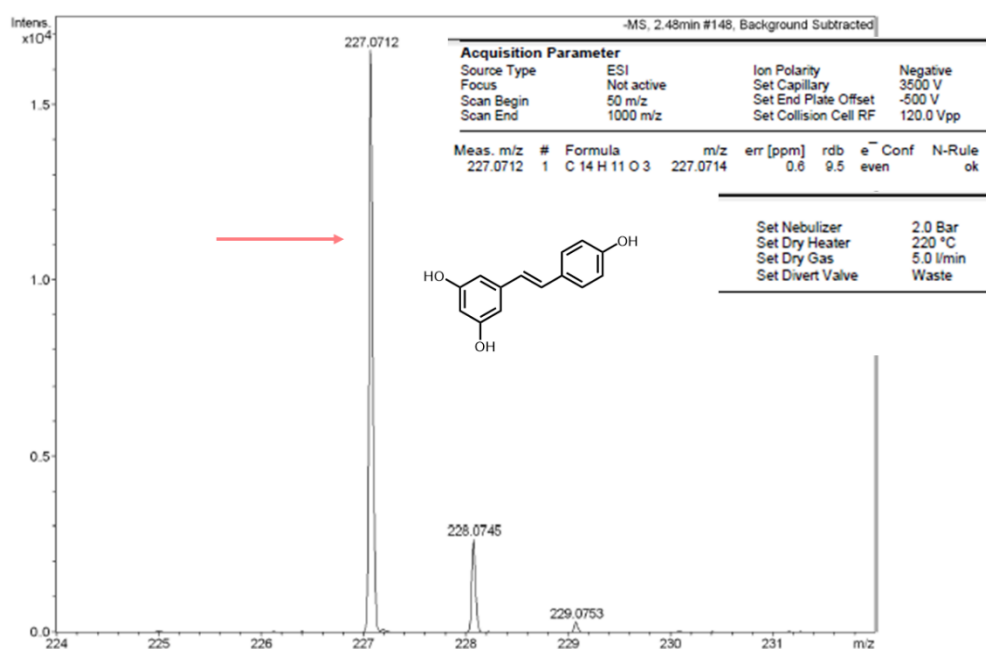


Figure 2.3: MS analysis of purified resveratrol fraction after *in vivo* precursor-directed combinatorial biosynthesis. The mass of the biosynthesized product corresponds to the mass of resveratrol.

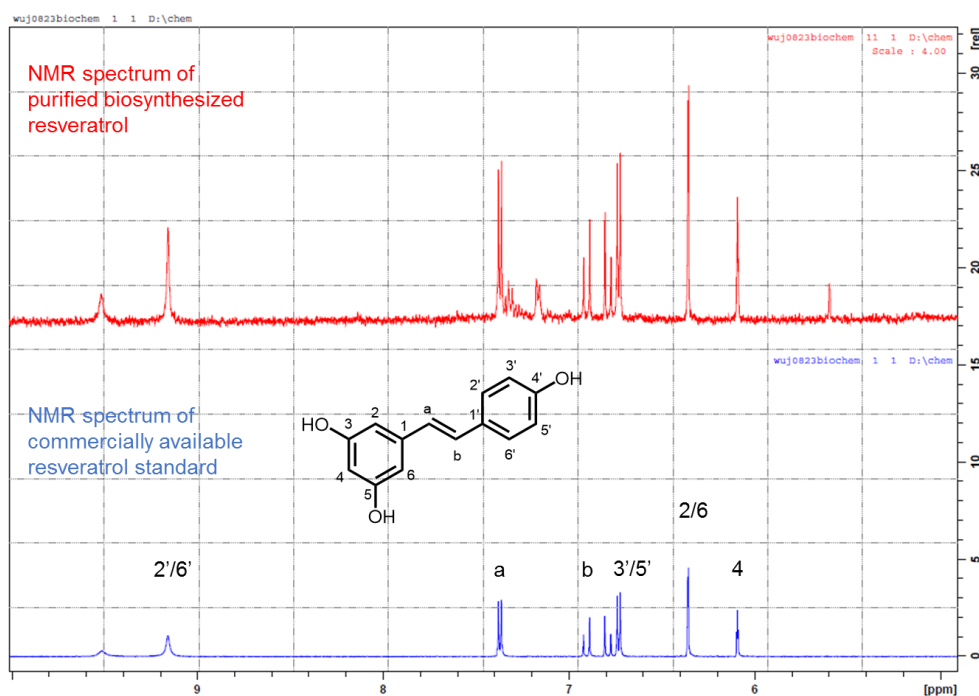


Figure 2.4: Overlay of NMR analyses of purified resveratrol fraction after *in vitro* precursor-directed combinatorial biosynthesis (red), and a commercially available resveratrol standard (blue). Both spectra are quite similar to each other, although there may be a low level of contamination in the purified resveratrol fraction.

Using precursor-directed biosynthesis via different combinations of 69 starter CoA thioesters and 12 extender malonyl-CoA derivatives, the substrate profile of CHS18 was established (Table 2.1), and a catalog of polyketides was obtained. CHS18 was found to be promiscuous in substrate utilization, consistent with previously characterized alfalfa CHS (Jez *et al.*, 2002). CHS18 was able to utilize unnatural starter and extender CoA thioesters as substrates for polyketide synthesis (Figure 2.5 and Figures A1 to A5), thus highlighting the feasibility of precursor-directed combinatorial biosynthesis of polyketides. From the matrix of substrates used, at least 413 novel polyketides were generated. Differences in the production yield of the novel polyketides suggested that both the CoA ligases and CHS18 have particular substrate preferences.

Table 2.1: Substrate profile of CHS18 using 69 starter CoA thioesters and 12 extender CoA thioesters. 413 out of 828 possible combinations (49.9%) gave rise to new polyketides.

Extender used	Malonyl-CoA	Methyl malonyl-CoA	Ethyl malonyl-CoA	Isopropyl malonyl-CoA	Butyl malonyl-CoA	Allyl malonyl-CoA
Successful combinations (for the 69 starters tested)	35	33	39	21	27	24

Extender used	Hydroxy malonyl-CoA	Fluoro malonyl-CoA	Chloro malonyl-CoA	Bromo malonyl-CoA	Phenyl malonyl-CoA	3-Thiophene malonyl-CoA
Successful combinations (for the 69 starters tested)	28	44	41	27	44	50

HPLC profile of CHS18 and control extracts when 2-fluorocinnamate and butylmalonate were added

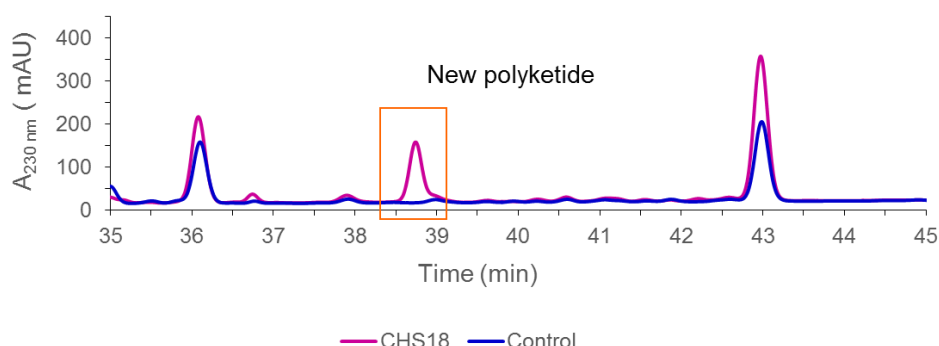


Figure 2.5: Biosynthesized products in spent minimal medium containing either *E. coli* with CoA ligases + CHS18 or *E. coli* with CoA ligases only (control construct) were extracted and subjected to HPLC analysis using an Atlantis Analytical C18 reverse-phase column. An additional peak at R_t 38.7 min was observed in the extract from the CHS18 construct, but was not present in the extract from the control construct, indicating that a new polyketide was biosynthesized when 2-fluorocinnamyl-CoA and butylmalonyl-CoA were supplemented to CHS18.

The finding that CHS18, together with most type III PKSs, is highly promiscuous is quite predictable, given the involvement of these enzymes in the generation of secondary metabolites in plants. Some of these metabolites can serve as anti-microbial agents, providing the plants with protection against harmful microorganisms in the environment (Staunton and Weissman, 2001). Others serve as antioxidants, providing another line of defence against threats in plants. Hence, it is possible that the promiscuity associated with these enzymes will enable the plants to respond quickly to any new threat that appears in the environment. This will provide the plant with a survival advantage over other members which only harbor PKSs with limited substrate selectivities.

2.3.2 Starter acyl-CoA substrate preference of CHS18

CHS18 was able to use a number of cinnamyl-CoA (Table A2 in Appendix), phenylpropanoyl-CoA (Table A2 in Appendix), benzoyl-CoA (Table A3 in Appendix), phenylacetyl-CoA (Table A4 in Appendix), bicyclic aromatic CoA (Table A4 in Appendix), and saturated and unsaturated aliphatic CoA thioester derivatives (Table A5 in Appendix), as the starter substrate, in combination with various malonyl-CoA derivatives as the extender substrate (Table 2.1). Interestingly, benzoyl-CoA derivatives were the most preferred starters (65.8% of the combinations led to new products formed), followed by unsaturated aliphatic CoA derivatives (61.7% of the combinations), phenylacetyl-CoA derivatives (51.4% of the combinations), cinnamyl-CoA derivatives (50% of the combinations), saturated aliphatic CoA derivatives (36.5% of the combinations), phenylpropanoyl-CoA derivatives (22.6% of the

combinations), and bicyclic aromatic CoA derivatives (12.5% of the combinations). Nevertheless, when the natural extender malonyl-CoA is used, the most preferred starters still contain a cinnamyl-CoA backbone, whereby 12 out of 14 cinnamyl-CoA derivatives tested were accepted by CHS18 to form novel polyketides. This is in line with the fact that cinnamyl-CoA and *p*-coumaroyl-CoA are natural starter substrates for alfalfa CHS. Hence, it is not surprising that due to structural similarities to the cognate substrate, cinnamyl-CoA derivatives, together with malonyl-CoA, are good substrates for CHS18.

Amongst the cinnamyl-CoA derivatives, *meta*-substituted and *para*-substituted derivatives were most preferred (62.5% and 60.7% of the combinations respectively led to new products formed), compared to *ortho*-substituted (25% of the combinations) and aliphatic chain-substituted (45.8% of the combinations) derivatives. This suggests that the presence of substituents at the *ortho* position may affect the interaction of the starter unit with the active site residues of CHS18, causing *ortho*-substituted cinnamyl-CoA derivatives to be accepted less efficiently. This is consistent with previous work on alfalfa CHS by Jez and co-workers, which reported that the catalytic efficiency of alfalfa CHS is lower when 2-hydroxycinnamyl-CoA is used, compared to 3-hydroxycinnamyl-CoA and 4-hydroxycinnamyl-CoA (Jez *et al.*, 2002). Interestingly, 2-hydroxyphenylacetyl-CoA (reacted with four out of twelve extenders) was also less readily accepted by CHS18 compared to 4-hydroxyphenylacetyl-CoA (reacted with eight out of twelve extenders), which is structurally similar to, but shorter than *p*-coumaroyl-CoA by a carbon unit.

Among the *para*-substituted cinnamyl-CoA derivatives, the OH and CH₃O substituent groups were most preferred (83.3% of the combinations led to new

products formed), followed by F (58.3% of the combinations), CH₃ (25% of the combinations), and Cl (16.7% of the combinations) substituent groups. This suggests that even though *para*-substituted cinnamyl-CoA derivatives are structurally similar to the natural substrate, the type of substituent in the *para* position can affect the catalytic efficiency of CHS18. The presence of the Cl substituent in the *para* position of cinnamyl-CoA derivatives was the least preferred, probably due to huge steric effects which hindered the formation of polyketide intermediates in the active site of CHS18.

When substituent groups are present on the extender acyl-CoA substrate, cinnamyl-CoA derivatives are no longer strongly preferred. Instead, smaller and more flexible starters like benzoyl-CoA derivatives and unsaturated aliphatic CoA derivatives are more easily accepted by CHS18, together with unnatural malonyl-CoA derivatives to form unique polyketides (Figure 2.6). Most benzoyl-CoA derivatives were utilized as starters, regardless of the position of the substituent groups (*ortho* position: 63.9% of the combinations led to new products formed, *meta* position: 62.5% of the combinations, *para* position: 58.3% of the combinations), suggesting that the benzoyl-CoA backbone is small enough to participate in reactions with bulky extenders. As for unsaturated aliphatic CoA derivatives, smaller starters with a butenoyl-CoA backbone were most preferred (70.8% of the combinations led to new products formed), followed by those with a pentenoyl-CoA backbone (62.5% of the combinations), and those with a hexenoyl-CoA backbone (41.7% of the combinations). This is consistent with previous studies on *S. baicalensis* CHS, which proposed that the more bulky starter substrates contributed to

unfavorable steric effects when additional substituent groups were present in the extender acyl-CoA used (Abe *et al.*, 2003).

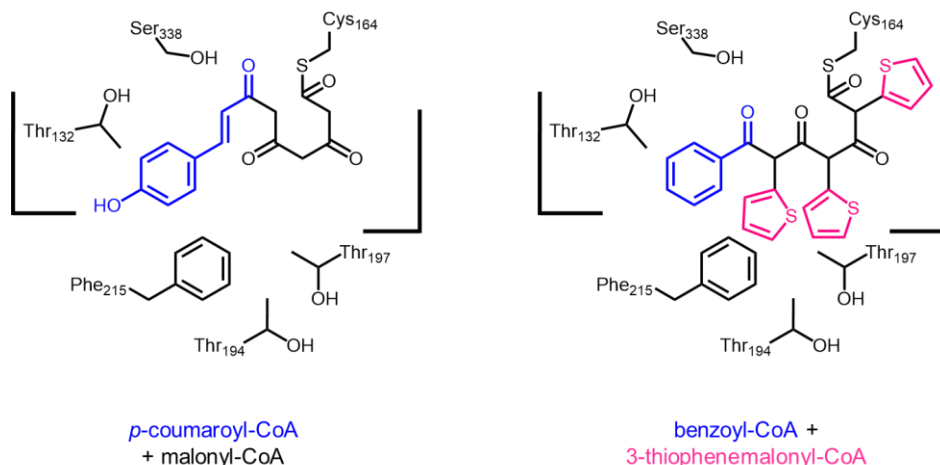


Figure 2.6: Unfavorable steric effects due to bulky extenders like 3-thiophenemalonoyl-CoA (substituent group highlighted in pink) resulted in a strong preference for smaller starters like benzoyl-CoA instead of the larger cinnamyl-CoA derivatives (starters which formed part of the linear polyketide intermediate are highlighted in blue). Hence, the active site cavity of CHS18 can accommodate benzoyl-CoA derivatives more easily than cinnamyl-CoA derivatives, or other more bulky starters.

Surprisingly, other than derivatives of the cognate substrates, CHS18 could utilize chemically distinct starter acyl-CoAs beyond its canonical substrate pool. In particular, it was shown for the first time that CHS18 could accept bicyclic aromatic CoA thioesters together with malonyl-CoA derivatives to form novel polyketides (6 out of 48 combinations led to new products formed). This substrate promiscuity could be attributed to substrate mimicry, illustrating how a slight substrate resemblance to the cognate substrates can play a role in starter unit recognition in CHS18 and subsequently, the biosynthesis of novel polyketides (Figure 2.7).

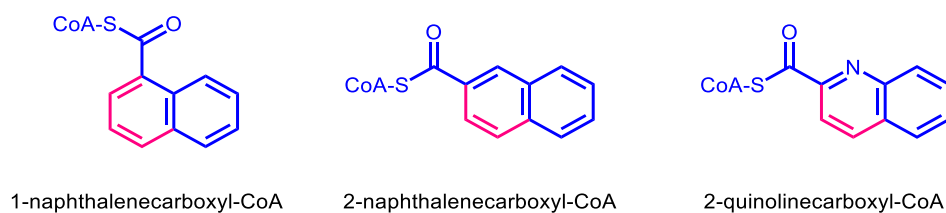


Figure 2.7: Structural mimicry of bicyclic aromatic CoA thioesters. The mimicry to phenylacetyl-CoA (for 1-naphthalenecarboxyl-CoA) and cinnamyl-CoA (for 2-naphthalenecarboxyl-CoA and 2-quinolinecarboxyl-CoA) are highlighted in blue.

2.3.3 Extender acyl-CoA substrate preference of CHS18

The repertoire of novel polyketides biosynthesized from the 69 x 12 assays also provided insights into the extender substrate preference of CHS18. By collating the number of starter acyl-CoAs that reacted with each extender substrate (Table 2.1), the order of preference for extender acyl-CoA substrates for CHS18 was discerned: 3-thiophenemalonyl-CoA > phenylmalonyl-CoA = fluoromalonyl-CoA > chloromalonyl-CoA > ethylmalonyl-CoA > malonyl-CoA > methylmalonyl-CoA > hydroxymalonyl-CoA > butylmalonyl-CoA = bromomalonyl-CoA > allylmalonyl-CoA > isopropylmalonyl-CoA. It was likely that the extender substrate preference of CHS18 was dependent on the stability of the carbanion intermediate generated during catalysis.

When the extender acyl-CoA enters the active site of CHS18, it is decarboxylated to form a carbanion intermediate which can attack the starter unit or elongating polyketide bound to the catalytic cysteine residue in the active site. This carbanion intermediate is stabilized by resonance effect in all the malonyl-CoA derivatives, aided by the nearby His303 and Asn336 residues (numbering in alfalfa CHS) (Figure 2.8). Certain substituent groups in the malonyl-CoA derivatives can affect the degree of stabilization of the

carbanion intermediate. For instance, 3-thiophenemalonyl-CoA and phenylmalonyl-CoA were strongly preferred compared to the other extender substrates (Table 2.1), perhaps due to the presence of the aromatic ring which can confer additional stability via resonance effect (Figure 2.9). Amongst the halogen-substituted malonyl-CoA derivatives, the fluoro-substituted malonyl-CoA derivative has the greatest inductive effect due to the high electronegativity of the fluorine atom. Thus, the carbanion intermediate is greatly stabilized and fluoromalonyl-CoA is the preferred extender, compared to chloromalonyl-CoA and bromomalonyl-CoA.

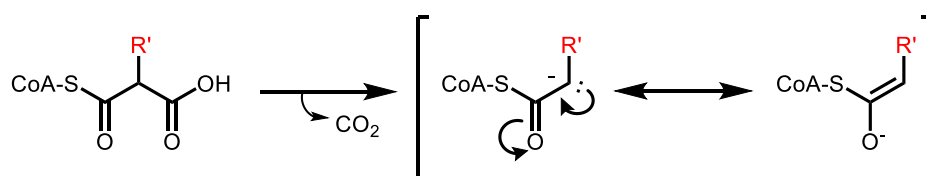


Figure 2.8: Stabilization of the carbanion intermediate after decarboxylation of the extender acyl-CoA.

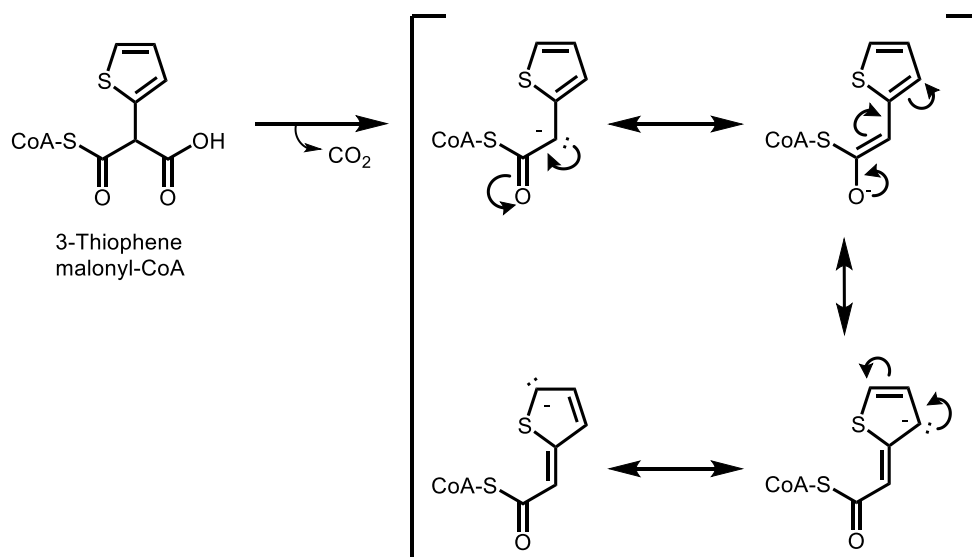


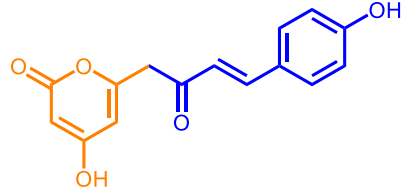
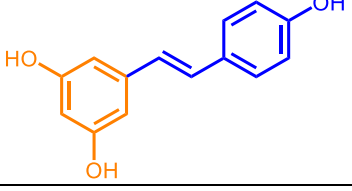
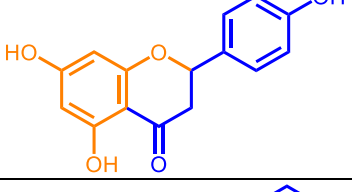
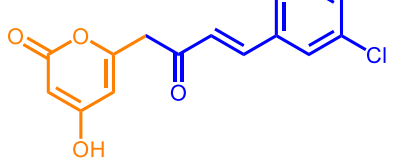
Figure 2.9: Resonance structures depicting the stabilization of the carbanion of 3-thiophenemalonyl-CoA after decarboxylation.

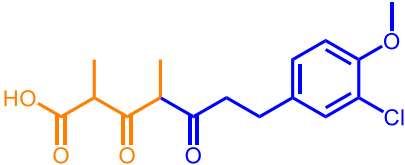
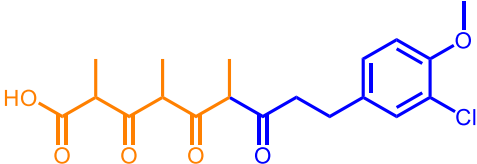
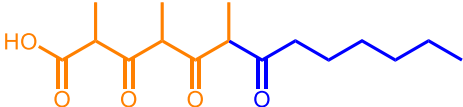
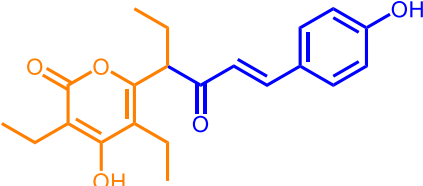
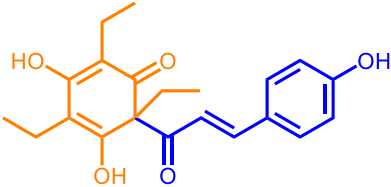
Compared to the aromatic malonyl-CoA derivatives, the aliphatic derivatives such as malonyl-CoA, methylmalonyl-CoA, ethylmalonyl-CoA, isopropylmalonyl-CoA, butylmalonyl-CoA, and allylmalonyl-CoA generated a smaller range of novel polyketides, each with 21 – 39 starters out of the 69 starter substrates tested. However, the order of preference did not display a significant trend. All in all, by determining the substrate preference of CHS18, a library of novel polyketides with potential anti-aging activities could be biosynthesized.

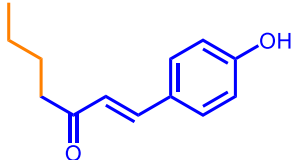
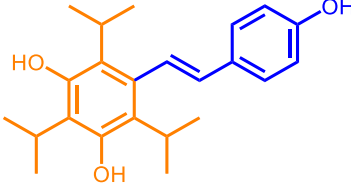
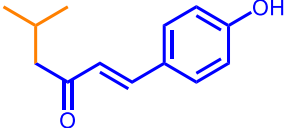
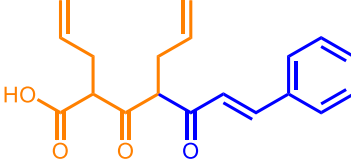
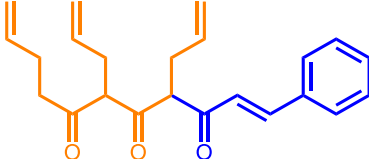
2.3.4 Mass spectrometry profiling of novel polyketides

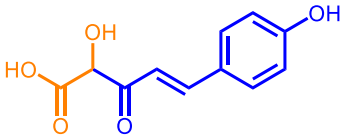
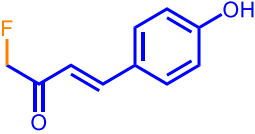
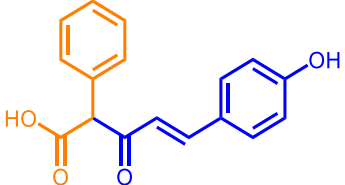
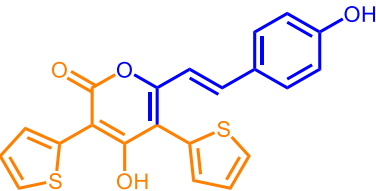
The substrate profile of CHS18 can be confirmed by determining the mass of the polyketide products using MS. Selected combinations of starters and extenders were used to generate polyketides *in vitro*, which were then purified by HPLC and sent for MS analysis. Most of the masses of the selected polyketides identified in this study matched their corresponding expected masses, and the potential chemical structures of the compounds were proposed (Table 2.2). Nevertheless, the exact identities of these products are not known as NMR analyses are needed. In some cases, cyclization of the polyketide intermediate may not occur at all, and the active site cysteine-bound intermediate hydrolyzes to form the corresponding acid, which may undergo decarboxylation to form a novel polyketide (Figure 2.10). In other cases, some of these polyketides could be truncation side products generated from the CHS18 reaction which include polyketides with fewer polyketide extension steps, or those that are biosynthesized through a lactonization, aldol or Claisen condensation of the linear polyketide intermediate (Figure 2.11).

Table 2.2: Potential polyketides biosynthesized by CHS18. HPLC retention times are based on analyses conducted using the Atlantis Prep C18 reverse-phase column. The part of the polyketide derived from the starter unit is highlighted in blue.

Combination of starter and extender	HPLC R_t (min)	Experimental mass [theoretical mass]	Chemical formula	Number of extender units added	Potential structure	Mode of Cyclization
<i>p</i> -coumaric acid + malonic acid	29.5	272.08 [272.25]	$C_{15}H_{12}O_5$	3		Lactonization
	33.7	228.06 [228.24]	$C_{14}H_{12}O_3$	3		Aldol
	40.9	272.05 [272.25]	$C_{15}H_{12}O_5$	3		Claisen
3-chlorocinnamic acid + malonic acid	27.3	290.00 [290.70]	$C_{15}H_{11}ClO_4$	3		Lactonization

Combination of starter and extender	HPLC R_t (min)	Experimental mass [theoretical mass]	Chemical formula	Number of extender units added	Potential structure	Mode of Cyclization
3-(3'-chloro-4'-methoxy)phenylpropanoic acid + methylmalonic acid	13.2	326.10 [326.77]	$C_{16}H_{19}ClO_5$	2		None
	26.8	382.12 [382.83]	$C_{19}H_{23}ClO_6$	3		None
Heptanoic acid + methylmalonic acid	42.0	298.22 [298.37]	$C_{16}H_{26}O_5$	3		None
<i>p</i> -coumaric acid + ethylmalonic acid	34.5	356.17 [356.41]	$C_{21}H_{24}O_5$	3		Lactonization
	45.2	356.17 [356.41]	$C_{21}H_{24}O_5$	3		Claisen

Combination of starter and extender	HPLC R_t (min)	Experimental mass [theoretical mass]	Chemical formula	Number of extender units added	Potential structure	Mode of Cyclization
<i>p</i> -coumaric acid + butylmalonic acid	44.7	218.07 [218.29]	$C_{14}H_{18}O_2$	1		Decarboxylation
<i>p</i> -coumaric acid + isopropylmalonic acid	29.2	354.22 [354.48]	$C_{23}H_{30}O_3$	3		Aldol
	33.0	204.05 [204.26]	$C_{13}H_{16}O_2$	1		Decarboxylation
Cinnamic acid + allylmalonic acid	19.0	312.24 [312.36]	$C_{19}H_{20}O_4$	2		None
	47.6	350.14 [350.45]	$C_{23}H_{26}O_3$	3		Decarboxylation

Combination of starter and extender	HPLC R_t (min)	Experimental mass [theoretical mass]	Chemical formula	Number of extender units added	Potential structure	Mode of Cyclization
<i>p</i> -coumaric acid + hydroxymalonic acid	45.1	222.06 [222.19]	$C_{11}H_{10}O_5$	1		None
<i>p</i> -coumaric acid + fluoromalonic acid	29.6	180.06 [180.18]	$C_{10}H_9FO_2$	1		Decarboxylation
<i>p</i> -coumaric acid + phenylmalonic acid	45.0	282.12 [282.29]	$C_{17}H_{14}O_4$	1		None
<i>p</i> -coumaric acid + 3-thiophenemalonic acid	45.0	394.04 [394.46]	$C_{21}H_{14}S_2O_4$	2		Lactonization

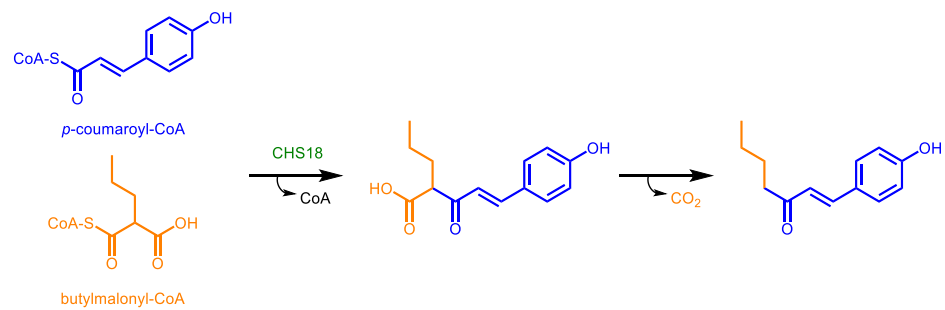


Figure 2.10: Potential polyketide formed from one unit of *p*-coumaroyl-CoA and butylmalonyl-CoA without cyclization occurring.

Figure 2.11: Novel polyketides formed via (A) lactonization, (B) Claisen condensation, (C) aldol condensation. The enol tautomer is the more stable form.

As indicated in Table 2.2, most of the new products formed did not cyclize, while lactonization was the preferred mode in those polyketides that completed cyclization. This was indicative of the ability of CHS18 to elongate the polyketide chain, but not perform cyclization in all cases. This is probably due to the unfavorable positioning of certain residues of the linear polyketide intermediate in the active site due to steric effects, hence aldol condensation could not be achieved. Indeed, when the peanut STS was incubated with other *p*-substituted cinnamyl-CoA analogues (-Cl, -Br, and -OCH₃), only triketide and tetraketide pyrones were obtained, indicating that truncation products are common and lactonization had occurred instead of an aldol condensation (Morita *et al.*, 2001). This suggested potential steric effects by substituents that are larger than that of the wild-type substrate (-OH in *p*-coumaroyl-CoA and -H in malonyl-CoA), which affected the stability and/or the conformation of polyketide intermediates in the cyclization pocket of the active site. However, as the 12 reactions were only a small subset of the 413 combinations which gave rise to new products, it is possible that cyclization may occur with other starter and extender combinations.

Many of the starter and extender substrates used in this research study have not been explored in the previous studies, and the product library biosynthesized is expected to comprise of novel polyketides with chalcone, stilbene, and lactone scaffolds. It has been shown that MS analysis provides an idea of the identity of the new products from precursor-directed combinatorial biosynthesis. These polyketides can then be further characterized by NMR to determine their chemical structure and properties. By obtaining a profile of

novel polyketides, the compound library can subsequently be applied to drug screening efforts, such as the development of anti-aging therapeutics.

2.3.5 Life span assays using resveratrol or novel polyketides

Studies on resveratrol have found that it is a potential CR mimetic (Chung *et al.*, 2012). By varying the dose of a commercially available resveratrol standard used for life span assays on wild-type N2 *C. elegans*, a significant life span extension was observed in worms exposed to 40 μ M and 50 μ M commercially available resveratrol when compared to controls fed with DMSO (Figure 2.12). In an attempt to validate the utility of our CHS18 combinatorial biosynthetic system, 50 μ M of biosynthesized resveratrol was purified and introduced to wild-type N2 *C. elegans*, and a significant life span extension was also observed when compared to controls fed with DMSO (Figure 2.13). However, the amount of increase in life span was not as large as when 50 μ M commercially available resveratrol was used. Hence this suggests that the biosynthesized resveratrol preparation could be slightly impure, and that the final concentration was over-estimated.

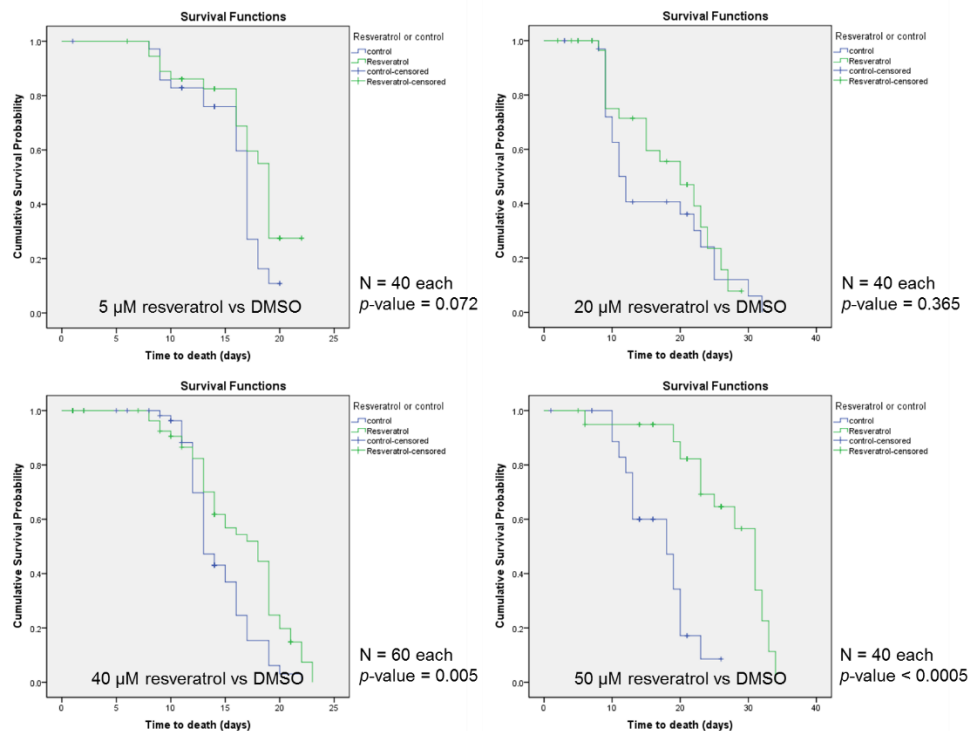


Figure 2.12: Survival plots of N2 *C. elegans* fed with 5 μ M, 20 μ M, 40 μ M, or 50 μ M commercially available resveratrol (green) or DMSO (blue). Worms exposed to 50 μ M resveratrol had a significantly longer mean life span (27.4 days) compared to the control (17.1 days). The p -values were calculated using log rank test, and a p -value < 0.05 is considered to be statistically significant.

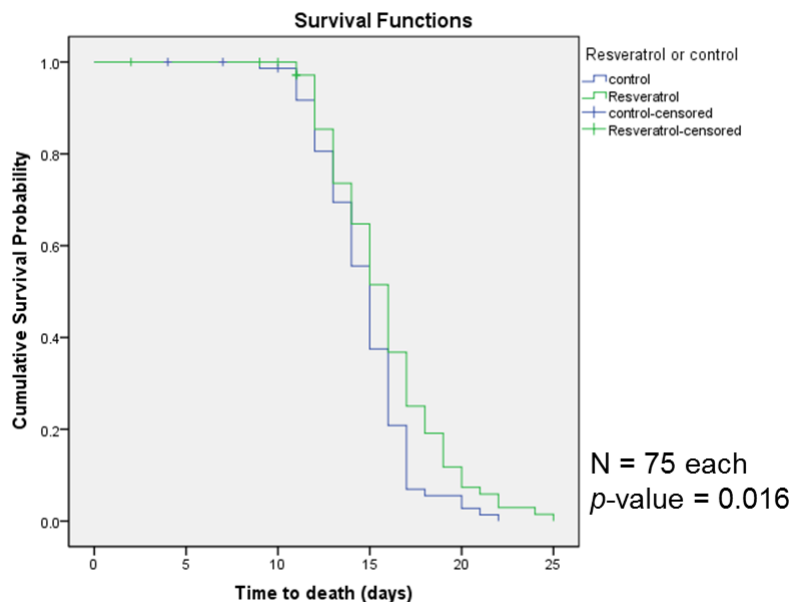


Figure 2.13: Survival plots of N2 *C. elegans* fed with either 50 μ M purified biosynthesized resveratrol (green) or DMSO (blue). The 'resveratrol' population had a significantly longer mean life span (15.9 days) compared to the control (14.8 days).

After establishing the substrate profile of CHS18, the polyketide-producing CHS18 strain (containing 4CL, MCS and CHS18) and the control *E. coli* strain (containing 4CL and MCS only) were fed to wild-type N2 *C. elegans* separately. Relevant combinations of starter and extender acids were incorporated into NGM agar for the biosynthesis of novel polyketides. 24 of the 413 novel polyketides were tested for anti-aging properties in a *C. elegans* life span assay (Table 2.3). Most of the tested combinations had no significant effects on the wild-type N2 *C. elegans* except for 3-chlorocinnamyl-CoA + malonyl-CoA and 3-(3'-chloro-4'-methoxy)phenylpropanoyl-CoA + methylmalonyl-CoA which had toxic effects and led to a shorter life span compared to the control (Figure 2.14).

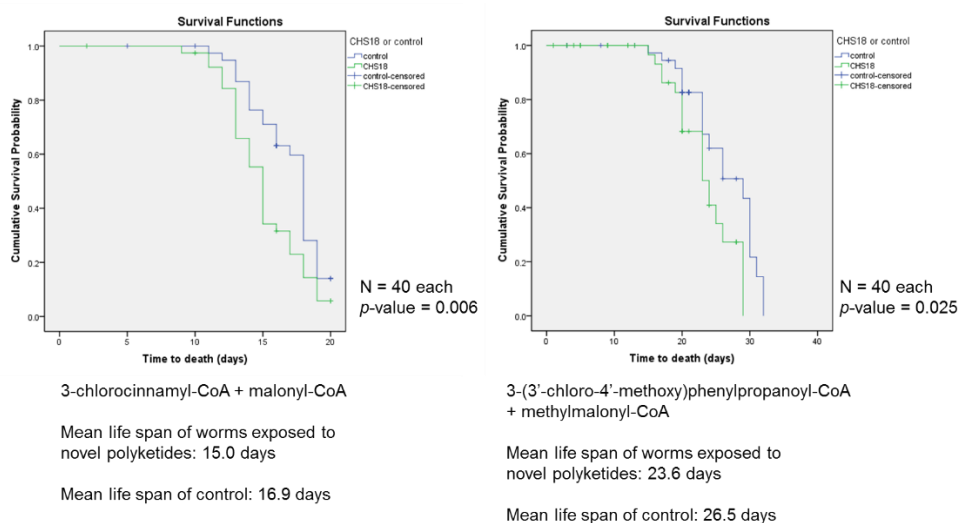


Figure 2.14: Survival plots of N2 *C. elegans* fed with either CHS18 *E. coli* strain (green) or control *E. coli* strain (blue) supplemented with 3-chlorocinnamic acid + malonic acid (left) or 3-(3'-chloro-4'-methoxy)phenylpropanoic acid + methylmalonic acid (right). Worms exposed to the novel polyketides produced from these two combinations of starter and extender acids had a significantly shorter mean life span compared to the control.

Table 2.3: Assessing the anti-aging properties of novel polyketides. A (✓) represents that particular combination was used in the *C. elegans* life span assay. A p -value < 0.05 is considered to be statistically significant. NA: Not applicable.

Starter acyl-CoA	Malonyl-CoA	Effect compared to control	Methylmalonyl-CoA	Effect compared to control
Cinnamyl-CoA	✓	No significant difference	-	NA
2-fluoro cinnamyl-CoA	-	NA	✓	No significant difference
3-fluoro cinnamyl-CoA	✓	No significant difference	✓	No significant difference
4-fluoro cinnamyl-CoA	✓	No significant difference	✓	No significant difference
3-chloro cinnamyl-CoA	✓	Shorter lifespan (p -value = 0.006)	✓	No significant difference
3-chloro-4-methoxycinnamyl-CoA	✓	No significant difference	-	NA
4-chloro cinnamyl-CoA	✓	No significant difference	-	NA
p -coumaroyl-CoA	✓	No significant difference	-	NA
3-methoxy-4-hydroxycinnamyl-CoA	✓	No significant difference	-	NA
4-methoxy cinnamyl-CoA	✓	No significant difference	-	NA
4-methyl cinnamyl-CoA	✓	No significant difference	-	NA
α -methyl cinnamyl-CoA	✓	No significant difference	-	NA
3-phenyl propanoyl-CoA	✓	No significant difference	✓	No significant difference
3-(3'-chloro) phenylpropanoyl-CoA	✓	No significant difference	✓	No significant difference
3-(3'-chloro-4'-methoxy)phenyl propanoyl-CoA	-	NA	✓	Shorter lifespan (p -value = 0.025)
3-(3'-methoxy) phenylpropanoyl-CoA	-	NA	✓	No significant difference
3-(4'-methoxy) phenylpropanoyl-CoA	-	NA	✓	No significant difference
3-(4'-fluoro) phenylpropanoyl-CoA	✓	No significant difference	✓	No significant difference

Interestingly, the mean life spans of the worms treated with the control strain and the respective combinations of carboxylic acids were different. For instance, worms treated with 3-chlorocinnamic acid, malonic acid, and the control *E. coli* construct had a mean life span of 16.9 days while worms treated with 3-(3'-chloro-4'-methoxy)phenylpropanoic acid, methylmalonic acid, and the control *E. coli* construct had a mean life span of 26.5 days. This suggests that the acids used or the CoA esters produced could have some effects on the life span of wild-type *C. elegans*. More studies are needed to verify the biological effects of these compounds.

Although the CHS18 strain can produce resveratrol when supplemented with *p*-coumaric acid and malonic acid, a significant life span extension effect was not observed (Figure 2.15). This is due to the low concentration of resveratrol (approximately 1 μ M) biosynthesized by the *E. coli* constructs growing on the NGM agar plates. Nevertheless, studies have shown that resveratrol is rapidly metabolized when ingested, and it has a broad spectrum of activity in various cellular components such as cyclooxygenases (COX1 and COX2) and norepinephrine transporters (Cottart *et al.*, 2010; Chung *et al.*, 2012) in addition to AMPK and sirtuins. Hence, issues of bioavailability and adverse effects warrant the need to look for other potential CR mimetics that are more potent than resveratrol. Even though the concentration of novel polyketides being biosynthesized is low, we hope to identify anti-aging compounds that can work well even at low doses.

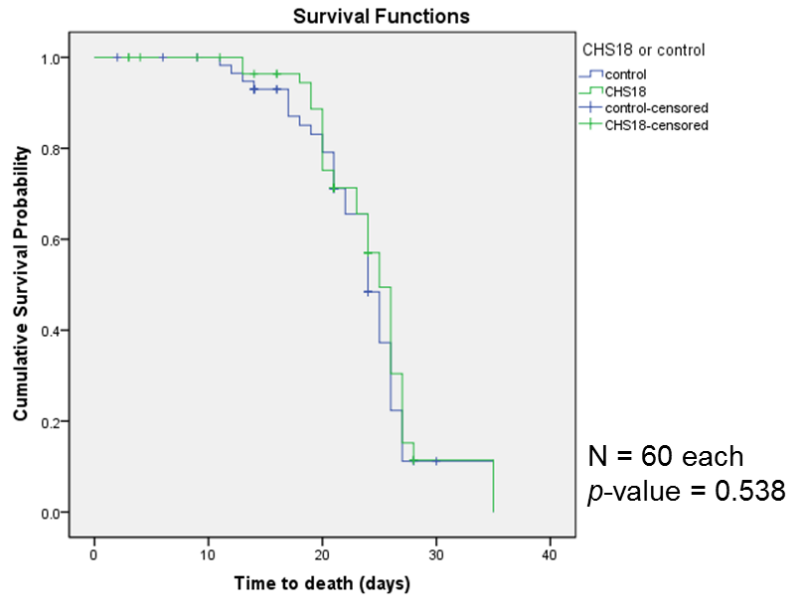


Figure 2.15: Survival plots of N2 *C. elegans* fed with either CHS18 *E. coli* strain (green) or control *E. coli* strain (blue) supplemented with *p*-coumaric acid and malonic acid. There was no significant difference in the mean life span between the two populations, due to the low concentration of resveratrol being synthesized by the *E. coli* constructs.

Despite the utility of life span assays, they are rather time-consuming as the average life span of wild-type *C. elegans* is approximately three weeks at 20°C. Hence, there is a need to develop a higher throughput method to screen our library of compounds for anti-aging properties. Since CR is known to promote longevity by modulating oxidative metabolism (Schulz *et al.*, 2007), it would be interesting to look at the mitochondrial activity of *C. elegans* when they are exposed to potential CR mimetics. By developing mitochondrial function assays, we can screen for anti-aging compounds more efficiently, and this will be further elaborated in Chapter 4 of this thesis.

CHAPTER 3: TOWARDS THE DEVELOPMENT OF NOVEL ANTI-AGING ALKALOIDS USING PRECURSOR-DIRECTED COMBINATORIAL BIOSYNTHESIS

3.1 Introduction

Alkaloids are the most structurally diverse secondary metabolites, providing an untapped potential for the creation of a bioactive compound library for anti-aging therapeutic development. Several studies have demonstrated the feasibility of performing precursor-directed combinatorial biosynthesis using promiscuous type III PKSs to generate novel alkaloids. A type III PKS from the club moss *Huperzia serrata* was found to be able to accept a broad range of starter substrates, including *N*-methylantraniloyl-CoA, and synthetic nitrogen-containing starter units like 2-carbamoylbenzoyl-CoA, to generate novel alkaloids with malonyl-CoA as the extender (Morita *et al.*, 2011). Similarly, CHS18 was able to utilize nitrogen-containing starter units such as 3-aminobenzoyl-CoA, 4-aminobenzoyl-CoA, and 2-quinolinecarboxyl-CoA to generate alkaloid products (Tables A3 and A4 in Appendix). Hence, this highlights an unconventional and simpler method to generate alkaloids by repurposing type III PKSs for alkaloid biosynthesis.

Since the diversity of the alkaloids biosynthesized by PKSs is partly dependent on the starter and extender units, variations in the choice of starters and extenders is important. However, there has been a lack of a toolkit that describes the means to introduce novel nitrogen-containing acyl-CoA precursors to PKSs for alkaloid biosynthesis. As nitrogen-containing acyl-CoA thioesters are not readily available in the market, chemical synthesis of

nitrogen-containing acyl-CoA thioesters from their respective carboxylic acid precursors is usually conducted, which involves a slow two-step process spanning at least two days. The process encompasses the synthesis of *N*-hydroxysuccinimide esters of the respective carboxylic acids, followed by a thiol ester exchange reaction with free CoA, to produce CoA thioester derivatives (Stockigt and Zenk, 1975) (Figure 3.1). An alternative way to generate a wide range of novel nitrogen-containing acyl-CoA esters is to make use of promiscuous acid-CoA ligases with different nitrogen-containing carboxylic acids. By determining substrate promiscuities of acid-CoA ligases and CHS18 beyond conventional substrate pools, we can establish novel enzymatic routes for the biosynthesis of unnatural alkaloids with potential anti-aging properties.

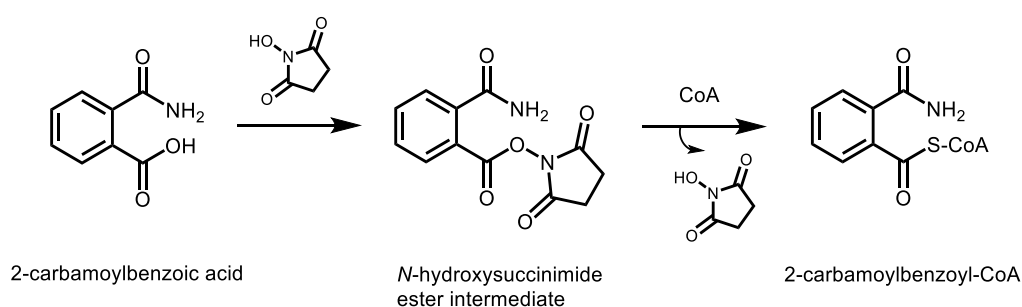


Figure 3.1: Chemical synthesis of nitrogen-containing acyl-CoA thioesters such as 2-carbamoylbenzoyl-CoA from the respective carboxylic acid precursors. Each step involves a reaction time of at least 24 h.

Previous studies on MCS, PCL, 4CL, and BZL showed that although they can utilize carboxylic acids to generate a total of 81 CoA esters, nitrogen-containing carboxylic acids were not good substrates (Go *et al.*, 2012). Consequently, another four acid-CoA ligases were selected based on the

availability of genomic DNA in the lab, and putative promiscuous CoA ligase functions as annotated in the National Center for Biotechnology Information website. The enzyme functions of these acid-CoA ligases were examined using a range of nitrogen-containing carboxylic acids, including all 20 standard amino acids. The new CoA thioesters produced were identified via HPLC and MS, and used as substrates for CHS18. By establishing a combinatorial biosynthetic pathway involving promiscuous acid-CoA ligases and CHS18 (Figure 1.9), a library of unnatural alkaloids with potential anti-aging properties can be biosynthesized.

3.2 Materials and methods

The carboxylic acid substrates for acid-CoA ligases were obtained from Sigma-Aldrich Co. (St. Louis, MO, USA), Tokyo Chemical Industry Co. (Tokyo, Japan), and Extrasynthese Co. (Genay Cedex, France). A total of 35 nitrogen-containing carboxylic acids were tested as potential precursors for acyl-CoA thioester biosynthesis: 4-nitrocinnamic acid, 3-aminobenzoic acid, 4-aminobenzoic acid, 4-amino-2-hydroxybenzoic acid, isoquinoline-1-carboxylic acid, 2-quinolinecarboxylic acid, 2-quinoxalinecarboxylic acid, 3-quinolinecarboxylic acid, 4-quinolinecarboxylic acid, pyrazine carboxylic acid, pyridine-2-carboxylic acid (picolinic acid), pyridine-3-carboxylic acid (nicotinic acid), 2-chloropyridine-3-carboxylic acid, pyridine-4-carboxylic acid (isonicotinic acid), carnitine, alanine, arginine, asparagine, aspartic acid, cysteine, glutamic acid, glutamine, glycine, histidine, isoleucine, leucine, lysine, methionine, phenylalanine, proline, serine, threonine, tryptophan, tyrosine and valine. All reagents were of the best quality grade that is available commercially. The chemical structures of all substrates tested are depicted in Figure A6 in the Appendix.

3.2.1 Cloning, expression and purification of novel acid-CoA ligases

Cg2, Sc1, Sc3, and Ec1

Putative long chain fatty acid-CoA ligase (Cg2) (GI: 499323704) and putative crotonobetaine / carnitine-CoA ligase (Ec1) (GI: 221142682) were cloned previously in the laboratory from *Corynebacterium glutamicum* ATCC 13032 and *E. coli* strain K12 MG1655 genomic DNA respectively. Putative long chain fatty acid-CoA ligase (Sc1) (GI: 499338447) and ligase (Sc3) (GI:

21218859) were cloned previously in the laboratory from *S. coelicolor* A3(2) genomic DNA. The four CoA ligases were each ligated into a Tom-15b vector and expressed in *E. coli* BL21(DE3) strain. Protein expression and purification were conducted as in section 2.2.3.

3.2.2 *In vitro* biosynthesis of nitrogen-containing acyl-CoA esters

A small scale reaction involving each nitrogen-containing carboxylic acid substrate was first conducted for each of the four acid-CoA ligases in order to determine the substrate profiles of the ligases. Biosynthesis of the nitrogen-containing acyl-CoA thioesters were carried out in 100 μ L reaction mixtures containing 100 mM Tris-HCL (pH 8.0), 5 mM $MgCl_2$, 5 mM ATP, 5 mM CoA, 5 mM nitrogen-containing carboxylic acid, and 2 mg/mL Cg2 / Ec1 / Sc1 / Sc3. After incubation for 6 h at 25°C, additional cofactors and CoA ligases were added to give a final reaction volume of 200 μ L, containing 100 mM Tris (pH 8.0), 5 mM $MgCl_2$, <5 mM ATP, <5 mM CoA, <5 mM nitrogen-containing carboxylic acid, and 2 mg/mL Cg2 / Ec1 / Sc1 / Sc3. The reactions were allowed to continue for another 16 h before they were pipetted out and centrifuged at 4°C through Amicon Ultracel membranes to remove all enzymes from the mixture. The filtrate containing reagents and/or products was collected and stored at -80°C until HPLC analysis.

The Atlantis Analytical C18 reverse-phase column was first equilibrated with 1% acetonitrile, 99% 100 mM ammonium acetate (pH 6.5) at a flow rate of 1 mL/min for 15 min. 10 μ L of sample was loaded and the column was washed with 1% acetonitrile, 99% 100 mM ammonium acetate (pH 6.5) at a flow rate of 1 mL/min for 4 min. The mobile phase was then changed to 70%

acetonitrile, 30% 100 mM ammonium acetate (pH 6.5) at a flow rate of 1 mL/min under a linear gradient over a period of 60 min. The eluted compounds were detected by measuring the absorbance at 230 nm, 240 nm, and 259 nm. New chromatogram peaks (minimum absorbance of 20 mAU) other than those due to the ATP, CoA, and carboxylic acid reference standards were identified and the respective nitrogen-containing carboxylic acid substrate and ligase combinations were scaled up to 2 ml reactions for subsequent MS analysis.

The same reagents were used for the 2 ml reaction mixtures, and biosynthesis of the nitrogen-containing acyl-CoA thioesters were conducted in a similar manner. In order to purify the novel nitrogen-containing acyl-CoA thioesters from the reaction mixture, HPLC analysis was carried out as above with minimal changes. The Atlantis Prep C18 reverse-phase column was first equilibrated with 1% acetonitrile, 99% 100 mM ammonium acetate (pH 6.5) at a flow rate of 5 mL/min for 15 min. Up to 800 μ L of sample was loaded and the column was washed with 1% acetonitrile, 99% 100 mM ammonium acetate (pH 6.5) at a flow rate of 5 mL/min for 4 min. The nitrogen-containing acyl-CoA thioesters were eluted with a linear gradient to 70% acetonitrile, 30% 100 mM ammonium acetate (pH 6.5) over a period of 60 min at a flow rate of 5 mL/min. Absorbance was monitored at 230 nm, 240 nm, and 259 nm, and fractions containing novel nitrogen-containing acyl-CoA thioesters were collected, lyophilized, and sent for low-resolution MS analyses.

3.2.3 Kinetic assays of acid-CoA ligase activity

After verifying that nitrogen-containing acyl-CoA esters were produced by the acid-CoA ligases using MS analyses, the kinetic parameters of the ligases were determined. Acid-CoA ligase activity was monitored spectrophotometrically by coupling the rate of formation of AMP (ligase activity) to oxidation of NADH (Figure 3.2) (Go *et al.*, 2012). A 200 μ l continuous spectrophotometric coupled-enzyme assay containing 100 mM Tris-HCL (pH 8.0), 10 mM $MgCl_2$, 5 mM ATP, 1.5 mM phosphoenolpyruvate (PEP), 1 mM CoA, 0.16 mM NADH, 2 units of pyruvate kinase, 2 units of lactate dehydrogenase, 1 unit of adenylate kinase, varying concentrations of carboxylic acid (0.010 – 10 mM), and Cg2 / Ec1 / Sc1 / Sc3 was conducted in Quartz cuvettes at 25°C. The reactions were monitored at 340 nm ($\epsilon = 6220 \text{ M}^{-1} \text{ cm}^{-1}$) for the oxidation of NADH using a Shimadzu UV-2550 UV-Visible Spectrophotometer. Since NADH absorbs at 340 nm, the rate of decrease of the absorbance at 340 nm will correlate with the rate of formation of the acyl-CoA ester. Initial velocity was measured and kinetic parameters were estimated using nonlinear regression to the Michaelis-Menten equation (EnzFitter software).

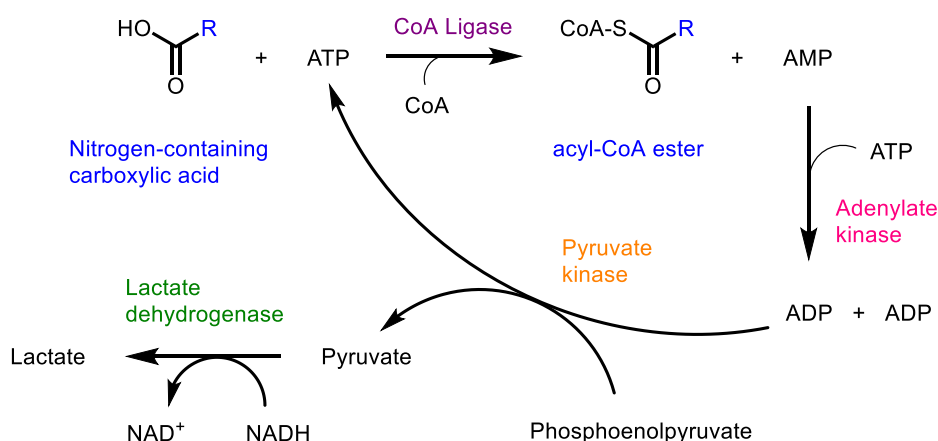


Figure 3.2: A continuous spectrophotometric coupled-enzyme assay was used to monitor the activities of acid-CoA ligases. Oxidation of NADH can be measured at 340 nm.

Interestingly, 2-quinoxalinecarboxylic acid can absorb at 340 nm, hence acid-CoA ligase activity for this acid was determined using a 5,5'-dithiobis-(2-nitrobenzoic acid) (DTNB) end-point assay which measures the amount of remaining free CoA (Kim and Bang, 1988). Briefly, a 100 μ L assay containing acid-CoA ligase, 100 mM Tris-HCl (pH 8.0), 10 mM MgCl₂, 5 mM ATP, 1 mM CoA, and varying concentrations of 2-quinoxalinecarboxylic acid (0.01 – 10 mM) was conducted. After incubation at 25°C for sufficient time to convert $\leq 10\%$ of the substrate to product, the reaction was quenched by the addition of 900 μ L of 222 μ M DTNB solution. The mixture was incubated at 25°C for another 5 min, and the remaining free CoA was quantitated by measuring the stoichiometrically equivalent amounts of 2-nitro-5-thiobenzoate dianion at 412 nm ($\epsilon = 14150 \text{ M}^{-1} \text{ cm}^{-1}$).

3.2.4 *In vitro* precursor-directed combinatorial biosynthesis of alkaloids and HPLC analysis

After verifying the biosynthesis of nitrogen-containing acyl-CoA thioesters, the respective carboxylic acid and their ligase were added to malonate, MCS and CHS18 for the biosynthesis of novel alkaloids. Initial biosyntheses of the nitrogen-containing starter CoA esters and extender CoA esters were carried out in 200 μ L reaction mixtures containing 100 mM Tris-HCL (pH 8.0), 10 mM $MgCl_2$, 10 mM ATP, 0.5 mM CoA, 2.5 mM starter acid, 5 mM malonic acid, 2 mg/mL Cg2 / Ec1 / Sc1 / Sc3, and 2 mg/mL MCS. After incubation for 6 h at 25°C, additional cofactors, CoA ligases, and 2 mg/mL CHS18 were added to give a final reaction volume of 400 μ L, containing 100 mM Tris (pH 8.0), 10 mM $MgCl_2$, <10 mM ATP, <0.5 mM CoA, <2.5 mM starter acid, <5 mM malonic acid, <0.5 mM starter CoA, <0.5 mM malonyl-CoA, 2 mg/mL Cg2 / Ec1 / Sc1 / Sc3, 2 mg/mL MCS, and 2 mg/mL CHS18. Due to the presence of a CoA regeneration system involving CoA ligases and CHS18, only a low amount of the expensive CoA is needed for the biosynthesis of alkaloids to take place. An aliquot of 80 μ L of the reaction mixture was immediately pipetted out and centrifuged at 4°C through Ultracel membranes to remove all enzymes from the mixture. The filtrate (representing time = 0 h) was collected and stored at -80°C until HPLC analysis. The remaining 320 μ L reaction mixture was then incubated at 25°C for another 20 h. Subsequently, enzymes were removed via centrifugation through Ultracel membranes, and the filtrate (representing time = 20 h) was collected and stored at -80°C until HPLC analysis. HPLC analysis was conducted as in section 2.2.2. By comparing the chromatograms of samples

from the 0 h (control) and 20 h (with CHS18) time-points, fractions that were only present in the 20 h time-point samples indicate alkaloid biosynthesis. The respective nitrogen-containing carboxylic acid substrate, malonic acid, ligases and CHS18 combinations were scaled up to 2 ml reactions for subsequent MS analysis.

The same reagents were used for the 2 ml reaction mixtures, and biosynthesis of the alkaloids were conducted in a similar manner. In order to purify the novel alkaloids from the reaction mixture, HPLC analysis was carried out as in section 2.2.4. Absorbance was monitored at 230 nm, 280 nm, and 320 nm, and fractions containing novel alkaloids were collected, lyophilized, and sent for low-resolution MS analyses.

3.2.5 Mass spectrometry profiling of novel nitrogen-containing acyl-CoA esters and alkaloids

MS analysis was conducted under the assistance of our collaborator, Dr. Manfred Raida, in A/P Markus Wenk's laboratory. The lyophilized nitrogen-containing acyl-CoA thioesters were dissolved in 100 μ L deionized water and subjected to high-resolution MS scanning and fragmentation. A neutral loss of 507 m/z was used for identification of the CoA ester group, and the mass of the parent ion was analyzed using Masshunter Qualitative Analysis software version 6. HPLC-MS/MS analysis of the purified alkaloids was carried out as in 2.2.5.

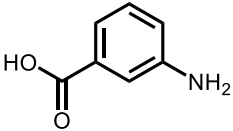
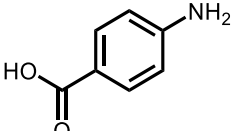
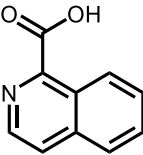
3.3 Results and discussion

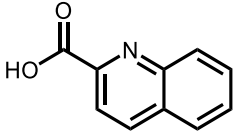
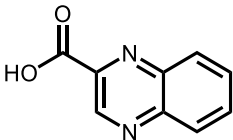
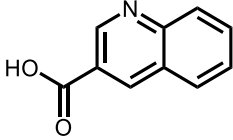
3.3.1 Catalytic functions of Cg2, Sc1, Sc3, and Ec1

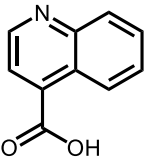
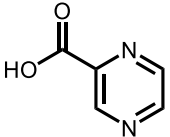
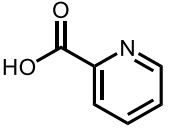
The enzyme functions of the CoA ligases Cg2, Ec1, Sc1, and Sc3 have not been determined before. Promiscuity of Cg2, Ec1, Sc1 and Sc3, and the type III PKS, CHS18, enabled the biosynthesis of alkaloids when various nitrogen-containing carboxylic acids were introduced as starters. The diversity of the alkaloids generated by CHS18 is dependent on its starter and extender units, which are the acyl-CoA thioesters produced by CoA ligases. Hence, there is a need to determine the substrate and product profiles of the promiscuous CoA ligases before selecting suitable nitrogen-containing carboxylic acid substrates for alkaloid biosynthesis.

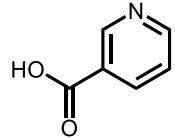
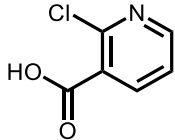
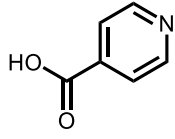
Small scale reactions were carried out, whereby the 20 standard amino acids and another 15 nitrogen-containing carboxylic acids were introduced individually as substrates for Cg2, Ec1, Sc1 and Sc3 *in vitro*. Out of the 35 acids tested, the acid-CoA ligases were found to generate a new acyl-CoA thioester peak for 14 substrates during HPLC analysis (Table 3.1). For instance, when 3-aminobenzoic acid was incubated with Ec1, a new acyl-CoA ester peak was observed at an R_t of 26.8 min (Figure 3.3). The reactions for the 14 nitrogen-containing carboxylic acids were scaled up and all the new peaks detected were purified and verified by MS analysis. Out of the 14 carboxylic acids tested, only 11 gave a correct and definitive MS result. 2-quinoxalinecarboxyl-CoA, and the CoA esters of cysteine and glutamic acid may be unstable and hence, these products were not detected in the MS analysis. The kinetic parameters for the biosynthesis of the various acyl-CoA esters were subsequently determined (Table 3.1).

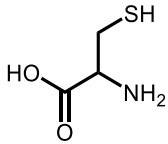
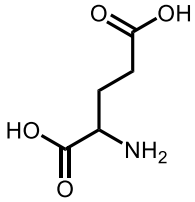
Table 3.1: Low-resolution MS analysis and kinetic parameters for the biosynthesis of new nitrogen-containing acyl-CoA esters. HPLC retention times are based on analyses conducted using the Atlantis Prep C18 reverse-phase column. ^a Saturation kinetics could not be achieved. *Italicized*: A definitive MS result was not obtained.

Carboxylic acid tested	Acid-CoA ligase used	HPLC R _t (min)	Experimental mass of CoA ester [theoretical mass]	<i>k</i> _{cat} (s ⁻¹)	<i>K</i> _M (mM)	<i>k</i> _{cat} / <i>K</i> _M (M ⁻¹ s ⁻¹)
 3-aminobenzoic acid	Cg2	26.4	886.00 [886.65]	<i>a</i>	<i>a</i>	0.21
	Ec1	26.8	886.10 [886.65]	<i>a</i>	<i>a</i>	0.35
 4-aminobenzoic acid	Cg2	26.2	886.10 [886.65]	<i>a</i>	<i>a</i>	1.9
	Ec1	26.4	886.10 [886.65]	<i>a</i>	<i>a</i>	0.037
 Isoquinoline-1-carboxylic acid	Cg2	32.0	922.00 [922.69]	(1.78 ± 0.06) x 10 ⁻³	9 ± 2	0.2
	Sc3	33.3	Not detected	<i>a</i>	<i>a</i>	1.9 x 10 ⁻⁵

Carboxylic acid tested	Acid-CoA ligase used	HPLC R _t (min)	Experimental mass of CoA ester [theoretical mass]	k_{cat} (s ⁻¹)	K_{M} (mM)	$k_{\text{cat}}/K_{\text{M}}$ (M ⁻¹ s ⁻¹)
 2-quinolinecarboxylic acid	Cg2	30.4	Not detected	$(1.6 \pm 0.1) \times 10^{-3}$	$(15.0 \pm 9.8) \times 10^{-3}$	110
	Sc3	32.0	Not detected	5.5 ± 0.2	0.22 ± 0.03	25000
	Ec1	33.4	922.10 [922.69]	$(6.0 \pm 0.3) \times 10^{-4}$	0.9 ± 0.2	0.64
 2-quinoxalinecarboxylic acid	Ec1	30.8	837.20 [923.67]	<i>a</i>	<i>a</i>	0.18
 3-quinolinecarboxylic acid	Ec1	27.8	922.10 [922.69]	$(2.1 \pm 0.2) \times 10^{-2}$	18 ± 3	1.1

Carboxylic acid tested	Acid-CoA ligase used	HPLC R _t (min)	Experimental mass of CoA ester [theoretical mass]	k_{cat} (s ⁻¹)	K_{M} (mM)	$k_{\text{cat}}/K_{\text{M}}$ (M ⁻¹ s ⁻¹)
 4-quinolinecarboxylic acid	Cg2	28.8	922.10 [922.69]	$(6.7 \pm 0.4) \times 10^{-3}$	0.52 ± 0.09	13
 Pyrazine carboxylic acid	Cg2	23.0	873.10 [873.61]	<i>a</i>	<i>a</i>	0.16
 Pyridine-2-carboxylic acid	Cg2	28.4	872.20 [872.63]	$(1.2 \pm 0.2) \times 10^{-2}$	4.2 ± 1.6	2.8

Carboxylic acid tested	Acid-CoA ligase used	HPLC R_t (min)	Experimental mass of CoA ester [theoretical mass]	k_{cat} (s^{-1})	K_M (mM)	k_{cat}/K_M ($M^{-1} s^{-1}$)
 Pyridine-3-carboxylic acid	Cg2	23.8	872.00 [872.63]	$(2.8 \pm 0.3) \times 10^{-3}$	1.7 ± 0.5	1.7
	Ec1	24.2	872.10 [872.63]	<i>a</i>	<i>a</i>	1.2×10^{-5}
 2-chloropyridine-3-carboxylic acid	Cg2	25.6	907.90 [907.07]	$(2.0 \pm 0.1) \times 10^{-3}$	1.3 ± 0.3	1.5
 Pyridine-4-carboxylic acid	Cg2	23.8	872.10 [872.63]	$(6.7 \pm 0.6) \times 10^{-3}$	2.4 ± 0.7	2.8

Carboxylic acid tested	Acid-CoA ligase used	HPLC R_t (min)	Experimental mass of CoA ester [theoretical mass]	k_{cat} (s^{-1})	K_M (mM)	k_{cat}/K_M ($\text{M}^{-1} \text{s}^{-1}$)
 Cysteine	Ec1	18.4	886.10 [870.68]	Reaction too slow to be detected	Reaction too slow to be detected	Reaction too slow to be detected
	Sc1	18.4	886.10 [870.68]	Reaction too slow to be detected	Reaction too slow to be detected	Reaction too slow to be detected
	Sc3	18.6	886.10 [870.68]	<i>a</i>	<i>a</i>	22
 Glutamic acid	Ec1	14.8	636.10 [896.65]	<i>a</i>	<i>a</i>	0.018

Biosynthesis of new acyl-CoA ester when 3-aminobenzoic acid is added to Ec1

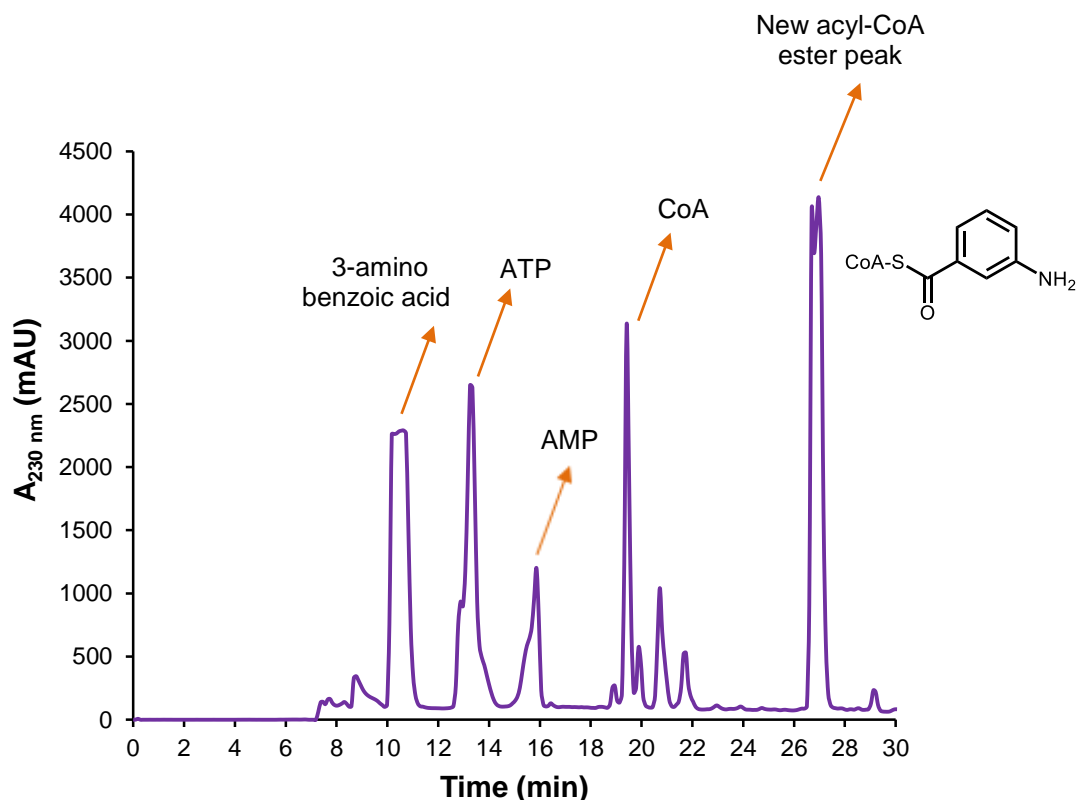


Figure 3.3: HPLC chromatogram showing the detection of a new acyl-CoA thioester peak at an R_t of 26.8 min, when 3-aminobenzoic acid was supplemented to Ec1. The identity of the other peaks were determined by running commercially available standards using the same HPLC program.

More nitrogen-containing starter carboxylic acids can be tested against the four CoA ligases in the future so as to gain more insights into their substrate preferences. After verifying the generation of nitrogen-containing starter acyl-CoA thioesters by MS, precursor-directed combinatorial biosynthesis of alkaloids using the promiscuous type III PKS, CHS18, can subsequently be performed.

3.3.2 Precursor-directed combinatorial biosynthesis is a novel means to produce alkaloids

CHS18 is a promiscuous PKS capable of using unnatural starter and extender acyl-CoA esters to biosynthesize novel polyketides. Hence, we hypothesized that CHS18 is likely to utilize nitrogen-containing starter units to produce alkaloids, and the substrate profile of CHS18 was determined. The 14 nitrogen-containing carboxylic acids with verified kinetic parameters were supplied to CHS18 together with the respective acid-CoA ligases. In addition, malonic acid and MCS were introduced to generate the extender, malonyl-CoA (Figure 3.4). CHS18 was able to catalyze the condensation of malonyl-CoA with three out of 14 starter acyl-CoA esters separately to form alkaloids. When CHS18 was supplemented with 3-aminobenzoyl-CoA generated by Ec1, and malonyl-CoA, a new alkaloid peak was observed at an R_t of 20.2 min (Figure 3.5). Similarly, CHS18 catalyzed the condensation of malonyl-CoA with the 3-aminobenzoyl-CoA thioester produced by Cg2, to form two alkaloids with R_t 20.2 min and 30.8 min (Figure 3.6). This could be due to different production yields of 3-aminobenzoyl-CoA by Ec1 and Cg2, leading to a skewed ratio of starter to extender units, and thus the incorporation of different numbers of extender units to form different alkaloid products. The combination comprising of 3-quinolinecarboxyl-CoA generated by Ec1 and malonyl-CoA also led to the biosynthesis of a new alkaloid product with an R_t of 26.0 min by CHS18 (Figure 3.7). Moreover, when pyridine-2-carboxyl-CoA produced by Cg2 and malonyl-CoA were introduced to CHS18, a new alkaloid with an R_t of 23.1 min was obtained (Figure 3.8).

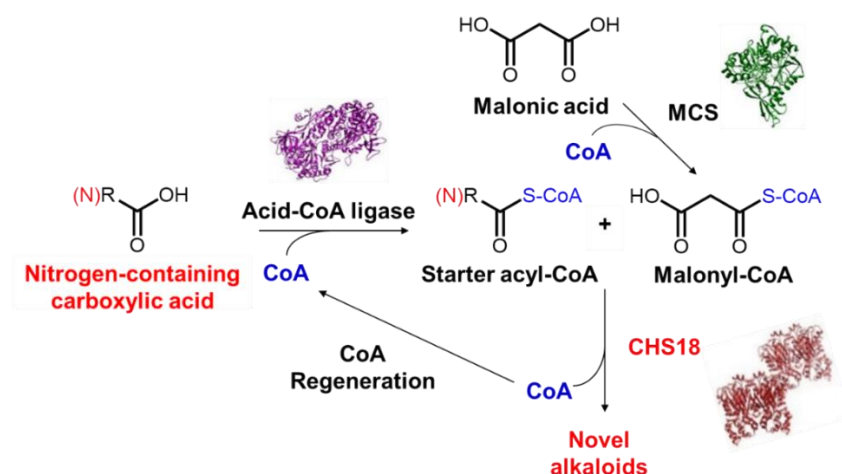


Figure 3.4: Precursor-directed combinatorial biosynthesis of novel alkaloids by supplying nitrogen-containing starter acyl-CoA esters and malonyl-CoA to CHS18.

Biosynthesis of new alkaloid when 3-aminobenzoic acid and malonate were added to Ec1, MCS and CHS18

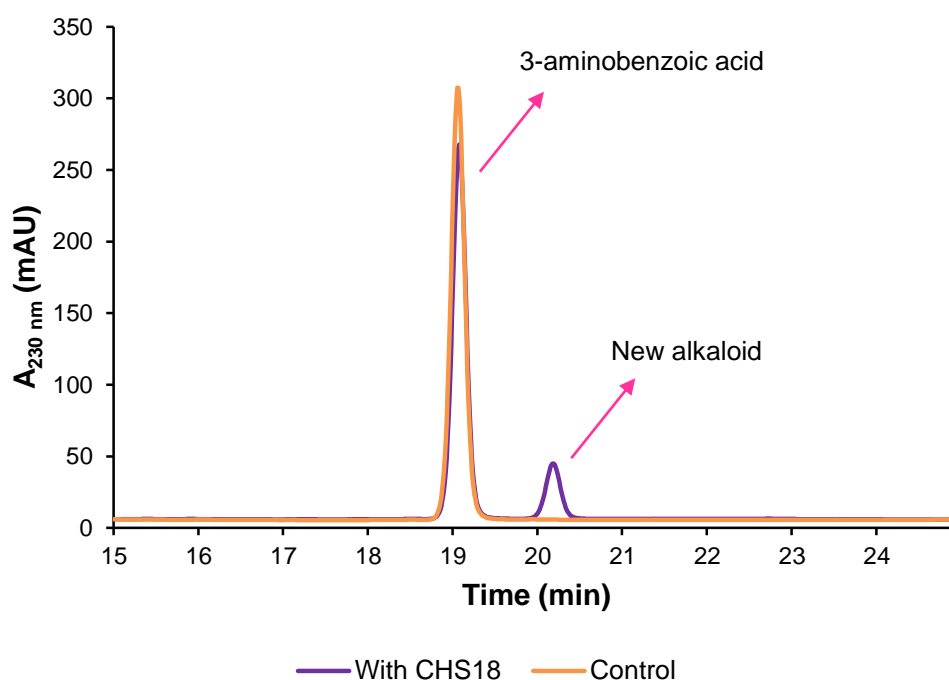


Figure 3.5: *In vitro* precursor-directed combinatorial biosynthesis involving 3-aminobenzoyl-CoA and malonyl-CoA produced by Ec1 and MCS respectively. HPLC analysis was conducted using an Atlantis Analytical C18 reverse-phase column. An additional peak at R_t 20.2 min was observed when CHS18 was incubated with the reagents for 20 h, indicating that a new alkaloid was biosynthesized.

Biosynthesis of new alkaloid when 3-aminobenzoic acid and malonate were added to Cg2, MCS and CHS18

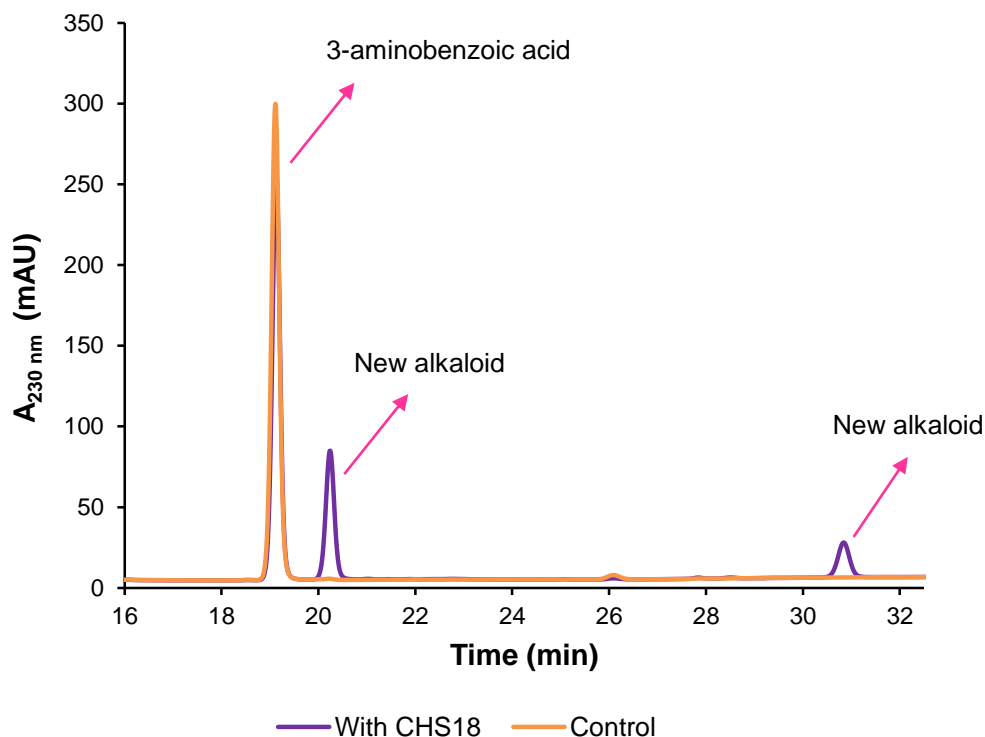


Figure 3.6: *In vitro* precursor-directed combinatorial biosynthesis involving 3-aminobenzoyl-CoA and malonyl-CoA produced by Cg2 and MCS respectively. HPLC analysis was conducted using an Atlantis Analytical C18 reverse-phase column. Additional peaks at R_t 20.2 min and 30.8 min were observed when CHS18 was incubated with the reagents for 20 h, indicating that new alkaloids were biosynthesized.

Biosynthesis of new alkaloid when 3-quinolinecarboxylic acid and malonate were added to Ec1, MCS and CHS18

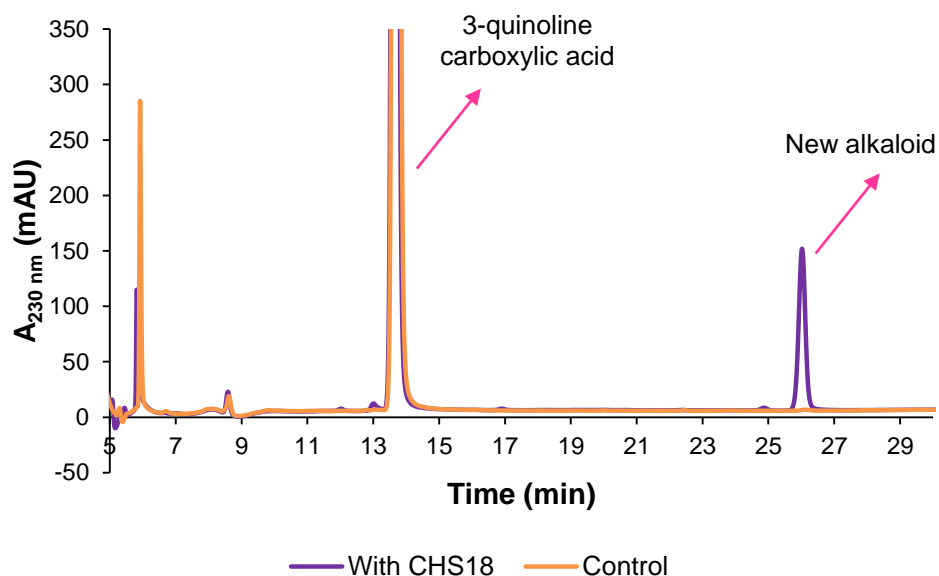


Figure 3.7: *In vitro* precursor-directed combinatorial biosynthesis involving 3-quinolinecarboxyl-CoA and malonyl-CoA produced by Ec1 and MCS respectively. HPLC analysis was conducted using an Atlantis Analytical C18 reverse-phase column. An additional peak at R_t 26.0 min was observed when CHS18 was incubated with the reagents for 20 h, indicating that a new alkaloid was biosynthesized.

Biosynthesis of new alkaloid when pyridine-2-carboxylic acid and malonate were added to Cg2, MCS and CHS18

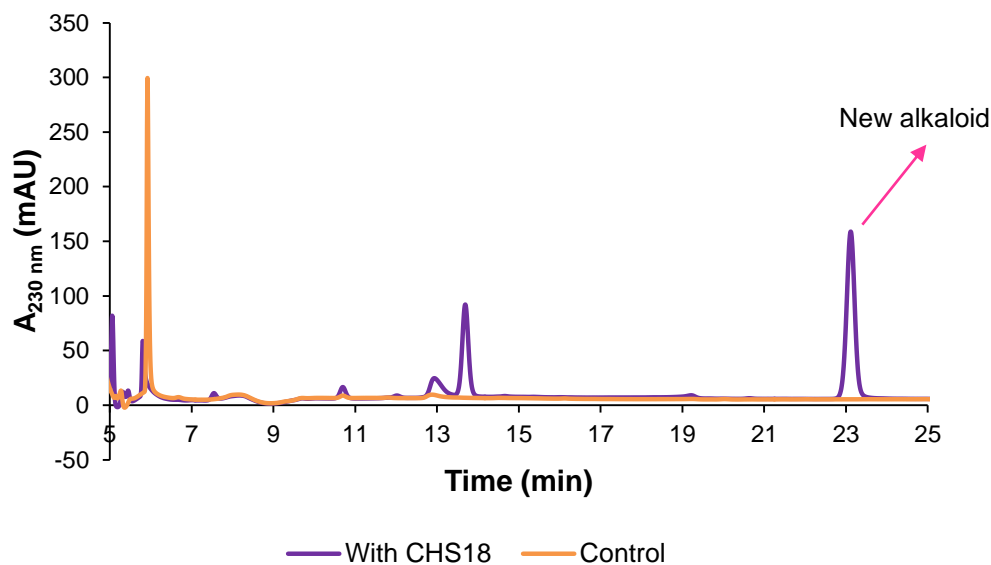
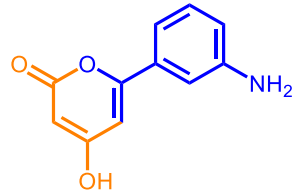
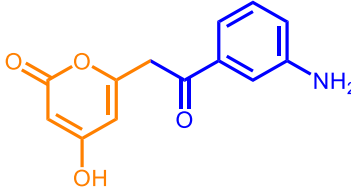
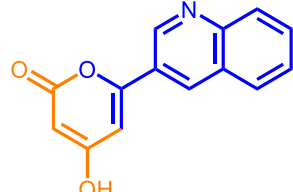
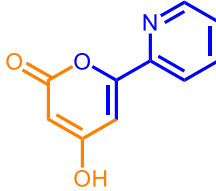


Figure 3.8: *In vitro* precursor-directed combinatorial biosynthesis involving pyridine-2-carboxyl-CoA and malonyl-CoA produced by Cg2 and MCS respectively. HPLC analysis was conducted using an Atlantis Analytical C18 reverse-phase column. An additional peak at R_t 23.1 min was observed when CHS18 was incubated with the reagents for 20 h, indicating that a new alkaloid was biosynthesized. Pyridine-2-carboxylic acid does not absorb at 230 nm.

The new peaks were collected and sent for MS analysis. The masses of the selected alkaloids identified in this study matched their corresponding expected masses, and the potential chemical structures of the compounds were proposed (Table 3.2). This suggested the feasibility of utilizing promiscuous acid-CoA ligases and non-alkaloid synthases, such as type III PKSs, to biosynthesize novel alkaloids in an unnatural way.

Table 3.2: Potential alkaloids biosynthesized by CHS18. The part of the alkaloid derived from the starter unit is highlighted in blue.

Combination of starter and extender	HPLC R_t (min)	Experimental mass [theoretical mass]	Chemical formula	Number of extender units added	Potential structure	Mode of Cyclization
3-aminobenzoyl-CoA + malonyl-CoA	20.2	203.07 [203.19]	$C_{11}H_9NO_3$	2		Lactonization
	30.8	245.08 [245.23]	$C_{13}H_{11}NO_4$	3		Lactonization
3-quinolinecarboxyl-CoA + malonyl-CoA	26.0	239.07 [239.23]	$C_{14}H_9NO_3$	2		Lactonization
Pyridine-2-carboxyl-CoA + malonyl-CoA	23.1	189.05 [189.17]	$C_{10}H_7NO_3$	2		Lactonization

Variations in the choice of starter and extender CoA esters can facilitate the creation of a diverse alkaloid library. Previous studies have shown that MCS and PCL are promiscuous enzymes capable of generating several novel extenders which are malonyl-CoA derivatives (Go *et al.*, 2012). By using CHS18 with different combinations of nitrogen-containing starters and malonyl-CoA derivatives, such as isopropylmalonyl-CoA, hydroxymalonyl-CoA and phenylmalonyl-CoA, a diverse and bioactive library of alkaloids can be created. Nitrogen-containing derivatives of malonyl-CoA, such as 2-[(aminocarbonyl)-amino]-malonyl-CoA and [2-(2-aminophenyl)-hydrazino]-malonyl-CoA (Figure 3.9), can also be utilized with suitable CoA ligases for an added diversity to the alkaloid library.

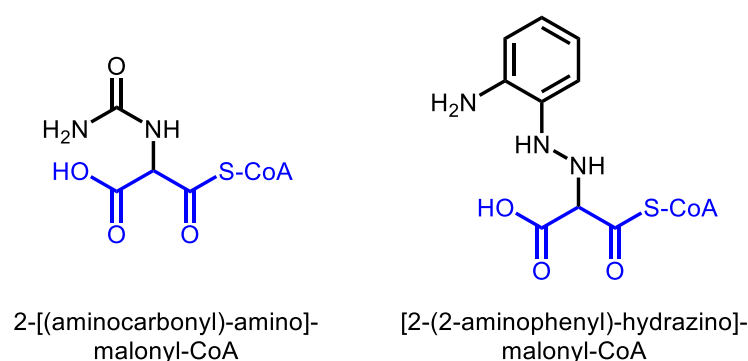


Figure 3.9: Nitrogen-containing derivatives of malonyl-CoA. The malonyl-CoA backbone is highlighted in blue.

Previously, CHS18 was derived from alfalfa CHS containing 18 mutations, and performed a predominantly C2 to C7 Aldol condensation rather than a C6 to C1 Claisen condensation, thus allowing CHS18 to acquire STS activity (Austin *et al.*, 2004). Manipulation of the type III PKS reactions by using rationally engineered mutant enzymes in conjunction with unnatural substrates can also result in a further generation of chemically and structurally

distinct alkaloids. The ‘gatekeeper’ Phe215 is generally conserved in most type III PKSs and is located between the CoA-binding tunnel and the entrance of the active site cavity. Intriguingly, although *N*-methylantraniloyl-CoA is not normally utilized by the wild type alfalfa CHS, the F215S mutant was found to accept the bulky starter to form *N*-methylantraniloyltriacetic acid lactone (Jez *et al.*, 2002). A modification into a serine residue at position 215 results in a reduction in steric hindrance and a wider active site entrance, thus allowing the entry of the bulky *N*-methylantraniloyl-CoA. This demonstrates that mutagenesis studies on CHS18 can be performed to further expand its substrate specificity. By rationally incorporating amino acid substitutions, the active site cavity of type III PKSs can be altered or expanded to facilitate the synthesis of more complex alkaloids in the future. This characteristic makes type III PKSs great candidates for structure-based engineering approaches to expand the chemical and structural diversity of natural products derived from these systems.

Overall, this study has demonstrated the utility in using precursor-directed combinatorial biosynthesis for the production of alkaloids. We can also conduct site-directed mutagenesis on residues near the active site cavity of CHS18, such as Phe215, so as to increase the product profile of CHS18. By constructing a natural product library of both alkaloids and polyketides, valuable drug compounds can be obtained more easily compared to extraction from natural sources or chemical synthesis. Hence, drug screening efforts, such as the development of anti-aging nutraceuticals, can be made more feasible.

CHAPTER 4: MITOCHONDRIAL FUNCTION ASSAY AS A NOVEL MEANS TO SCREEN FOR CALORIC RESTRICTION MIMETICS

4.1 Introduction

Drugs that mimic CR are being developed to improve longevity. These include derivatives of the polyketide resveratrol (Gertz *et al.*, 2012) and isoquinoline alkaloids such as berberine (Chow and Sato, 2013). The conventional method of anti-aging drug screening is via life span assays, which are time consuming and impractical to screen for a large compound library. Identification of drug hits via microarray profiling is also a feasible method (Dhahbi *et al.*, 2005), but it is expensive, invasive and require sufficient amount of organ tissue for analysis. Therefore, there is a need to develop another high throughput method to screen our library of polyketides and alkaloids for anti-aging properties.

Reduced mitochondrial function and aerobic capacity is one of the hallmarks of aging (Lopez-Otin *et al.*, 2013). During the aging process, the accumulation of mutations in the nuclear DNA and mitochondrial DNA (mtDNA), especially in genes encoding subunits of the ETC, can result in an age-related decline in mitochondrial capacity for oxidative phosphorylation (Bua *et al.*, 2006; Seo and Leeuwenburgh, 2015). Since CR is known to promote longevity by modulating oxidative metabolism (Schulz *et al.*, 2007), exposing *C. elegans* to potential CR mimetics is likely to affect their mitochondrial activity. Hence, by establishing a link between life span

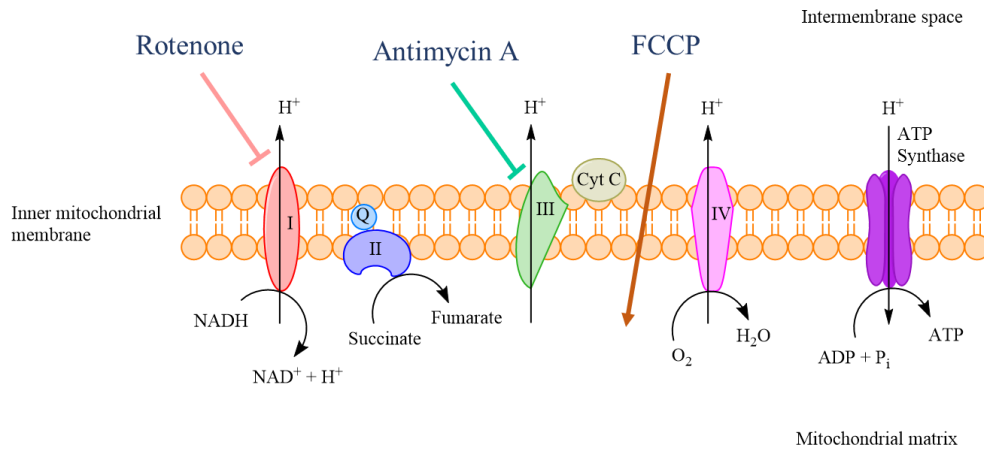
extension, CR, and mitochondrial function, we can design a more effective screening assay for CR mimetics with anti-aging properties.

Resveratrol is able to extend life span in model organisms and is likely to be a potential CR mimetic. It is thought to activate AMPK (Um *et al.*, 2010; Park *et al.*, 2012) and increase Sirt1-mediated PGC-1 α activation (Lagouge *et al.*, 2006). Thus, resveratrol-mediated longevity could be due to alterations in metabolism. PGC-1 α is an important regulator of mitochondrial biogenesis and function (Wu *et al.*, 1999). Indeed, resveratrol treatment in mice has been shown to improve mitochondrial oxidative phosphorylation and aerobic capacity, as evidenced by an induction of genes for mitochondrial content, and increased oxygen consumption and physical endurance (Lagouge *et al.*, 2006; Um *et al.*, 2010; Park *et al.*, 2012).

By using resveratrol treatment to mimic CR and establish a reference for mitochondrial function assays, screening of potential CR mimetics can be facilitated. Mitochondrial function assays using an extracellular flux analyzer were adopted to screen for drug hits, in which the real-time mitochondrial respiration of *C. elegans* can be looked into non-invasively at the molecular level (Ferrick *et al.*, 2008). In this approach, OCR is used as an indicator of metabolic rate, which is considered as the most reliable method of determination compared to carbon dioxide production assays and direct calorimetry due to size limitations of *C. elegans* (Braeckman *et al.*, 2002). Mitochondrial inhibitors such as carbonyl cyanide *p*-(trifluoromethoxy)phenylhydrazone (FCCP), antimycin A and rotenone were added during the assay to perturb the ETC of *C. elegans* (Figure 4.1).

FCCP is an uncoupling agent which disrupts the proton gradient across the inner mitochondrial membrane. This interferes with the generation of ATP as protons are transported down a potential gradient back into the mitochondrial matrix before being utilized to provide the energy for ATP synthesis (Benz and McLaughlin, 1983). This uncoupling of phosphorylation of 5'-Adenosine Diphosphate (ADP) from electron transport causes OCR to increase as cells attempt to maintain intracellular ATP levels. The greater the increase in OCR upon FCCP addition, the more efficient the mitochondria were in producing ATP under basal conditions.

Antimycin A and rotenone inhibit Complex III and Complex I respectively, causing the ETC to shut down and result in a decrease in OCR below basal levels (Schuh *et al.*, 2012) (Figure 4.1). The introduction of FCCP, antimycin A, and rotenone during the mitochondrial function assay enables a mitochondrial respiration profile to be generated. This profile allows the determination of four mitochondrial respiration parameters, namely basal respiration, maximal respiration, spare respiratory capacity, and non-mitochondrial respiration (Figure 4.1). Future work on screening for CR mimetics can be performed by using the mitochondrial respiration profile obtained from this study as a reference. This can narrow down the number of drug hits for further validation studies.



Mitochondrial Respiration

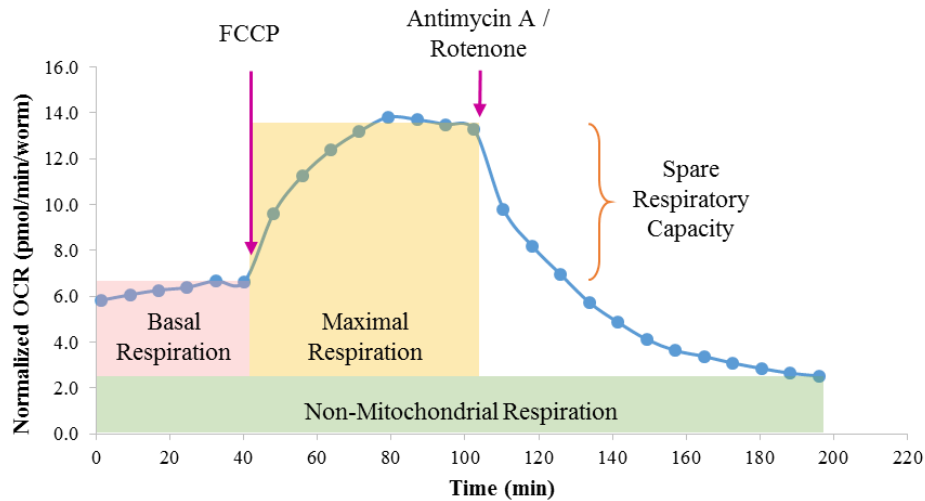


Figure 4.1: Four parameters of *C. elegans* mitochondrial respiration can be acquired by using mitochondrial inhibitors such as FCCP, antimycin A and rotenone to perturb mitochondrial function. FCCP is an uncoupler while antimycin A and rotenone are inhibitors of Complex III and Complex I respectively.

4.2 Materials and methods

4.2.1 Optimization of mitochondrial function assays in *Caenorhabditis elegans*

Mitochondrial function assays were conducted as in Dancy *et al.* (2013) with some modifications. Age-synchronized adult wild-type *C. elegans* N2 strain were grown on NGM plates containing 90 μ M FUdR, 90 μ M FUdR + 0.1% DMSO, or 90 μ M FUdR + 50 μ M resveratrol (dissolved in DMSO) for different durations up to 14 days, with each treatment having replicates prior to the mitochondrial function assay. This is because it has been shown that worms exposed to 50 μ M resveratrol had a significantly longer mean life span compared to worms exposed to DMSO only (Figure 2.11), suggesting that resveratrol is a potential CR mimetic at 50 μ M. Oxygen consumption was measured using the Seahorse XFe24 Extracellular Flux Analyzer (Seahorse Bioscience).

Briefly, fluorescent probes in 24-well islet microplates were hydrated a day before the assay and calibrated just before assays were conducted. *C. elegans* were recovered from NGM plates using M9 minimal medium, and washed three times to eliminate eggs and residual bacteria (Dancy *et al.*, 2013). Worms were transferred to 24-well Seahorse islet plates (10 – 25 worms in 675 μ L M9 minimal medium per well) and covered with an islet capture screen. Basal oxygen consumption was measured for 6 cycles before performing FCCP treatment at a final concentration of 20 μ M. Each cycle of reading consisted of a mixing of media for 2 min, waiting for worms to equilibrate to the environment for 2 min, and a measurement of oxygen levels in the media for 3 min. After addition of FCCP to the media, maximal oxygen

consumption was subsequently measured for 8 cycles. OCR was then brought down to minimal levels by treatment with 20 μ M antimycin A and 10 μ M rotenone.

OCR values were normalized to the number of worms in each well. Kruskal-Wallis test and Dunn's multiple comparisons test in the GraphPad Prism 6 program were used to determine the significance of differences in medians. After determining the optimum number of days for exposure to potential CR mimetics in order to see any effects on mitochondrial respiration, *C. elegans* were subjected to 25 μ M, 40 μ M, or 50 μ M resveratrol treatment to determine any dose-dependent effects on respiration. Mutant *eat-2* *C. elegans* which undergo chronic CR, and *daf-2* mutants which have compromised IGF-1 signaling, were also subjected to 50 μ M resveratrol treatment, and their mitochondrial respiration rates were compared to that of the wild-type N2 worms.

4.2.2 Screening for more potent caloric restriction mimetics

After completing the optimization studies, selected compounds in our polyketide and alkaloid libraries were introduced to age-synchronized adult wild-type *C. elegans* for eight days. *C. elegans* were grown on NGM plates containing 90 μ M FUdR, 0.5 mM starter acids, 1 mM extender acids, 0.1 mM IPTG, 34 μ g/mL chloramphenicol, 100 μ g/mL ampicillin, 30 μ g/mL kanamycin, and either the corresponding CoA ligases + CHS18 *E. coli* constructs, or constructs without CHS18. *E. coli* were prepared as in section 2.2.6. The mitochondrial respiration of *C. elegans* exposed to the CoA

thioesters and novel polyketides / alkaloids were compared to the mitochondrial respiration of worms exposed to CoA thioesters only, using Kruskal-Wallis test and Dunn's multiple comparisons test.

4.3 Results and discussion

4.3.1 Optimization of mitochondrial function assays in *Caenorhabditis elegans*

The development of anti-aging therapeutics involves the generation of a diverse bioactive compound library as well as a methodology to screen for potential drug hits. These two arms of therapeutic development complement each other to enable the discovery of novel bioactive drugs that can lead to life span extension in organisms. Mitochondrial function assays were developed and optimized in order to establish a correlation between OCR, mitochondrial activity, and longevity.

C. elegans were treated with a CR mimetic, resveratrol, for a range of duration before measuring their mitochondrial respiration rates. The results were analyzed using Kruskal-Wallis test to determine if there was a significant difference in the median OCR of the groups, as the samples were not normally distributed. Subsequently, Dunn's multiple comparisons test was used to determine if the medians varied significantly between any two selected groups.

It was observed that *C. elegans* exposed to 50 μ M resveratrol for at least seven days have a higher average basal OCR (Figure 4.2) and higher average maximal OCR (Figure 4.3) when compared to their controls. However, an increase in spare respiratory capacity was only significant after eight days of exposure to 50 μ M resveratrol (Figure 4.4). This suggests that exposure to a potential CR mimetic for at least eight days can counteract the age-related decline in mitochondrial function in *C. elegans* by increasing the average basal OCR, average maximal OCR, and spare respiratory capacity. The increase in

sparse respiratory capacity was indicative of the improvements in the ability of the mitochondria to cope with changes in the demand for ATP.

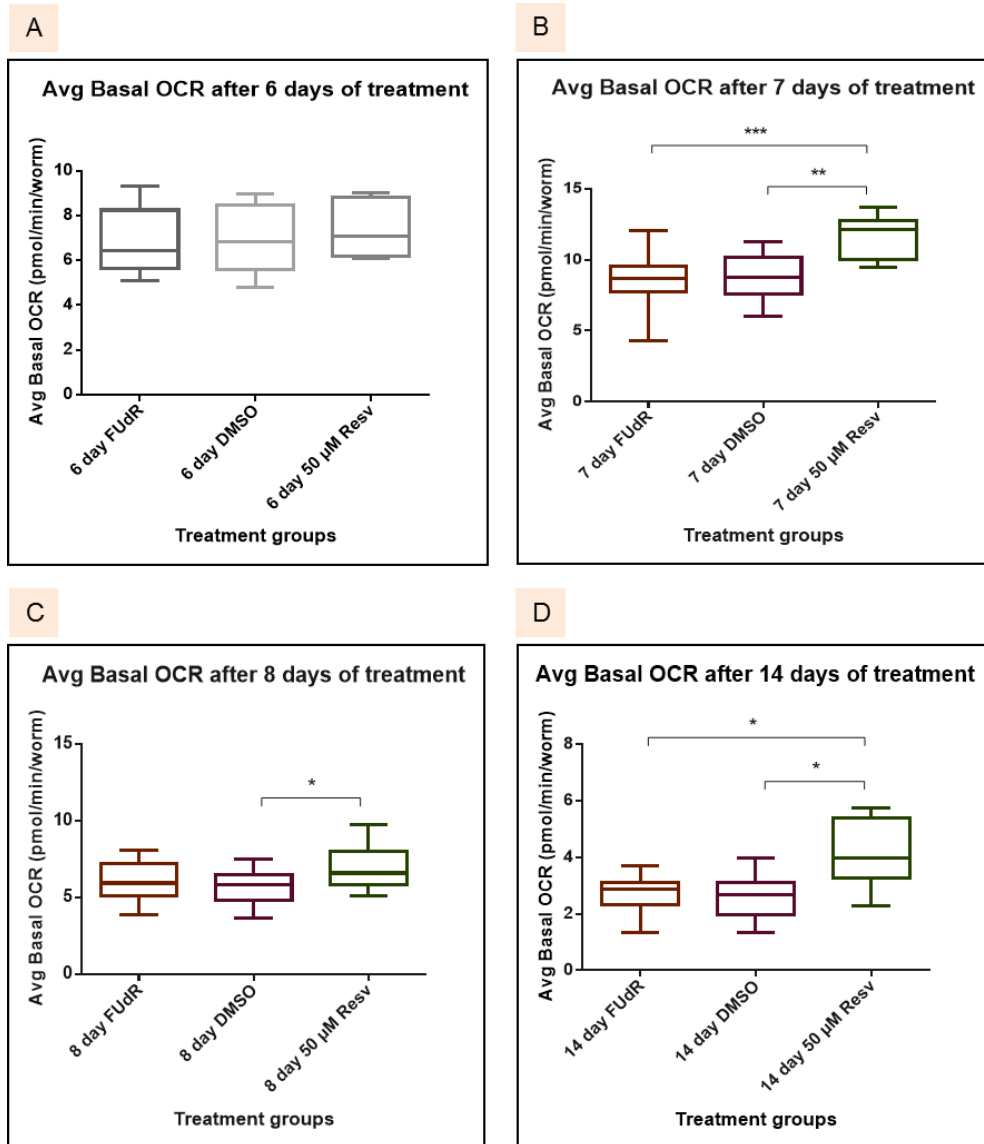


Figure 4.2: Average basal OCR readings of *C. elegans* exposed to (A) 6 days, (B) 7 days, (C) 8 days, and (D) 14 days of FUDR + 50 μ M resveratrol (Resv). Control groups were exposed to FUDR or FUDR + 0.1% DMSO. *C. elegans* exposed to the CR mimetic, resveratrol, for at least seven days have a higher rate of average basal respiration as compared to the control. * p -value ≤ 0.05 ; ** p -value ≤ 0.01 ; *** p -value ≤ 0.001 .

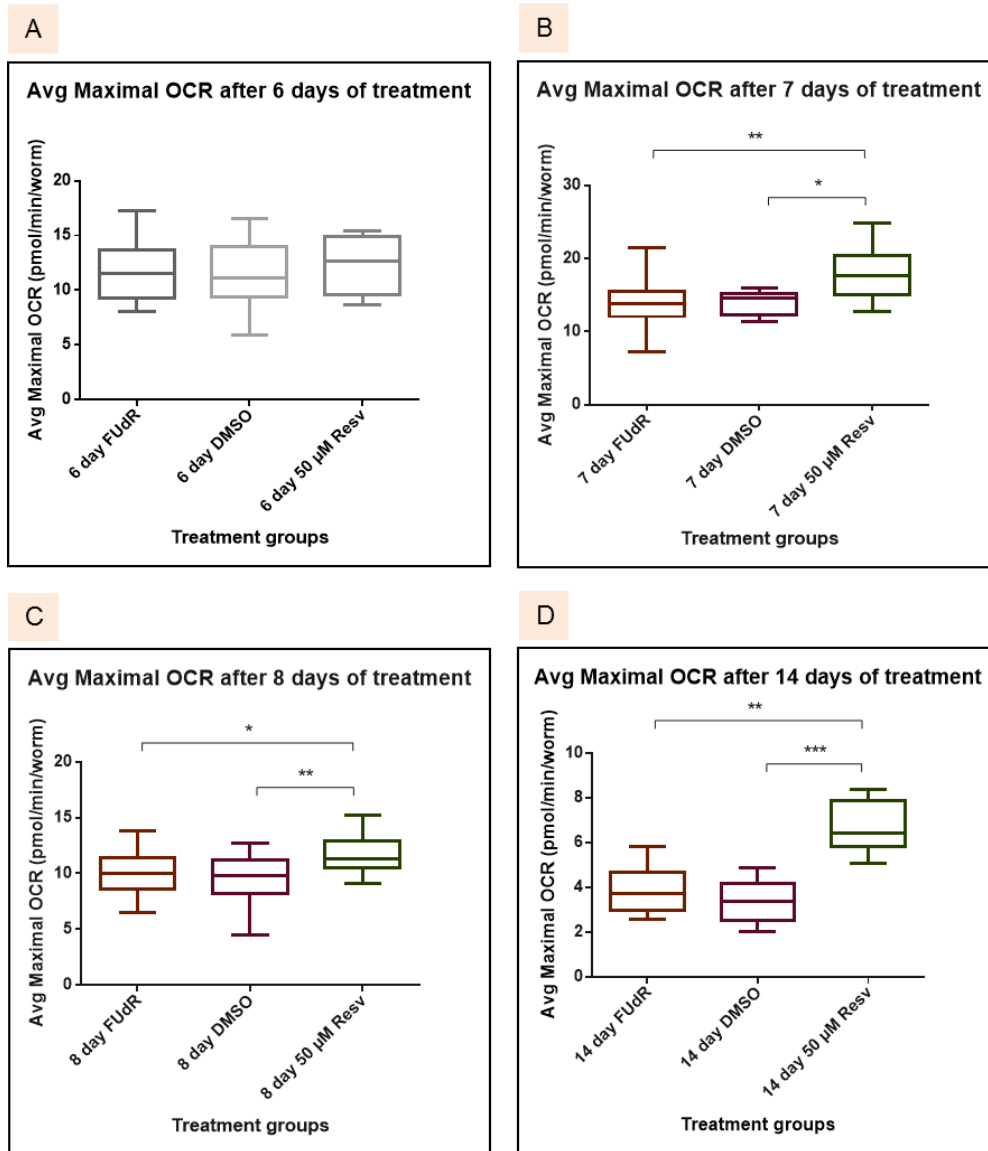


Figure 4.3: Average maximal OCR readings of *C. elegans* exposed to (A) 6 days, (B) 7 days, (C) 8 days, and (D) 14 days of FUDR + 50 μ M resveratrol (Resv). Control groups are the same as in Figure 4.2. *C. elegans* exposed to the CR mimetic, resveratrol, for at least seven days have a higher rate of average maximal respiration as compared to the control. * p -value ≤ 0.05 ; ** p -value ≤ 0.01 ; *** p -value ≤ 0.001 .

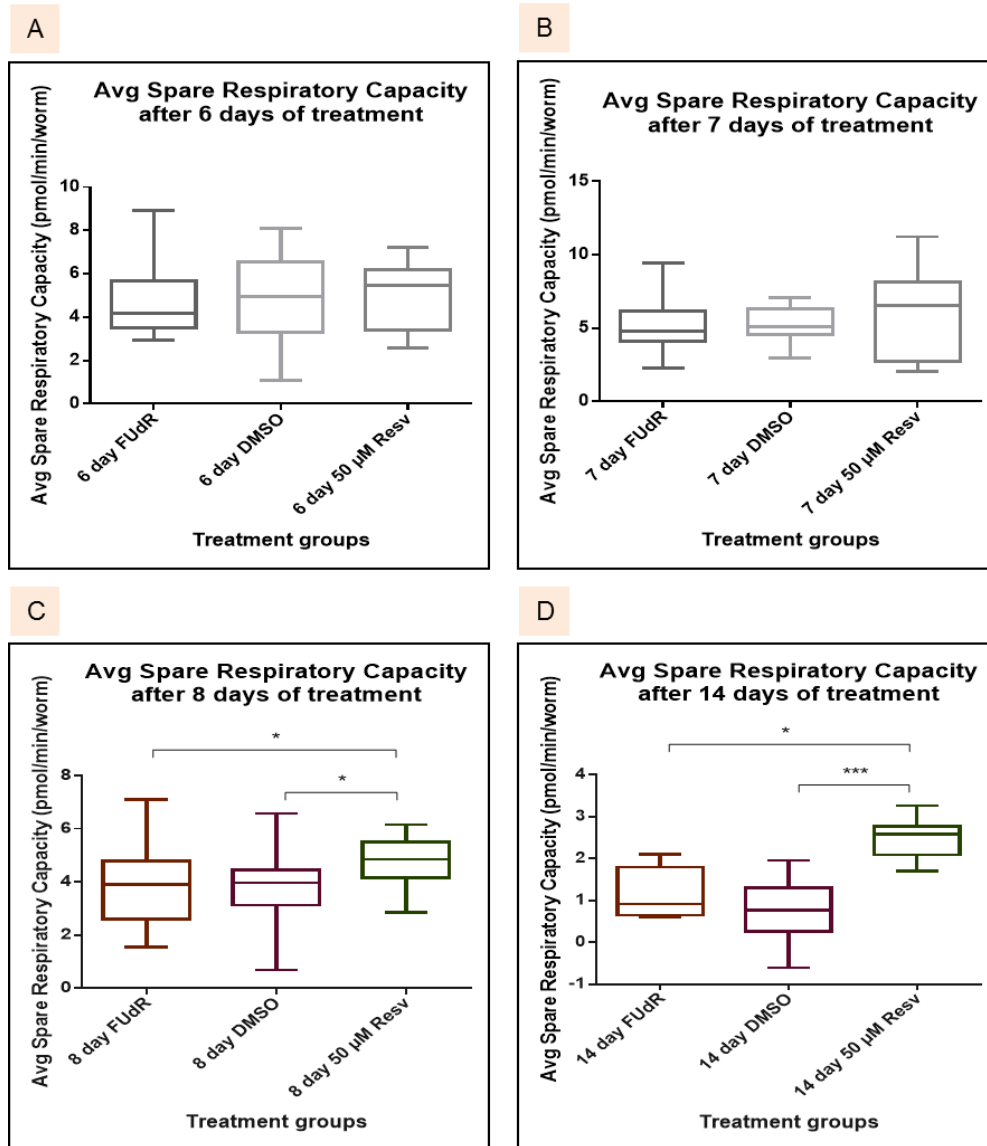


Figure 4.4: Average spare respiratory capacity of *C. elegans* exposed to (A) 6 days, (B) 7 days, (C) 8 days, and (D) 14 days of FUDR + 50 μ M resveratrol (Resv). Control groups are the same as in Figure 4.2. *C. elegans* exposed to the CR mimetic, resveratrol, for at least eight days have a higher average spare respiratory capacity as compared to the control. Hence, an 8-day treatment period is optimal for detecting the effects of CR mimetics like resveratrol on mitochondrial function. * p -value ≤ 0.05 ; ** p -value ≤ 0.01 ; *** p -value ≤ 0.001 .

Our discovery supported a recent study which also observed a rise in *C. elegans* basal mitochondrial respiration rates when resveratrol was introduced to the worms (Houtkooper *et al.*, 2013). A likely hypothesis for this intriguing observation is that resveratrol can mimic a CR state, and causes metabolism to

shift away from glycolysis towards respiration so as to sustain body function. Therefore, there is an elevated electron transport, basal respiration, and ROS generation similar to the effects of CR (Lin *et al.*, 2002; Moroz *et al.*, 2014). This low exposure to a greater oxidative stress triggers a secondary adaptive response called mitohormesis in the host's defence system, leading to improved stress resistance and life span extension (Schulz *et al.*, 2007; Kim *et al.*, 2015).

In addition, the increase in spare respiratory capacity in *C. elegans* after prolonged resveratrol treatment also supported other similar studies in mice, whereby the aerobic capacity was improved after a 15-week administration of resveratrol (Lagouge *et al.*, 2006). The effect of resveratrol treatment on spare respiratory capacity also appeared to mirror that of CR, which has been shown to improve spare respiratory capacity in mice fed with 60% of *ad libitum* diet (Cerqueira *et al.*, 2012). This further substantiates the ability of resveratrol to function as a CR mimetic in living systems, and supports the use of resveratrol as a reference compound to be compared against during drug hit identification via mitochondrial function assays after an 8-day treatment. Therefore, this can facilitate the screening of potential CR mimetics. The anti-aging properties of selected drug hits can subsequently be validated by life span assays.

4.3.2 Establishing a reference mitochondrial function profile using resveratrol as a caloric restriction mimetic

When the dose of resveratrol was varied during the 8-day treatment, both 40 μ M resveratrol and 50 μ M resveratrol treatments can elicit an increase in basal respiration (Figure 4.5). However, only the 8-day 50 μ M resveratrol treatment can cause a significant increase in maximal respiration and spare respiratory capacity. This suggests a dose-dependent effect of resveratrol on mitochondrial function. Since our polyketide and alkaloid library of compounds can only be biosynthesized to sub-micro molar amounts by the *E. coli* constructs growing on the NGM agar plates, any identified drug lead from mitochondrial function assays will be more potent than resveratrol as a CR mimetic. This may help to minimize any adverse effects which are common with resveratrol treatment.

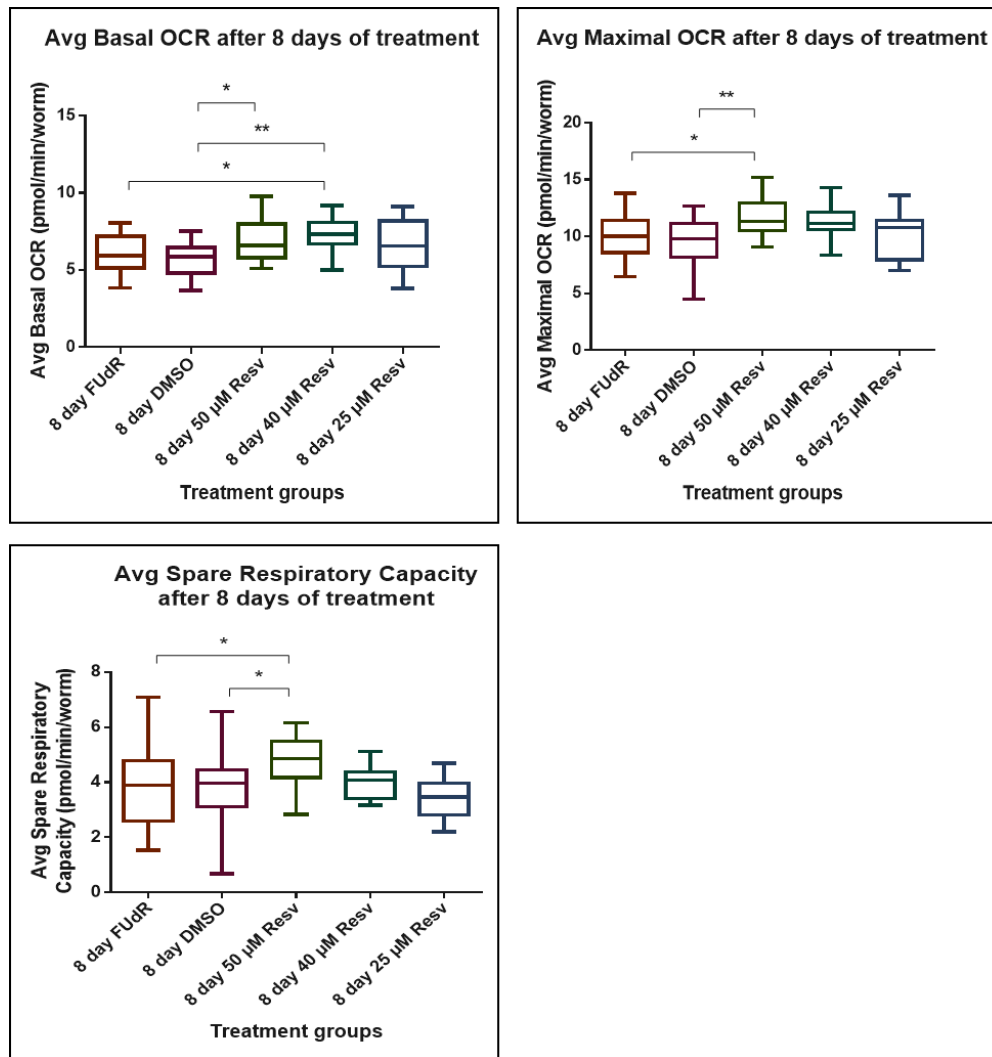


Figure 4.5: Average basal OCR, maximal OCR, and spare respiratory capacity of *C. elegans* exposed to 8 days of FUDR + varying concentrations of resveratrol (Resv). Control groups are the same as in Figure 4.2. Dose-dependent effects of resveratrol are present, and only *C. elegans* exposed to 50 μ M resveratrol had a significantly higher basal respiration, maximal respiration, and spare respiratory capacity compared to controls. * p -value ≤ 0.05 ; ** p -value ≤ 0.01 .

C. elegans eat-2 mutants have a pharyngeal muscle pumping defect, leading to a compromised food intake and allowing mutants to undergo chronic CR and subsequently life span extension. Indeed, *eat-2* mutants can live approximately 38% longer than wild-type *C. elegans* (Figure 4.6). *C. elegans eat-2* mutants were also found to have a higher basal respiration,

maximal respiration, and spare respiratory capacity compared to wild-type worms (Figure 4.7). This is consistent with the effects of resveratrol on mitochondrial function, highlighting the potential of mitochondrial function assays in screening for CR mimetics. Nevertheless, subjecting *eat-2* mutants to resveratrol treatment did not increase the basal OCR, maximal OCR, and spare respiratory capacity further. This suggests that resveratrol may cause a strain on the mitochondrial function of the *eat-2* mutants which were already experiencing chronic CR. Indeed, exposing *eat-2* mutants to 50 μ M resveratrol treatment resulted in a shorter mean life span (15.9 days) compared to *eat-2* mutants which were exposed to 0.1% DMSO (20.0 days) (Figure 4.8). Therefore, subjecting the mutants to a further exposure of a CR mimetic may result in some detrimental effects on mitochondrial function, leading to a shorter life span.

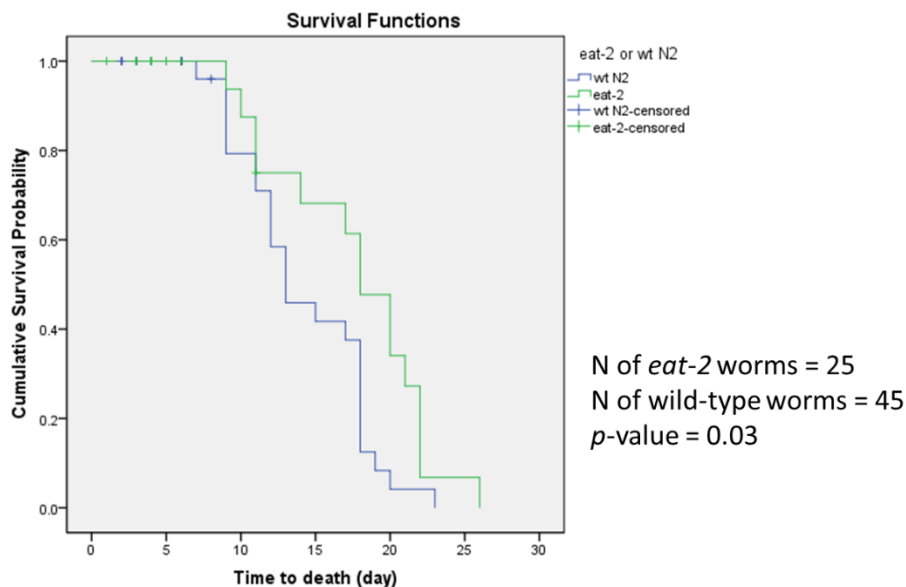


Figure 4.6: The mean life span of *C. elegans eat-2* mutants (17.6 days) was significantly longer than the mean life span of wild-type worms (14.3 days).

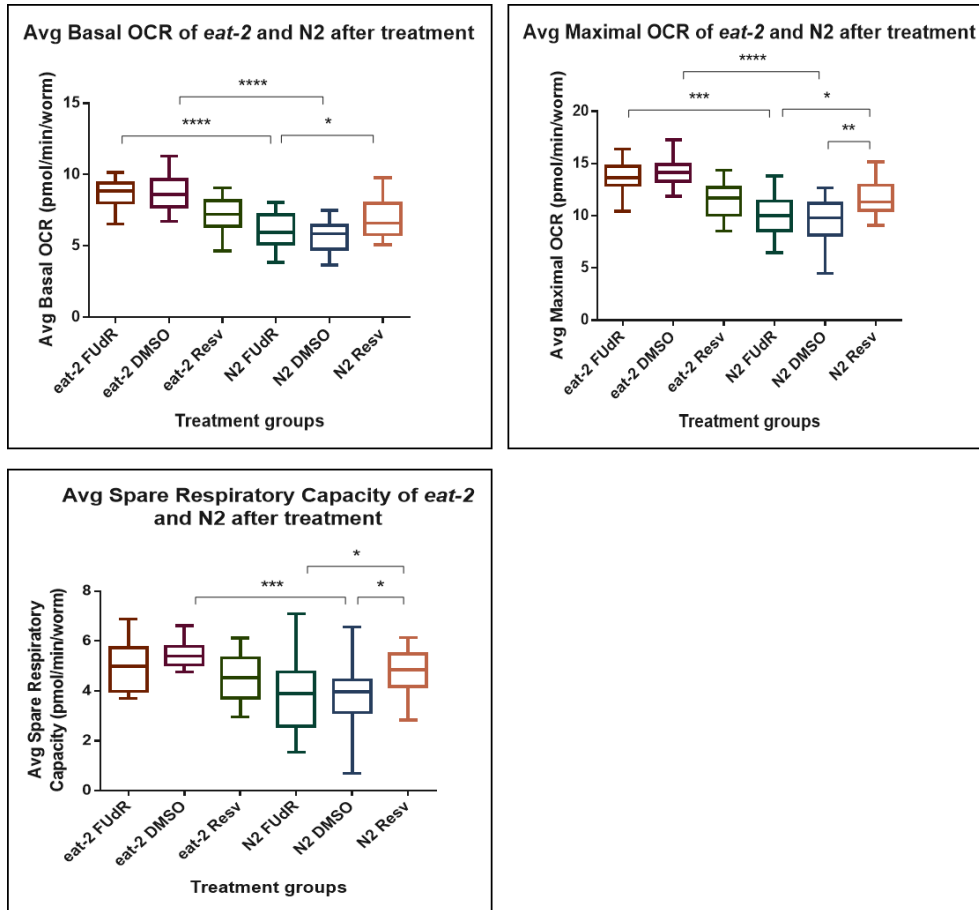


Figure 4.7: Consistent with results using the CR mimetic resveratrol, *eat-2* mutants undergo chronic CR and have a higher basal respiration, maximal respiration, and spare respiratory capacity compared to wild-type *C. elegans*. Introducing 50 μ M resveratrol to *eat-2* mutants does not improve their mitochondrial function further. FUDR: worms exposed to FUDR treatment only; DMSO: worms exposed to FUDR + DMSO; Resv: worms exposed to FUDR + 50 μ M resveratrol. * p -value ≤ 0.05 ; ** p -value ≤ 0.01 ; *** p -value ≤ 0.001 ; **** p -value ≤ 0.0001 .

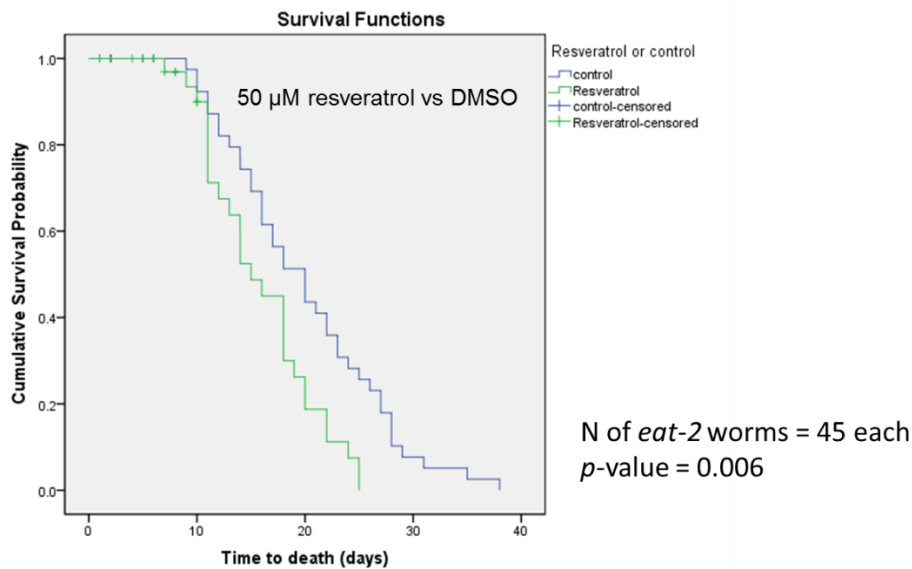


Figure 4.8: The mean life span of *C. elegans eat-2* mutants subjected to 50 μ M resveratrol treatment (15.9 days) was significantly shorter than the mean life span of *C. elegans eat-2* mutants subjected to 0.1% DMSO treatment only (20.0 days).

Resveratrol was found to activate AMPK and sirtuins, resulting in PGC-1 α activation and increasing mitochondrial biogenesis and respiration rate (Lagouge *et al.*, 2006; Um *et al.*, 2010; Gertz *et al.*, 2012; Park *et al.*, 2012). CR on the other hand, can activate AMPK and sirtuins while inhibiting the IGF-1 and mTOR pathways (Kenyon, 2010; Moroz *et al.*, 2014). Interestingly, *C. elegans daf-2* mutants, which have compromised IGF-1 signaling and also live longer compared to wild-type worms, do not have the same improvement in mitochondrial function as *eat-2* mutants or wild-type worms subjected to CR mimetic treatment (Figure 4.9). This is in contrast to previous studies which found *daf-2* mutants to have a higher basal respiration than wild-type worms (Houthoofd *et al.*, 2005). This could be due to the fact that *daf-2* mutants are approximately 37% smaller in volume compared to wild-type worms, and previous studies normalized the OCR to protein content in the

worms rather than worm number. However, normalizing metabolic data to protein content can still be inaccurate as the true amount of metabolically active mass is always unknown (Braeckman *et al.*, 2002).

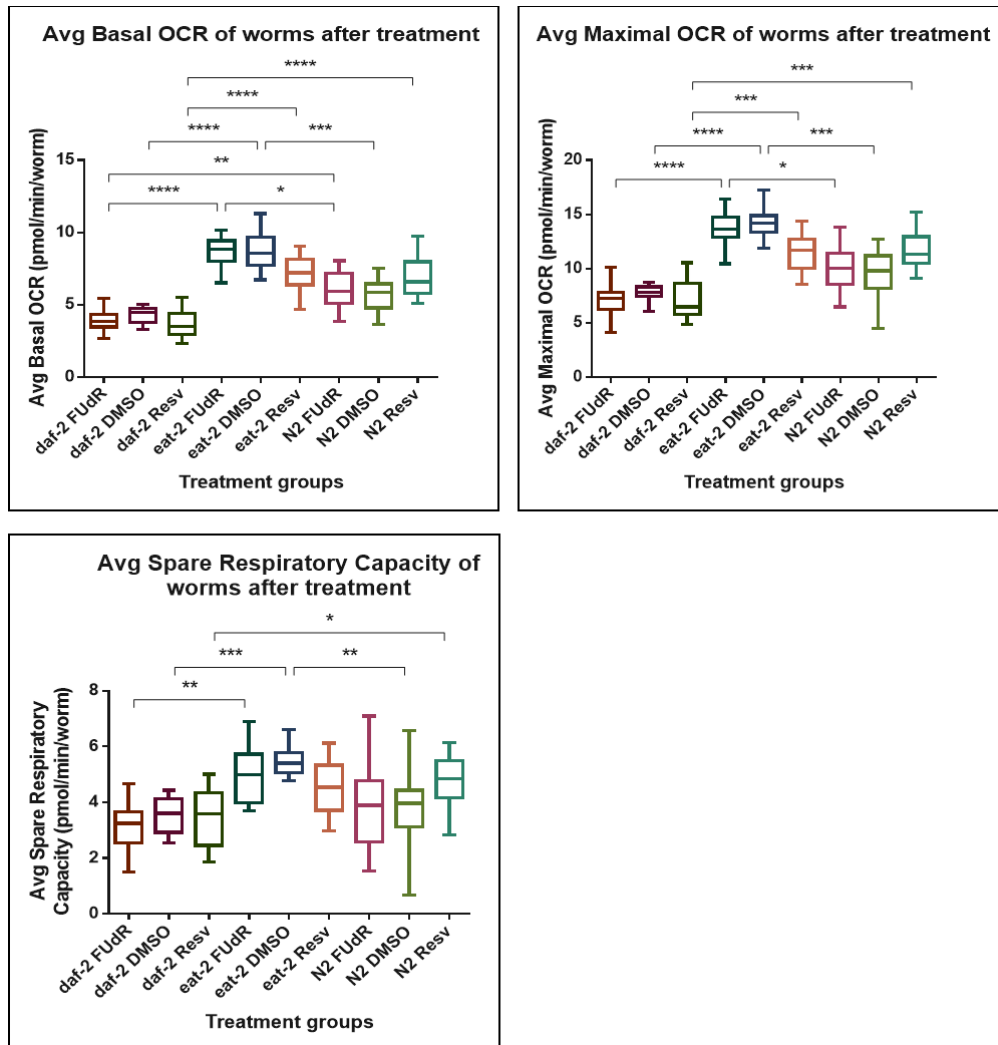


Figure: 4.9: *C. elegans daf-2* mutants seem to have a lower basal respiration, maximal respiration, and spare respiratory capacity compared to *eat-2* and wild-type *C. elegans*. Introducing 50 μ M resveratrol to *eat-2* and *daf-2* mutants does not improve their mitochondrial function further. FUDR: worms exposed to FUDR treatment only; DMSO: worms exposed to FUDR + DMSO; Resv: worms exposed to FUDR + 50 μ M resveratrol. * p -value ≤ 0.05 ; ** p -value ≤ 0.01 ; *** p -value ≤ 0.001 ; **** p -value ≤ 0.0001 .

Nevertheless, the results also show that *daf-2* mutants are resistant to the effects of resveratrol, since subjecting *daf-2* mutants to resveratrol treatment failed to improve their mitochondrial function further. This suggests that CR mimetics may act partly through the insulin/IGF-1 pathway too. A recent study on mouse intestinal fibroblasts found that resveratrol can inhibit the binding of IGF-1 to its receptor, in addition to activating Sirt1 (Li *et al.*, 2014). More studies are needed to investigate the actual mechanisms of resveratrol, so as to validate whether CR biochemical pathways are indeed targeted.

All in all, sufficient evidence has pointed to the fact that resveratrol can mimic some aspects of CR, and can extend the life span of several model organisms, although the detailed mechanism of action is still unknown. Using the OCR profile of wild-type *C. elegans* exposed to 8 days of 50 μ M resveratrol, and the OCR profile of *eat-2* mutants as references, we can screen our library of polyketides and alkaloids for potential CR mimetics. A molecular screening platform where novel compound libraries are screened in *C. elegans*-based mitochondrial function assays is thus developed.

4.3.3 Screening for more potent caloric restriction mimetics

Since life span assays are not efficient in screening for anti-aging compounds, *E. coli* constructs and selected combinations of starters and extenders leading to the biosynthesis of novel polyketides or alkaloids were supplemented to *C. elegans*, and their mitochondrial function was analyzed using an extracellular flux analyzer. This will serve as a higher-throughput platform to identify other promising CR mimetic drug hits from our library of

compounds, which have a similar metabolic flux profile to resveratrol. Due to time constraint, only a few novel polyketides and alkaloids from our compound library were tested, and none of them significantly improved the mitochondrial function of wild-type *C. elegans*.

For instance, when ethylmalonic acid and *p*-coumaric acid were incorporated into the NGM agar together with either the control or the CHS18 *E. coli* construct, N2 worms exposed to the novel polyketides, ethylmalonyl-CoA, and *p*-coumaroyl-CoA did not have a significantly higher basal respiration, maximal respiration, and spare respiratory capacity compared to worms exposed to the CoA esters only (Figure 4.10). Similarly, worms exposed to the novel polyketides, butylmalonyl-CoA, and *p*-coumaroyl-CoA did not have a significantly higher basal respiration, maximal respiration, and spare respiratory capacity compared to worms exposed to the CoA esters only (Figure 4.11). Also, when malonic acid and the nitrogen-containing 3-aminobenzoic acid were incorporated into the NGM agar together with the respective *E. coli* constructs, worms exposed to the novel alkaloids, malonyl-CoA, and 3-aminobenzoyl-CoA did not have a significantly higher basal respiration, maximal respiration, and spare respiratory capacity compared to worms exposed to the CoA esters only (Figure 4.12).

Interestingly, either the carboxylic acids used or the CoA esters produced by the ligases seem to increase the respiration of N2 worms when compared to worms exposed to FUdR only. This is similar to the conclusions derived from life span assays, whereby N2 worms exposed to the control *E. coli* construct and certain combinations of carboxylic acids had a longer life span compared to other worms which were exposed to the same control *E. coli* strain but

different combination of acids (Figure 2.13). However, when N2 worms were treated with 1 mM butylmalonic acid and 0.5 mM *p*-coumaric acid only in NGM agar with OP50 *E. coli* as the food source, the basal respiration, maximal respiration, and spare respiratory capacity were not significantly improved compared to worms exposed to FUDR only (Figure 4.13). This rules out any potential effect on mitochondrial function that is due to an exposure to a low dose of carboxylic acids. More studies are needed to find out whether the CoA esters indeed play a role in affecting the mitochondrial function of *C. elegans*. All in all, by developing mitochondrial function assays, we can screen our libraries for anti-aging compounds more efficiently.

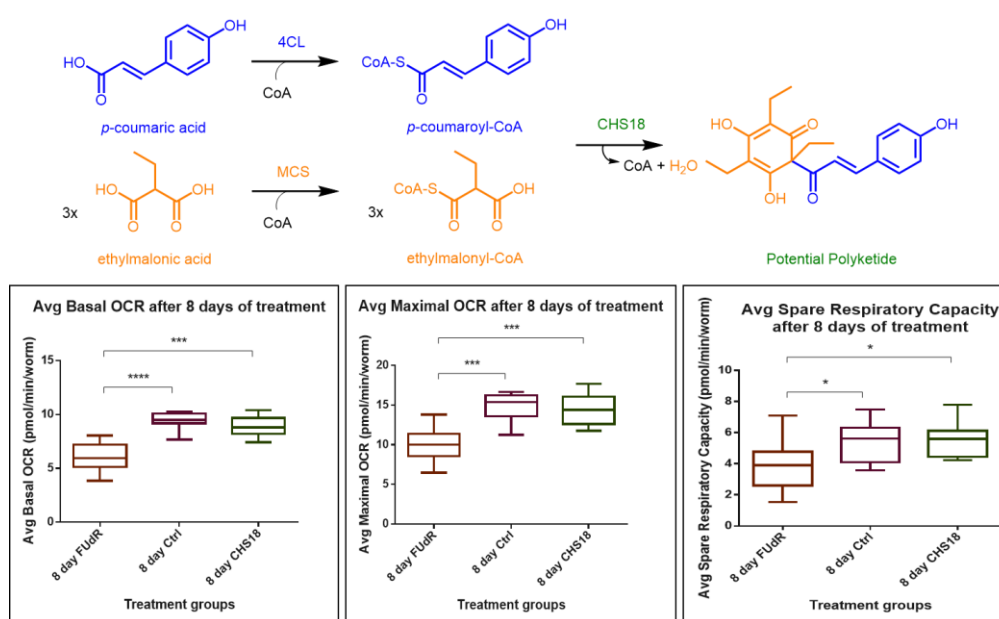


Figure 4.10: Ethylmalonic acid and *p*-coumaric acid were incorporated into NGM agar together with either the control (Ctrl) or CHS18 *E. coli* construct. *C. elegans* exposed to novel polyketides and CoA esters produced by the CHS18 *E. coli* construct (contains CoA ligases + CHS18) do not have a higher basal respiration, maximal respiration, and spare respiratory capacity compared to *C. elegans* exposed to CoA esters only (control construct contains CoA ligases only). FUDR: worms exposed to FUDR treatment only. * *p*-value ≤ 0.05; ** *p*-value ≤ 0.01; *** *p*-value ≤ 0.001; **** *p*-value ≤ 0.0001.

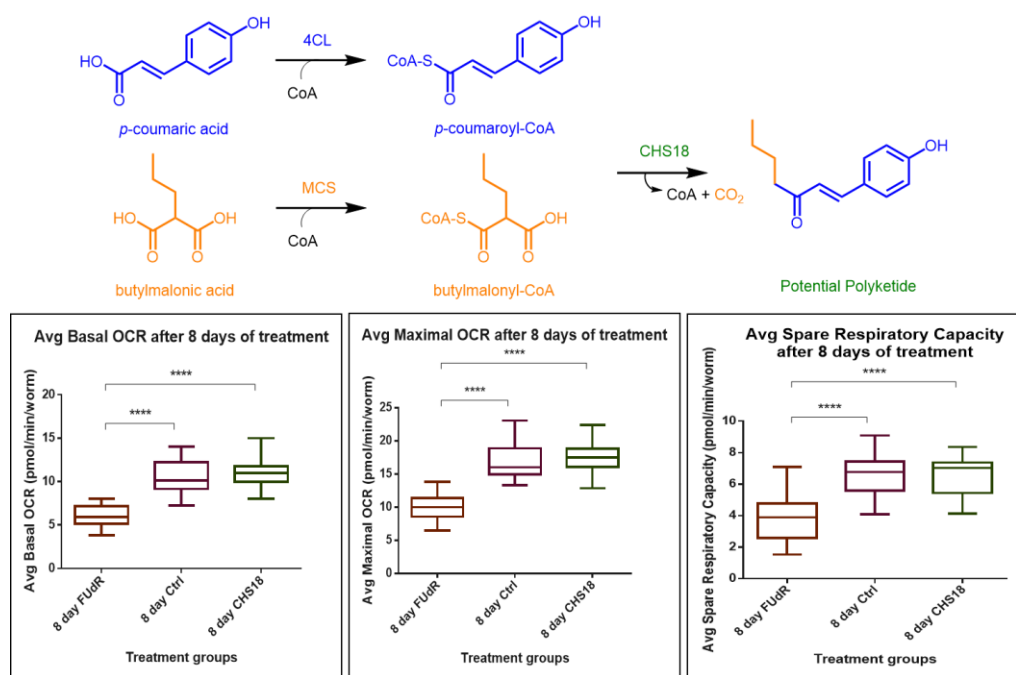


Figure 4.11: Butylmalonic acid and *p*-coumaric acid were incorporated into NGM agar together with either the control (Ctrl) or CHS18 *E. coli* construct. *C. elegans* exposed to novel polyketides and CoA esters produced by the CHS18 *E. coli* construct (contains CoA ligases + CHS18) do not have a higher basal respiration, maximal respiration, and spare respiratory capacity compared to *C. elegans* exposed to CoA esters only (control construct contains CoA ligases only). FUDR: worms exposed to FUDR treatment only. **** *p*-value ≤ 0.0001.

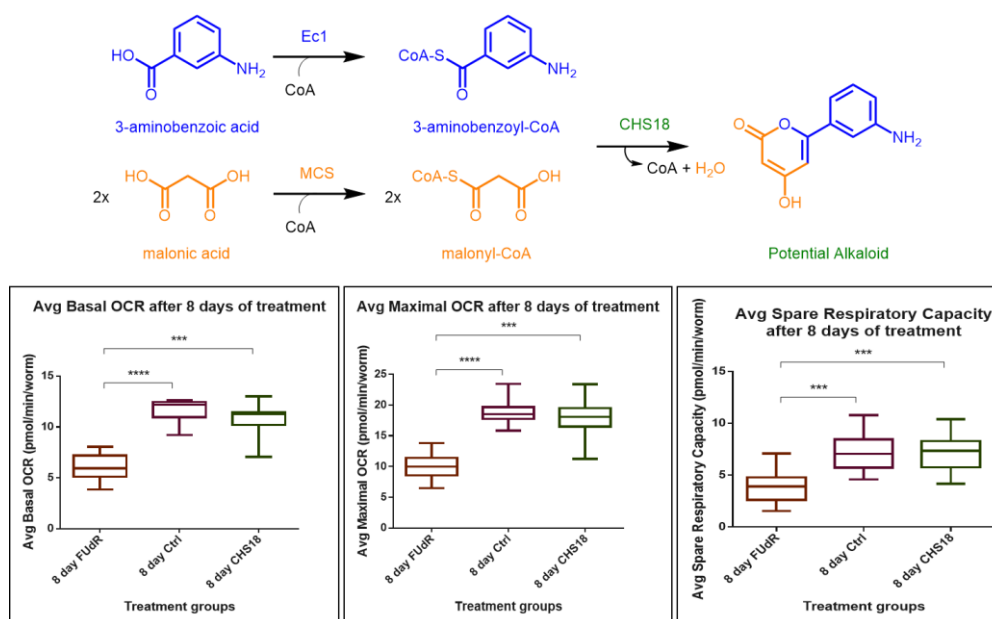


Figure 4.12: Malonic acid and 3-aminobenzoic acid were incorporated into NGM agar together with either the control (Ctrl) or CHS18 *E. coli* construct. *C. elegans* exposed to novel alkaloids and CoA esters produced by the CHS18 *E. coli* construct (contains CoA ligases + CHS18) do not have a higher basal respiration, maximal respiration, and spare respiratory capacity compared to *C. elegans* exposed to CoA esters only (control construct contains CoA ligases only). FUDR: worms exposed to FUDR treatment only. *** p -value ≤ 0.001 ; **** p -value ≤ 0.0001 .

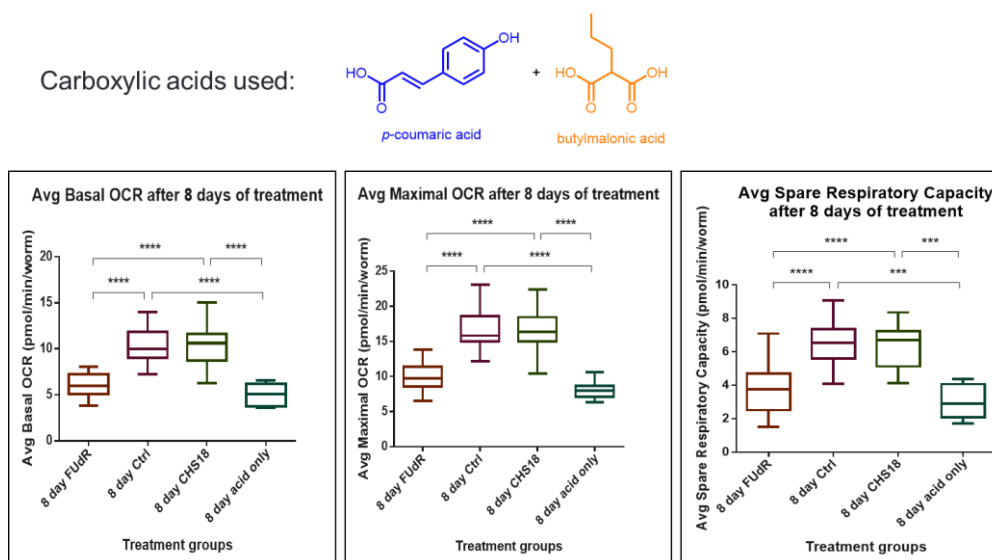


Figure 4.13: *C. elegans* exposed to p-coumaric acid and butylmalonic acid only do not have a higher basal respiration, maximal respiration, and spare respiratory capacity compared to *C. elegans* exposed to FUDR only. *** p -value ≤ 0.001 ; **** p -value ≤ 0.0001 .

CHAPTER 5: FUTURE DIRECTIONS IN ANTI-AGING NUTRACEUTICAL DEVELOPMENT AND CONCLUSION

Ever since the discovery of the first “longevity gene”, *age-1*, in *C. elegans*, there has been a steady progress in understanding how we age, hence allowing us to develop strategies to counter the effects of aging. CR is currently still the best means to achieve a longer and healthier life span, but it is difficult to have the discipline to adhere to such a rigorous intervention. Furthermore, there could be side effects like depression and hypotension. By studying the biology of aging and targeting the biochemical pathways affected by CR without restricting calorie intake, it is hoped that maximal life span can one day be increased and bring upon a reduction in the severity of age-related diseases like cancer and diabetes. However, we first need a library of potential drug compounds and an effective screening platform, before we can embark on the journey to develop anti-aging drug leads.

Since the diversity of the compounds biosynthesized by PKSs is partly dependent on the starter and extender units, variations in the choice of starters and extenders is important. However, combinatorial biosynthesis is limited by the means to introduce novel acyl-CoA precursors to PKSs for the biosynthesis of novel compounds. Precursor-directed combinatorial biosynthesis using CoA ligases and a type III PKS, CHS18 was demonstrated to be a viable approach that can be utilized for the biosynthesis of novel polyketides. By using a combination of 69 starters and 12 extenders, the diversity and complexity of the polyketides produced were enhanced, and at least 413 unnatural polyketides were generated. As the crystal structures of other type III PKSs are continuously made accessible from the Protein Data

Bank (PDB), more rational approaches of structure-based engineering can be adopted in addition to precursor-directed combinatorial biosynthesis, for the production of more novel polyketides. This strategy is advantageous because other than the choice of starter and extender, the number of rounds of polyketide chain extension and the intramolecular mode of cyclization of the linear polyketide intermediate can affect the diversity of the polyketide produced. By incorporating choice mutations into the active site cavity of the PKS, polyketide chain elongation and the cyclization mode of the intermediate can be modified.

In fact, a recent report demonstrated that although octaketides are not usually synthesized by the wild type *S. baicalensis* CHS, the S338V mutant CHS was found to produce trace amounts of SEK4 and SEK4b using eight units of malonyl-CoA (Abe *et al.*, 2006). This S338V mutation was proposed to facilitate the extension of the linear polyketide intermediate into a buried pocket in the active site cavity of the enzyme by providing steric guidance. Therefore, it was demonstrated for the first time that CHS could be engineered to generate longer polyketides such as octaketides. This suggests that rational site-directed mutagenesis efforts can be used to generate PKSs with different substrate selectivities and altered product profiles, thereby producing more diverse novel polyketides.

Yields of certain target compounds can also be increased by conducting site-directed mutagenesis on CHS18 to find mutants with better activity. A previous study in our lab showed that a S341N mutation in a chalcone synthase from *Oryza sativa* led to an improved yield of a tetraketide pyrone from 3-(4'-methoxy)phenylpropanoyl-CoA and malonyl-CoA (Go *et al.*,

2015). Hence, we can also carry out a similar mutation in CHS18 to increase the activity of CHS18 and subsequently, the yield of various products.

Since the polyketides only contribute to a relatively small group of natural products, the project was extended to look into the biosynthesis of other natural product classes such as the alkaloids, which are also known to possess important biological activities. Therefore, the precursor-directed combinatorial biosynthesis of novel natural products was expanded by testing more nitrogen-containing substrates and looking into the substrate specificities of more CoA ligases. This allows the introduction of novel nitrogen-containing acyl-CoA precursors to PKSs for alkaloid biosynthesis, highlighting a unique and simpler method to generate a large library of novel alkaloids. CHS18 was able to catalyze the condensation of malonyl-CoA with three out of 14 nitrogen-containing starter acyl-CoA esters separately to form alkaloids. The next step will be to test the nitrogen-containing starters with the rest of the 11 malonyl-CoA derivatives in order to produce a library of bioactive alkaloids. We can also look into the biosynthesis of other natural product classes such as isoprenoids, so as to further enrich our compound library for anti-aging drug screening.

After developing a substantial library of novel compounds, we then focused on the development of an efficient screening platform for anti-aging drug hits. Since life span assays are time consuming and not practical for screening a huge compound library, mitochondrial function assays were used as sufficient evidence has pointed to a link between metabolism, CR mimetics, and anti-aging. Although a consensus has not been reached regarding the exact pathways targeted, both CR and CR mimetics like resveratrol can induce a

physiological shift towards respiration away from glycolysis in order to maintain body function. This leads to a small increase in ROS production and causes an elevated and improved oxidative stress response via mitohormesis, enabling the host to better counteract the effects of aging and live longer.

In fact, many studies have continually disproved the mitochondrial free radical theory of aging and an increase in ROS is viewed as a consequence rather than a cause of aging (Lagouge and Larsson, 2013). ROS are now viewed as important mediators and signaling molecules of the stress response to age-associated damage. This explains why many antioxidant therapies have failed to delay the progression of age-associated diseases and extend life span in clinical trials.

On the other hand, CR in *C. elegans* has been shown to induce catalase enzyme activity and improve oxidative stress resistance, resulting in a longer life span (Schulz *et al.*, 2007). Further research by other researchers (Lagouge *et al.*, 2006; Moroz *et al.*, 2014) and this study led to the conclusion that life span, mitochondrial function, CR and CR mimetics are intricately linked. By supplying our compound library to *C. elegans* for eight days and looking at their respiration rates and mitochondrial function, we can quickly narrow down potential CR mimetics without having to go through a lengthy life span assay.

Beyond the *in vivo* screening, additional evaluation of *in vivo* effects are necessary. Reduced body temperature, lower plasma insulin levels, increased mitochondrial biogenesis, and enhanced protection against oxidative stress are also important biomarkers of CR (Ingram *et al.*, 2006). Hence, after a drug hit

is identified through mitochondrial function assays, it will be useful to test the compound in mice or rats and evaluate the effects on these biomarkers, in addition to mitochondrial function and toxicity studies.

Once we have identified a promising anti-aging drug lead with minimal adverse effects, we can either use the drug directly in humans or incorporate the combinatorial biosynthetic pathway into a probiotic strain such as *E. coli* Nissle 1917. Hence, in addition to preventing diseases of the gastrointestinal tract, the probiotic Nissle strain can lead to a stable biosynthesis of anti-aging drugs within the human host. More research still needs to be done, and currently we are building a combinatorial biosynthetic pathway involving phenylalanine ammonia lyase (PAL) as an enzyme upstream of the CoA ligases and CHS18. PAL is able to deaminate phenylalanine and tyrosine to cinnamic acid and coumaric acid respectively, while 4CL can utilize these carboxylic acids to produce starter acyl-CoAs for CHS18 for the biosynthesis of potential anti-aging compounds. Nutraceuticals are food or parts of food that provide health or medical benefits such as the prevention or treatment of diseases (De and Ghosh, 2012). It will be very interesting if we can make use of nutraceuticals such as an engineered strain of *E. coli* Nissle to deliver anti-aging compounds constantly to the body.

Nevertheless, as drug candidates undergo different validation assessments, it is important to note that aging is a complex process affecting different biochemical pathways, macromolecules, organelles and tissues. There are nine hallmarks of aging which are interconnected and we have only focused mainly on interventions targeting deregulated nutrient sensing and mitochondrial dysfunction (Lopez-Otin *et al.*, 2013). Hence, the key to the Fountain of Youth

may lie in a ‘cocktail’ of drug compounds rather than a single drug approach. This study is a primer towards the development of therapeutic drugs in the emerging field of anti-aging research.

REFERENCES

- Abe, I.** (2012). Novel applications of plant polyketide synthases. Curr Opin Chem Biol 16(1-2): 179-185.
- Abe, I. and Morita, H.** (2010). Structure and function of the chalcone synthase superfamily of plant type III polyketide synthases. Nat Prod Rep 27(6): 809-838.
- Abe, I., Takahashi, Y., Lou, W. and Noguchi, H.** (2003). Enzymatic formation of unnatural novel polyketides from alternate starter and nonphysiological extension substrate by chalcone synthase. Org Lett 5(8): 1277-1280.
- Abe, I., Watanabe, T., Morita, H., Kohno, T. and Noguchi, H.** (2006). Engineered biosynthesis of plant polyketides - manipulation of chalcone synthase. Org Lett 8(3): 499-502.
- Alberts, A. W., Chen, J., Kuron, G., Hunt, J., Huff, J., Hoffman, C., Rothrock, J., Lopez, M., Joshua, H., Harris, E., Patchett, A., Monaghan, R., Currie, S., Stapley, E., Albers-Schonberg, G., Hensens, O., Hirshfield, J., Hoogsteen, K., Liesch, J. and Springer, J.** (1980). Mevinolin - A highly potent competitive inhibitor of hydroxymethylglutaryl-coenzyme A reductase and a cholesterol-lowering agent. Proc Natl Acad Sci U S A 77(7): 3957-3961.
- Aldawsari, F. S., Elshenawy, O. H., El Gendy, M. A., Aguayo-Ortiz, R., Baksh, S., El-Kadi, A. O. and Velazquez-Martinez, C. A.** (2015). Design and synthesis of resveratrol-salicylate hybrid derivatives as CYP1A1 inhibitors. J Enzyme Inhib Med Chem 30(6): 884-895.
- Anisimov, V. N.** (2013). Metformin: do we finally have an anti-aging drug? Cell Cycle 12(22): 3483-3489.
- Anisimov, V. N., Berstein, L. M., Egormin, P. A., Piskunova, T. S., Popovich, I. G., Zabezhinski, M. A., Tyndyk, M. L., Yurova, M. V., Kovalenko, I. G., Poroshina, T. E. and Semenchenko, A. V.** (2008). Metformin slows down aging and extends life span of female SHR mice. Cell Cycle 7(17): 2769-2773.
- Appadurai, P. and Rathinasamy, K.** (2014). Indicine N-oxide binds to tubulin at a distinct site and inhibits the assembly of microtubules: A mechanism for its cytotoxic activity. Toxicol Lett 225(1): 66-77.
- Austin, M. B., Bowman, M. E., Ferrer, J. L., Schroder, J. and Noel, J. P.** (2004). An aldol switch discovered in stilbene synthases mediates cyclization specificity of type III polyketide synthases. Chem Biol 11(9): 1179-1194.
- Austin, M. B. and Noel, J. P.** (2003). The chalcone synthase superfamily of type III polyketide synthases. Nat Prod Rep 20(1): 79-110.

Bass, T. M., Weinkove, D., Houthoofd, K., Gems, D. and Partridge, L. (2007). Effects of resveratrol on lifespan in *Drosophila melanogaster* and *Caenorhabditis elegans*. Mech Ageing Dev 128(10): 546-552.

Benz, R. and McLaughlin, S. (1983). The molecular mechanism of action of the proton ionophore FCCP (carbonylcyanide p-trifluoromethoxyphenylhydrazone). Biophys J 41(3): 381-398.

Beuerle, T. and Pichersky, E. (2002). Enzymatic synthesis and purification of aromatic coenzyme A esters. Anal Biochem 302(2): 305-312.

Birch, A. J. and Donovan, F. W. (1953). Studies in relation to biosynthesis. I. Some possible routes to derivatives of orcinol and phloroglucinol. Aust J Chem 6: 360-368.

Bishop, N. A. and Guarente, L. (2007). Two neurons mediate diet-restriction-induced longevity in *C. elegans*. Nature 447(7144): 545-549.

Bolen, S., Feldman, L., Vassy, J., Wilson, L., Yeh, H. C., Marinopoulos, S., Wiley, C., Selvin, E., Wilson, R., Bass, E. B. and Brancati, F. L. (2007). Systematic review: comparative effectiveness and safety of oral medications for type 2 diabetes mellitus. Ann Intern Med 147(6): 386-399.

Braeckman, B. P., Houthoofd, K. and Vanfleteren, J. R. (2002). Assessing metabolic activity in aging *Caenorhabditis elegans*: concepts and controversies. Aging Cell 1: 82-88.

Brenner, S. (1974). The genetics of *Caenorhabditis elegans*. Genetics 77(1): 71-94.

Bua, E., Johnson, J., Herbst, A., Delong, B., McKenzie, D., Salamat, S. and Aiken, J. M. (2006). Mitochondrial DNA-deletion mutations accumulate intracellularly to detrimental levels in aged human skeletal muscle fibers. Am J Hum Genet 79(3): 469-480.

Calne, R. Y., Collier, D. S., Lim, S., Pollard, S. G., Samaan, A., White, D. J. and Thiru, S. (1989). Rapamycin for immunosuppression in organ allografting. Lancet 2(8656): 227.

Cameron, D. E., Bashor, C. J. and Collins, J. J. (2014). A brief history of synthetic biology. Nat Rev Microbiol 12(5): 381-390.

Cerqueira, F. M., Cunha, F. M., Laurindo, F. R. and Kowaltowski, A. J. (2012). Calorie restriction increases cerebral mitochondrial respiratory capacity in a NO*-mediated mechanism: impact on neuronal survival. Free Radic Biol Med 52(7): 1236-1241.

Cesari, M., Vellas, B. and Gambassi, G. (2013). The stress of aging. Exp Gerontol 48(4): 451-456.

- Chemler, J. A. and Koffas, M. A.** (2008). Metabolic engineering for plant natural product biosynthesis in microbes. Curr Opin Biotechnol 19(6): 597-605.
- Chow, Y. L. and Sato, F.** (2013). Screening of isoquinoline alkaloids for potent lipid metabolism modulation with *Caenorhabditis elegans*. Biosci Biotechnol Biochem 77(12): 2405-2412.
- Chung, J. H., Manganiello, V. and Dyck, J. R. B.** (2012). Resveratrol as a calorie restriction mimetic: therapeutic implications. Trends Cell Biol 22(10): 546-554.
- Collie, J. N.** (1907). Derivatives of the multiple keten group. J Chem Soc, Trans 91: 1806-1813.
- Cordell, G. A.** (2013). Fifty years of alkaloid biosynthesis in Phytochemistry. Phytochemistry 91: 29-51.
- Cordell, G. A., Quinn-Beattie, M. L. and Farnsworth, N. R.** (2001). The potential of alkaloids in drug discovery. Phytother Res 15(3): 183-205.
- Cottart, C. H., Nivet-Antoine, V., Laguillier-Morizot, C. and Beaudeux, J. L.** (2010). Resveratrol bioavailability and toxicity in humans. Mol Nutr Food Res 54(1): 7-16.
- Cox, R. J.** (2007). Polyketides, proteins and genes in fungi: programmed nano-machines begin to reveal their secrets. Org Biomol Chem 5(13): 2010-2026.
- Crowell, J. A., Korytko, P. J., Morrissey, R. L., Booth, T. D. and Levine, B. S.** (2004). Resveratrol-associated renal toxicity. Toxicol Sci 82(2): 614-619.
- Daly, J. W., Myers, C. W. and Whittaker, N.** (1987). Further classification of skin alkaloids from neotropical poison frogs (Dendrobatidae), with a general survey of toxic/noxious substances in the amphibia. Toxicon 25(10): 1023-1095.
- Dancy, B. M., Kayser, E., Sedensky, M. M. and Morgan, P. G.** (2013). Live worm respiration in 24-well format. WBG 19(4): 11-12.
- De, D. and Ghosh, D.** (2012). Resveratrol: a potent antidiabetic nutraceutical. J Community Nutr Health 1(2): 65-70.
- Dhahbi, J. M., Mote, P. L., Fahy, G. M. and Spindler, S. R.** (2005). Identification of potential caloric restriction mimetics by microarray profiling. Physiol Genomics 23(3): 343-350.
- Dirks, A. J. and Leeuwenburgh, C.** (2006). Caloric restriction in humans: potential pitfalls and health concerns. Mech Ageing Dev 127(1): 1-7.
- Dodds, E. C.** (1946). The search for morphine substitutes. Br Med Bull 4(2): 88-91.

Dorman, J. B., Albinder, B., Shroyer, T. and Kenyon, C. (1995). The age-1 and daf-2 genes function in a common pathway to control the lifespan of *Caenorhabditis elegans*. Genetics *141*(4): 1399-1406.

Dunn, B. J. and Khosla, C. (2013). Engineering the acyltransferase substrate specificity of assembly line polyketide synthases. J R Soc Interface *10*(85): 20130297.

Facchini, P. J. (2001). Alkaloid biosynthesis in plants: Biochemistry, cell biology, molecular regulation and metabolic engineering applications. Annu Rev Plant Physiol Plant Mol Biol *52*: 29-66.

Ferrer, J. L., Jez, J. M., Bowman, M. E., Dixon, R. A. and Noel, J. P. (1999). Structure of chalcone synthase and the molecular basis of plant polyketide biosynthesis. Nat Struct Biol *6*(8): 775-784.

Ferrick, D. A., Neilson, A. and Beeson, C. (2008). Advances in measuring cellular bioenergetics using extracellular flux. Drug Discov Today *13*(5-6): 268-274.

Finkel, T. and Holbrook, N. J. (2000). Oxidants, oxidative stress and the biology of ageing. Nature *408*(6809): 239-247.

Finley, L. W., Lee, J., Souza, A., Desquirit-Dumas, V., Bullock, K., Rowe, G. C., Procaccio, V., Clish, C. B., Arany, Z. and Haigis, M. C. (2012). Skeletal muscle transcriptional coactivator PGC-1 α mediates mitochondrial, but not metabolic, changes during calorie restriction. Proc Natl Acad Sci U S A *109*(8): 2931-2936.

Fontana, L., Meyer, T. E., Klein, S. and Holloszy, J. O. (2004). Long-term calorie restriction is highly effective in reducing the risk for atherosclerosis in humans. Proc Natl Acad Sci U S A *101*(17): 6659-6663.

Friedman, D. B. and Johnson, T. E. (1988). A mutation in the age-1 gene in *Caenorhabditis elegans* lengthens life and reduces hermaphrodite fertility. Genetics *118*(1): 75-86.

Gems, D. and Partridge, L. (2013). Genetics of longevity in model organisms: debates and paradigm shifts. Annu Rev Physiol *75*: 621-644.

Gertz, M., Nguyen, G. T., Fischer, F., Suenkel, B., Schlicker, C., Franzel, B., Tomaschewski, J., Aladini, F., Becker, C., Wolters, D. and Steegborn, C. (2012). A molecular mechanism for direct sirtuin activation by resveratrol. PLoS One *7*(11): e49761.

Go, M. K., Chow, J. Y., Cheung, V. W., Lim, Y. P. and Yew, W. S. (2012). Establishing a toolkit for precursor-directed polyketide biosynthesis: exploring substrate promiscuities of acid-CoA ligases. Biochemistry *51*(22): 4568-4579.

Go, M. K., Wongsantichon, J., Cheung, V. W. N., Chow, J. Y., Robinson, R. C. and Yew, W. S. (2015). Synthetic Polyketide Enzymology: Platform for Biosynthesis of Antimicrobial Polyketides. ACS Catalysis 5(7): 4033-4042.

Goldberg, D. M., Yan, J. and Soleas, G. J. (2003). Absorption of three wine-related polyphenols in three different matrices by healthy subjects. CLB 36(1): 79-87.

Greer, E. L. and Brunet, A. (2009). Different dietary restriction regimens extend lifespan by both independent and overlapping genetic pathways in *C. elegans*. Aging Cell 8(2): 113-127.

Gruber, J., Ng, L. F., Poovathingal, S. K. and Halliwell, B. (2009). Deceptively simple but simply deceptive--*Caenorhabditis elegans* lifespan studies: considerations for aging and antioxidant effects. FEBS Lett 583(21): 3377-3387.

Gruber, J., Tang, S. Y. and Halliwell, B. (2007). Evidence for a trade-off between survival and fitness caused by resveratrol treatment of *Caenorhabditis elegans*. Ann N Y Acad Sci 1100: 530-542.

Guarente, L. (2013). Calorie restriction and sirtuins revisited. Genes Dev 27(19): 2072-2085.

Hansen, M., Taubert, S., Crawford, D., Libina, N., Lee, S. J. and Kenyon, C. (2007). Lifespan extension by conditions that inhibit translation in *Caenorhabditis elegans*. Aging Cell 6(1): 95-110.

Heilbronn, L. K. and Ravussin, E. (2003). Caloric restriction and aging: review of the literature and implications for studies in humans. Am J Clin Nutr 78(3): 361-369.

Honda, Y. and Honda, S. (2002). Oxidative stress and life span determination in the nematode *Caenorhabditis elegans*. Ann N Y Acad Sci 959: 466-474.

Houthoofd, K., Fidalgo, M. A., Hoogewijs, D., Braeckman, B. P., Lenaerts, I., Brys, K., Matthijssens, F., De Vreese, A., Van Eygen, S., Munoz, M. J. and Vanfleteren, J. R. (2005). Metabolism, physiology and stress defense in three aging *Ins/IGF-1* mutants of the nematode *Caenorhabditis elegans*. Aging Cell 4(2): 87-95.

Houthoofd, K. and Vanfleteren, J. R. (2006). The longevity effect of dietary restriction in *Caenorhabditis elegans*. Exp Gerontol 41(10): 1026-1031.

Houtkooper, R. H., Mouchiroud, L., Ryu, D., Moullan, N., Katsyuba, E., Knott, G., Williams, R. W. and Auwerx, J. (2013). Mitonuclear protein imbalance as a conserved longevity mechanism. Nature 497(7450): 451-457.

Houtkooper, R. H., Williams, R. W. and Auwerx, J. (2010). Metabolic networks of longevity. Cell 142(1): 9-14.

Ingram, D. K., Zhu, M., Mamczarz, J., Zou, S., Lane, M. A., Roth, G. S. and deCabo, R. (2006). Calorie restriction mimetics: an emerging research field. Aging Cell 5(2): 97-108.

Jez, J. M., Bowman, M. E. and Noel, J. P. (2002). Expanding the biosynthetic repertoire of plant type III polyketide synthases by altering starter molecule specificity. Proc Natl Acad Sci U S A 99(8): 5319-5324.

Jez, J. M., Ferrer, J. L., Bowman, M. E., Dixon, R. A. and Noel, J. P. (2000). Dissection of malonyl-coenzyme A decarboxylation from polyketide formation in the reaction mechanism of a plant polyketide synthase. Biochemistry 39(5): 890-902.

Jia, K., Chen, D. and Riddle, D. L. (2004). The TOR pathway interacts with the insulin signaling pathway to regulate *C. elegans* larval development, metabolism and life span. Development 131(16): 3897-3906.

Karmase, A., Jagtap, S. and Bhutani, K. K. (2013). Anti adipogenic activity of *Aegle marmelos* Correa. Phytomedicine 20(14): 1267-1271.

Katsuyama, Y., Funa, N., Miyahisa, I. and Horinouchi, S. (2007). Synthesis of unnatural flavonoids and stilbenes by exploiting the plant biosynthetic pathway in *Escherichia coli*. Chem Biol 14(6): 613-621.

Kenyon, C. J. (2010). The genetics of ageing. Nature 464(7288): 504-512.

Kim, M. I., Kwon, S. J. and Dordick, J. S. (2009). In vitro precursor-directed synthesis of polyketide analogues with coenzyme A regeneration for the development of antiangiogenic agents. Org Lett 11(17): 3806-3809.

Kim, S. E., Mori, R., Komatsu, T., Chiba, T., Hayashi, H., Park, S., Sugawa, M. D., Dencher, N. A. and Shimokawa, I. (2015). Upregulation of cytochrome c oxidase subunit 6b1 (Cox6b1) and formation of mitochondrial supercomplexes: implication of Cox6b1 in the effect of calorie restriction. Age (Dordr) 37(3): 9787.

Kim, Y. S. and Bang, S. K. (1988). Assays for malonyl-coenzyme A synthase. Anal Biochem 170(1): 45-49.

Klass, M. R. (1977). Aging in the nematode *Caenorhabditis elegans*: major biological and environmental factors influencing life span. Mech Ageing Dev 6(6): 413-429.

Ko, B. S., Choi, S. B., Park, S. K., Jang, J. S., Kim, Y. E. and Park, S. (2005). Insulin sensitizing and insulinotropic action of berberine from *Cortidis rhizoma*. Biol Pharm Bull 28(8): 1431-1437.

Kobayashi, S., Ueno, M., Suzuki, R., Ishitani, H., Kim, H. S. and Wataya, Y. (1999). Catalytic asymmetric synthesis of antimalarial alkaloids febrifugine and isofebrifugine and their biological activity. J Org Chem 64(18): 6833-6841.

Kwon, S. J., Kim, M. I., Ku, B., Coulombel, L., Kim, J. H., Shawky, J. H., Linhardt, R. J. and Dordick, J. S. (2010). Unnatural polyketide analogues selectively target the HER signaling pathway in human breast cancer cells. Chembiochem 11(4): 573-580.

Lagouge, M., Argmann, C., Gerhart-Hines, Z., Meziane, H., Lerin, C., Daussin, F., Messadeq, N., Milne, J., Lambert, P., Elliott, P., Geny, B., Laakso, M., Puigserver, P. and Auwerx, J. (2006). Resveratrol improves mitochondrial function and protects against metabolic disease by activating SIRT1 and PGC-1 α . Cell 127(6): 1109-1122.

Lagouge, M. and Larsson, N. G. (2013). The role of mitochondrial DNA mutations and free radicals in disease and ageing. J Intern Med 273(6): 529-543.

Lakowski, B. and Hekimi, S. (1998). The genetics of caloric restriction in *Caenorhabditis elegans*. Proc Natl Acad Sci U S A 95(22): 13091-13096.

Lanza, I. R. and Nair, K. S. (2010). Mitochondrial function as a determinant of life span. Pflugers Arch 459(2): 277-289.

Laurent, P., Braekman, J. C., Daloze, D. and Pasteels, J. (2003). Biosynthesis of defensive compounds from beetles and ants. Eur J Org Chem 2003(15): 2733-2743.

Lesch, J. E. (1981). Conceptual change in an empirical science: the discovery of the first alkaloids. Hist Stud Phys Sci 11(2): 305-328.

Li, P., Liang, M. L., Zhu, Y., Gong, Y. Y., Wang, Y., Heng, D. and Lin, L. (2014). Resveratrol inhibits collagen I synthesis by suppressing IGF-1R activation in intestinal fibroblasts. World J Gastroenterol 20(16): 4648-4661.

Lin, S. J., Kaeberlein, M., Andalis, A. A., Sturtz, L. A., Defossez, P. A., Culotta, V. C., Fink, G. R. and Guarente, L. (2002). Calorie restriction extends *Saccharomyces cerevisiae* lifespan by increasing respiration. Nature 418(6895): 344-348.

Liu, Y., Liu, W. and Liang, Z. (2015). Endophytic bacteria from *Pinellia ternata*, a new source of purine alkaloids and bacterial manure. Pharm Biol 53(10): 1545-1548.

Lopez-Otin, C., Blasco, M. A., Partridge, L., Serrano, M. and Kroemer, G. (2013). The hallmarks of aging. Cell 153(6): 1194-1217.

Maglioni, S., Schiavi, A., Runci, A., Shaik, A. and Ventura, N. (2014). Mitochondrial stress extends lifespan in *C. elegans* through neuronal hormesis. Exp Gerontol 56: 89-98.

Martin, G. M. (2011). The biology of aging: 1985-2010 and beyond. FASEB J 25(11): 3756-3762.

- McCay, C. M., Crowell, M. F. and Maynard, L. A.** (1935). The effect of retarded growth upon the length of life span and upon the ultimate body size. J Nutr 10(1): 63-79.
- Meneses, A.** (1998). Physiological, pathophysiological and therapeutic roles of 5-HT systems in learning and memory. Rev Neurosci 9(4): 275-289.
- Menzies, K. J. and Hood, D. A.** (2012). The role of SirT1 in muscle mitochondrial turnover. Mitochondrion 12(1): 5-13.
- Minami, H., Kim, J. S., Ikezawa, N., Takemura, T., Katayama, T., Kumagai, H. and Sato, F.** (2008). Microbial production of plant benzyloquinoline alkaloids. Proc Natl Acad Sci U S A 105(21): 7393-7398.
- Minois, N.** (2014). Molecular basis of the 'anti-aging' effect of spermidine and other natural polyamines - a mini-review. Gerontology 60(4): 319-326.
- Mitchell, D. H., Stiles, J. W., Santelli, J. and Sanadi, D. R.** (1979). Synchronous growth and aging of *Caenorhabditis elegans* in the presence of fluorodeoxyuridine. J Gerontol 34(1): 28-36.
- Moran, B. W., Anderson, F. P., Devery, A., Cloonan, S., Butler, W. E., Varughese, S., Draper, S. M. and Kenny, P. T.** (2009). Synthesis, structural characterisation and biological evaluation of fluorinated analogues of resveratrol. Bioorg Med Chem 17(13): 4510-4522.
- Morita, H., Noguchi, H., Schroder, J. and Abe, I.** (2001). Novel polyketides synthesised with a higher plant stilbene synthase. Eur J Biochem 268(13): 3759-3766.
- Morita, H., Yamashita, M., Shi, S. P., Wakimoto, T., Kondo, S., Kato, R., Sugio, S., Kohno, T. and Abe, I.** (2011). Synthesis of unnatural alkaloid scaffolds by exploiting plant polyketide synthase. Proc Natl Acad Sci U S A 108(33): 13504-13509.
- Moroz, N., Carmona, J. J., Anderson, E., Hart, A. C., Sinclair, D. A. and Blackwell, T. K.** (2014). Dietary restriction involves NAD⁺-dependent mechanisms and a shift toward oxidative metabolism. Aging Cell 13(6): 1075-1085.
- Morris, J. Z., Tissenbaum, H. A. and Ruvkun, G.** (1996). A phosphatidylinositol-3-OH kinase family member regulating longevity and diapause in *Caenorhabditis elegans*. Nature 382(6591): 536-539.
- Mouchiroud, L., Houtkooper, R. H., Moullan, N., Katsyuba, E., Ryu, D., Cantó, C., Mottis, A., Jo, Y. S., Viswanathan, M., Schoonjans, K., Guarente, L. and Auwerx, J.** (2013). The NAD⁺/Sirtuin Pathway Modulates Longevity through Activation of Mitochondrial UPR and FOXO Signaling. Cell 154(2): 430-441.

Navrotskaya, V. V., Oxenkrug, G., Vorobyova, L. I. and Summergrad, P. (2012). Berberine Prolongs Life Span and Stimulates Locomotor Activity of. Am J Plant Sci 3(7A): 1037-1040.

Newman, D. J. and Cragg, G. M. (2012). Natural products as sources of new drugs over the 30 years from 1981 to 2010. J Nat Prod 75(3): 311-335.

Olshansky, S. J., Goldman, D. P., Zheng, Y. and Rowe, J. W. (2009). Aging in America in the twenty-first century: demographic forecasts from the MacArthur Foundation Research Network on an aging society. Milbank Q 87(4): 842-862.

Park, S. J., Ahmad, F., Philp, A., Baar, K., Williams, T., Luo, H., Ke, H., Rehmann, H., Taussig, R., Brown, A. L., Kim, M. K., Beaven, M. A., Burgin, A. B., Manganiello, V. and Chung, J. H. (2012). Resveratrol Ameliorates Aging-Related Metabolic Phenotypes by Inhibiting cAMP Phosphodiesterases. Cell 148(3): 421-433.

Pirola, L. and Frojdo, S. (2008). Resveratrol: one molecule, many targets. IUBMB Life 60(5): 323-332.

Schuh, R. A., Jackson, K. C., Khairallah, R. J., Ward, C. W. and Spangenburg, E. E. (2012). Measuring mitochondrial respiration in intact single muscle fibers. Am J Physiol Regul Integr Comp Physiol 302(6): R712-719.

Schulz, T. J., Zarse, K., Voigt, A., Urban, N., Birringer, M. and Ristow, M. (2007). Glucose restriction extends *Caenorhabditis elegans* life span by inducing mitochondrial respiration and increasing oxidative stress. Cell Metab 6(4): 280-293.

Schuz, R., Heller, W. and Hahlbrock, K. (1983). Substrate specificity of chalcone synthase from *Petroselinum hortense*. J Biol Chem 258(11): 6730-6734.

Seo, A. Y. and Leeuwenburgh, C. (2015). The Role of Genome Instability in Frailty: Mitochondria versus Nucleus. Nestle Nutr Inst Workshop Ser 83: 19-27.

Servillo, L., D'Onofrio, N., Longobardi, L., Sirangelo, I., Giovane, A., Cautela, D., Castaldo, D., Giordano, A. and Balestrieri, M. L. (2013). Stachydrine ameliorates high-glucose induced endothelial cell senescence and SIRT1 downregulation. J Cell Biochem 114(11): 2522-2530.

Shen, B. (2003). Polyketide biosynthesis beyond the type I, II and III polyketide synthase paradigms. Curr Opin Chem Biol 7(2): 285-295.

Shomura, Y., Torayama, I., Suh, D. Y., Xiang, T., Kita, A., Sankawa, U. and Miki, K. (2005). Crystal structure of stilbene synthase from *Arachis hypogaea*. Proteins 60(4): 803-806.

Sohal, R. S. and Weindruch, R. (1996). Oxidative stress, caloric restriction, and aging. Science 273(5271): 59-63.

Staunton, J. and Weissman, K. J. (2001). Polyketide biosynthesis: a millennium review. Nat Prod Rep 18(4): 380-416.

Stein, P. K., Soare, A., Meyer, T. E., Cangemi, R., Holloszy, J. O. and Fontana, L. (2012). Caloric restriction may reverse age-related autonomic decline in humans. Aging Cell 11(4): 644-650.

Stewart, C., Jr., Vickery, C. R., Burkart, M. D. and Noel, J. P. (2013). Confluence of structural and chemical biology: plant polyketide synthases as biocatalysts for a bio-based future. Curr Opin Plant Biol 16(3): 365-372.

Stiernagle, T. (2006). Maintenance of *C. elegans*. WormBook: 1-11.

Stockigt, J. and Zenk, M. H. (1975). Chemical syntheses and properties of hydroxycinnamoyl-coenzyme A derivatives. Z Naturforsch C 30(3): 352-358.

Tatar, M., Kopelman, A., Epstein, D., Tu, M. P., Yin, C. M. and Garofalo, R. S. (2001). A mutant *Drosophila* insulin receptor homolog that extends life-span and impairs neuroendocrine function. Science 292(5514): 107-110.

Tatsuta, K. and Hosokawa, S. (2006). Total syntheses of polyketide-derived bioactive natural products. Chem Rec 6(4): 217-233.

Tissenbaum, H. A. and Ruvkun, G. (1998). An insulin-like signaling pathway affects both longevity and reproduction in *Caenorhabditis elegans*. Genetics 148(2): 703-717.

Tropf, S., Lanz, T., Rensing, S. A., Schroder, J. and Schroder, G. (1994). Evidence that stilbene synthases have developed from chalcone synthases several times in the course of evolution. J Mol Evol 38(6): 610-618.

Um, J. H., Park, S. J., Kang, H., Yang, S., Foretz, M., McBurney, M. W., Kim, M. K., Viollet, B. and Chung, J. H. (2010). AMP-activated protein kinase-deficient mice are resistant to the metabolic effects of resveratrol. Diabetes 59(3): 554-563.

Vendelbo, M. H. and Nair, K. S. (2011). Mitochondrial longevity pathways. Biochim Biophys Acta 1813(4): 634-644.

Walford, R. L., Harris, S. B. and Weindruch, R. (1987). Dietary restriction and aging: historical phases, mechanisms and current directions. J Nutr 117(10): 1650-1654.

Walford, R. L., Mock, D., Verdery, R. and MacCallum, T. (2002). Caloric restriction in biosphere 2: alterations in physiologic, hematologic, hormonal, and biochemical parameters in humans restricted for a 2-year period. J Gerontol A Biol Sci Med Sci 57(6): B211-224.

Wang, D. T., He, J., Wu, M., Li, S. M., Gao, Q. and Zeng, Q. P. (2015). Artemisinin mimics calorie restriction to trigger mitochondrial biogenesis and compromise telomere shortening in mice. PeerJ 3: e822.

Wang, H., Mu, W., Shang, H., Lin, J. and Lei, X. (2014). The antihyperglycemic effects of Rhizoma Coptidis and mechanism of actions: a review of systematic reviews and pharmacological research. Biomed Res Int 2014: 798093.

Wattanathorn, J., Chonpathompikunlert, P., Muchimapura, S., Priprem, A. and Tankamnerdthai, O. (2008). Piperine, the potential functional food for mood and cognitive disorders. Food Chem Toxicol 46(9): 3106-3110.

Weindruch, R., Walford, R. L., Fligiel, S. and Guthrie, D. (1986). The retardation of aging in mice by dietary restriction: longevity, cancer, immunity, and lifetime energy intake. J Nutr 116(4): 641-654.

Wright, L. F. and Hopwood, D. A. (1976). Actinorhodin is a chromosomally-determined antibiotic in *Streptomyces coelicolor* A3(2). J Gen Microbiol 96(2): 289-297.

Wu, Z., Puigserver, P., Andersson, U., Zhang, C., Adelmant, G., Mootha, V., Troy, A., Cinti, S., Lowell, B., Scarpulla, R. C. and Spiegelman, B. M. (1999). Mechanisms Controlling Mitochondrial Biogenesis and Respiration through the Thermogenic Coactivator PGC-1. Cell 98(1): 115-124.

Yamaguchi, T., Kurosaki, F., Suh, D. Y., Sankawa, U., Nishioka, M., Akiyama, T., Shibuya, M. and Ebizuka, Y. (1999). Cross-reaction of chalcone synthase and stilbene synthase overexpressed in *Escherichia coli*. FEBS Lett 460(3): 457-461.

Young, C. A., Schardl, C. L., Panaccione, D. G., Florea, S., Takach, J. E., Charlton, N. D., Moore, N., Webb, J. S. and Jaromczyk, J. (2015). Genetics, genomics and evolution of ergot alkaloid diversity. Toxins (Basel) 7(4): 1273-1302.

Yuan, Y., Kadiyala, C. S., Ching, T. T., Hakimi, P., Saha, S., Xu, H., Yuan, C., Mullangi, V., Wang, L., Fivenson, E., Hanson, R. W., Ewing, R., Hsu, A. L., Miyagi, M. and Feng, Z. (2012). Enhanced energy metabolism contributes to the extended life span of calorie-restricted *Caenorhabditis elegans*. J Biol Chem 287(37): 31414-31426.

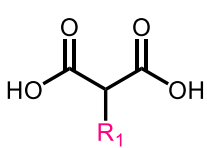

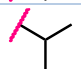
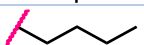
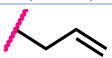
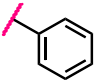
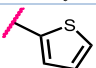
Zhao, H. and Darzynkiewicz, Z. (2014). Attenuation of replication stress-induced premature cellular senescence to assess anti-aging modalities. Curr Protoc Cytom 69: 9.47.41-49.47.10.

Zhou, G., Myers, R., Li, Y., Chen, Y., Shen, X., Fenyk-Melody, J., Wu, M., Ventre, J., Doebber, T., Fujii, N., Musi, N., Hirshman, M. F., Goodyear, L. J. and Moller, D. E. (2001). Role of AMP-activated protein kinase in mechanism of metformin action. J Clin Invest 108(8): 1167-1174.

Ziegler, J. and Facchini, P. J. (2008). Alkaloid biosynthesis: metabolism and trafficking. Annu Rev Plant Biol 59: 735-769.

APPENDIX

Table A1: Carboxylic acids and the corresponding CoA ligases used for the precursor-directed combinatorial biosynthesis of polyketides.

Malonate type	R ₁	Extender carboxylic acid	CoA ligase used
	-H	Malonic acid	MCS
	-CH ₃	Methylmalonic acid	MCS
		Ethylmalonic acid	MCS
		Isopropylmalonic acid	MCS
		Butylmalonic acid	MCS
		Allylmalonic acid	MCS
	-OH	Hydroxymalonic acid	MCS
	-F	Fluoromalonic acid	MCS
	-Cl	Chloromalonic acid	MCS
	-Br	Bromomalonic acid	MCS
		Phenylmalonic acid	PCL
		3-thiophenemalonic acid	PCL

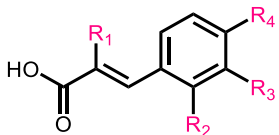
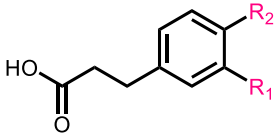
Cinnamate type	R _x	Starter carboxylic acid	CoA ligase used
	None	Cinnamic acid	4CL
	R ₂ : -F	2-fluorocinnamic acid	4CL
	R ₃ : -F	3-fluorocinnamic acid	4CL
	R ₄ : -F	4-fluorocinnamic acid	4CL
	R ₁ : -F	α-fluorocinnamic acid	4CL
	R ₃ : -Cl	3-chlorocinnamic acid	4CL
	R ₃ : -Cl R ₄ : -OCH ₃	3-chloro-4-methoxy cinnamic acid	4CL
	R ₄ : -Cl	4-chlorocinnamic acid	4CL
	R ₂ : -OH	2-hydroxycinnamic acid	4CL
	R ₄ : -OH	4-hydroxycinnamic acid	4CL
	R ₃ : -OCH ₃ R ₄ : -OH	3-methoxy-4-hydroxy cinnamic acid	4CL
	R ₄ : -OCH ₃	4-methoxycinnamic acid	4CL
	R ₄ : -CH ₃	4-methylcinnamic acid	4CL
	R ₁ : -CH ₃	α-methylcinnamic acid	4CL

Table A1 (continued)

Phenylpropanoate type	R _x	Starter carboxylic acid	CoA ligase used
	None	3-phenylpropanoic acid	4CL
	R ₁ : -Cl	3-(3'-chloro) phenylpropanoic acid	4CL
	R ₁ : -Cl R ₂ : -OCH ₃	3-(3'-chloro-4'-methoxy) phenylpropanoic acid	4CL
	R ₁ : -OH R ₂ : -OH	3-(3',4'-dihydroxy) phenylpropanoic acid	4CL
	R ₁ : -OCH ₃	3-(3'-methoxy) phenylpropanoic acid	4CL
	R ₂ : -OCH ₃	3-(4'-methoxy) phenylpropanoic acid	4CL
	R ₂ : -F	3-(4'-fluoro) phenylpropanoic acid	4CL

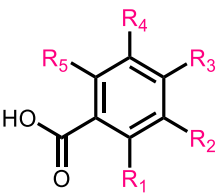
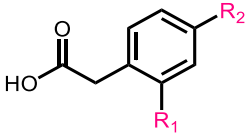
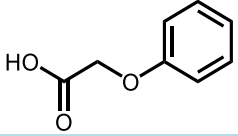
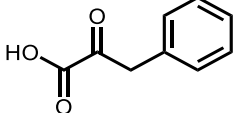
Benzoate type	R _x	Starter carboxylic acid	CoA ligase used
	None	Benzoic acid	BZL
	R ₁ : -F	2-fluorobenzoic acid	BZL
	R ₂ : -F	3-fluorobenzoic acid	BZL
	R ₃ : -F	4-fluorobenzoic acid	BZL
	R ₁ : -F R ₅ : -F	2,6-difluorobenzoic acid	BZL
	R ₁ : -Cl	2-chlorobenzoic acid	BZL
	R ₂ : -Cl	3-chlorobenzoic acid	BZL
	R ₃ : -Cl	4-chlorobenzoic acid	BZL
	R ₁ : -Br	2-bromobenzoic acid	BZL
	R ₂ : -Br	3-bromobenzoic acid	BZL
	R ₃ : -Br	4-bromobenzoic acid	BZL
	R ₁ : -I	2-iodobenzoic acid	BZL
	R ₁ : -OH	2-hydroxybenzoic acid	BZL
	R ₁ : -OH R ₂ : -OH	2,3-dihydroxybenzoic acid	BZL
	R ₁ : -OH R ₃ : -OH	2,4-dihydroxybenzoic acid	BZL
	R ₁ : -OH R ₄ : -OH	2,5-dihydroxybenzoic acid	BZL
	R ₁ : -OCH ₃	2-methoxybenzoic acid	BZL
	R ₁ : -CH ₃	2-methylbenzoic acid	BZL
	R ₂ : -NH ₂	3-aminobenzoic acid	BZL
	R ₃ : -NH ₂	4-aminobenzoic acid	BZL

Table A1 (continued)

Phenylacetate type	R _x	Starter carboxylic acid	CoA ligase used
	None	Phenylacetic acid	PCL
	R ₁ : -OH	2-hydroxyphenylacetic acid	PCL
	R ₂ : -OH	4-hydroxyphenylacetic acid	PCL
	R ₂ : -OCH ₃	4-methoxyphenylacetic acid	PCL
	None	Phenoxyacetic acid	PCL
	None	Phenylpyruvic acid	PCL

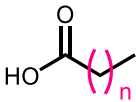
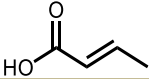
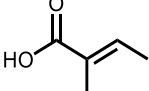
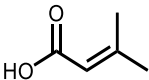
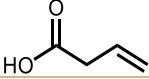
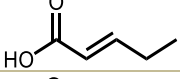
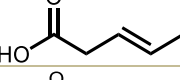
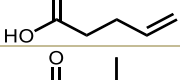

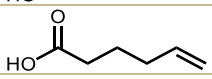

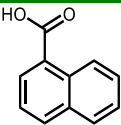
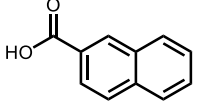
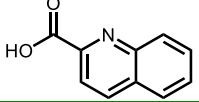
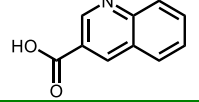
Saturated aliphatic type	n	Starter carboxylic acid	CoA ligase used
	1	Propanoic acid	BZL
	2	Butanoic acid	BZL or PCL
	3	Pentanoic acid	PCL
	4	Hexanoic acid	4CL
	5	Heptanoic acid	4CL
	6	Octanoic acid	4CL
	7	Nonanoic acid	4CL
	8	Decanoic acid	4CL

Table A1 (continued)

Unsaturated aliphatic type	Starter carboxylic acid	CoA ligase used
	2-butenic acid	BZL
	2-methyl-2-butenic acid	BZL
	3-methyl-2-butenic acid	BZL
	3-butenic acid	BZL
	2-pentenic acid	BZL
	3-pentenic acid	PCL
	4-pentenic acid	BZL
	3-methyl-4-pentenic acid	PCL
	3-hexenic acid	PCL
	5-hexenic acid	PCL

Naphthalene and quinoline type	Starter carboxylic acid	CoA ligase used
	1-naphthalenecarboxylic acid	4CL
	2-naphthalenecarboxylic acid	4CL
	2-quinolinecarboxylic acid	4CL
	3-quinolinecarboxylic acid	4CL

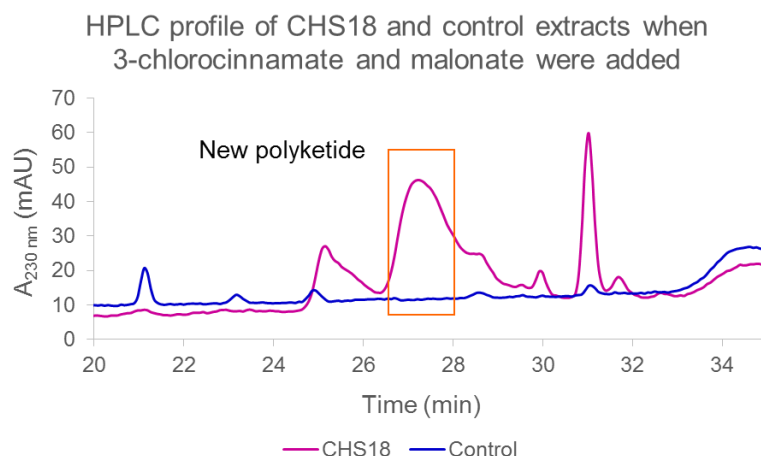


Figure A1: Biosynthesized products in spent minimal medium containing either *E. coli* with CoA ligases + CHS18 or *E. coli* with CoA ligases only (control construct) were extracted and subjected to HPLC analysis. An additional peak at R_t 27.3 min was observed in the extract from the CHS18 construct, but was not present in the extract from the control construct, indicating that a new polyketide was biosynthesized when 3-chlorocinnamyl-CoA and malonyl-CoA were supplemented to CHS18.

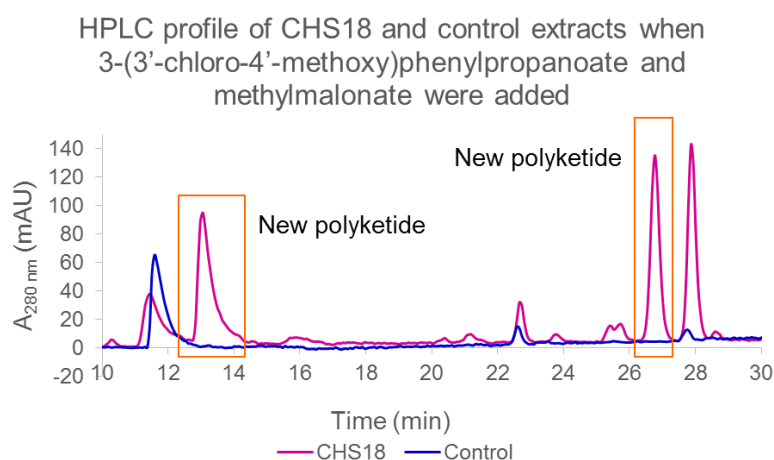


Figure A2: Biosynthesized products in spent minimal medium containing either *E. coli* with CoA ligases + CHS18 or *E. coli* with CoA ligases only (control construct) were extracted and subjected to HPLC analysis. Additional peaks at R_t 13.2 min and 26.8 min were observed in the extract from the CHS18 construct, but were absent in the extract from the control construct, indicating that new polyketides were biosynthesized when 3-(3'-chloro-4'-methoxy)phenylpropanoyl-CoA and methylmalonyl-CoA were supplemented to CHS18.

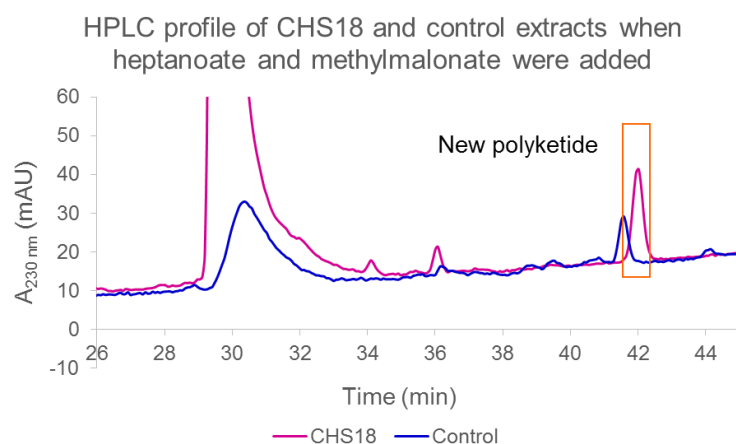


Figure A3: Biosynthesized products in spent minimal medium containing either *E. coli* with CoA ligases + CHS18 or *E. coli* with CoA ligases only (control construct) were extracted and subjected to HPLC analysis. An additional peak at R_t 42.0 min was observed in the extract from the CHS18 construct, but was not present in the extract from the control construct, indicating that a new polyketide was biosynthesized when heptanoyl-CoA and methylmalonyl-CoA were supplemented to CHS18.

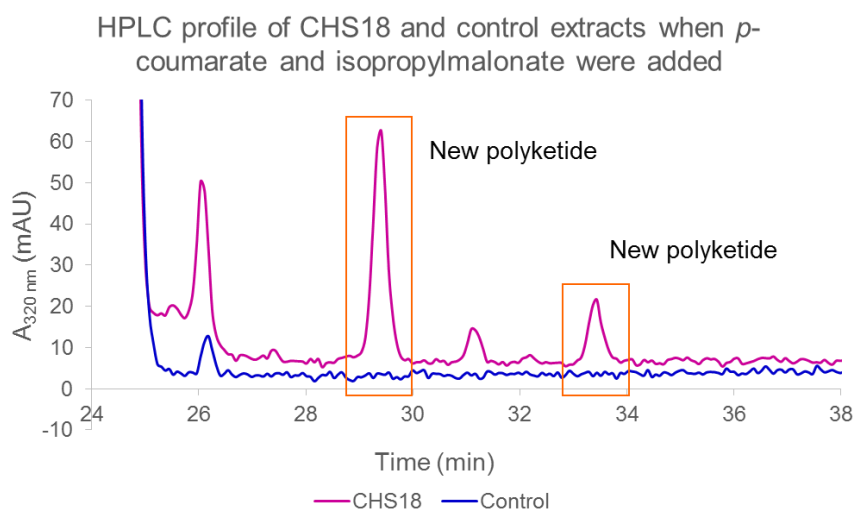


Figure A4: Biosynthesized products in spent minimal medium containing either *E. coli* with CoA ligases + CHS18 or *E. coli* with CoA ligases only (control construct) were extracted and subjected to HPLC analysis. Additional peaks at R_t 29.2 min and 33.0 min were observed in the extract from the CHS18 construct, but were not present in the extract from the control construct, indicating that new polyketides were biosynthesized when *p*-coumaroyl-CoA and isopropylmalonyl-CoA were supplemented to CHS18.

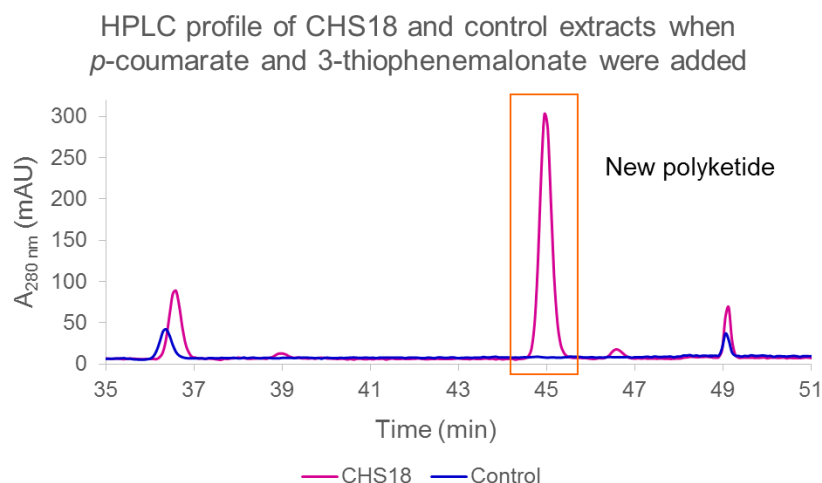


Figure A5: Biosynthesized products in spent minimal medium containing either *E. coli* with CoA ligases + CHS18 or *E. coli* with CoA ligases only (control construct) were extracted and subjected to HPLC analysis. An additional peak at R_t 45.0 min was observed in the extract from the CHS18 construct, but was absent in the extract from the control construct, indicating that a new polyketide was biosynthesized when *p*-coumaroyl-CoA and 3-thiophenemalonoyl-CoA were supplemented to CHS18.

Table A2: Substrate profile of CHS18 involving 12 extender acyl-CoAs with cinnamyl-CoA and phenylpropanoyl-CoA derivatives as starters. For cinnamyl-CoA derivatives as starters, 84 out of 168 combinations (50.0%) produced at least one new product, while 19 out of 84 combinations (22.6%) produced at least one new product for phenylpropanoyl-CoA derivatives as starters. A (√) represents at least one new product is formed. Extender acyl-CoAs are abbreviated as follows: malonyl-CoA (Mal), methylmalonyl-CoA (MeMal), ethylmalonyl-CoA (EtMal), isopropylmalonyl-CoA (IsoMal), butylmalonyl-CoA (ButMal), allylmalonyl-CoA (AlMal), hydroxymalonyl-CoA (OHMal), fluoromalonyl-CoA (FMal), chloromalonyl-CoA (ClMal), bromomalonyl-CoA (BrMal), phenylmalonyl-CoA (PhMal), and 3-thiophenemalonyl-CoA (3ThMal).

Substrate	Mal	MeMal	EtMal	IsoMal	ButMal	AlMal	OHMal	Fmal	ClMal	BrMal	PhMal	3ThMal
Cinnamic acid	√					√	√	√	√			
2-fluorocinnamic acid	√	√						√			√	√
3-fluorocinnamic acid	√	√	√		√		√		√	√	√	
4-fluorocinnamic acid	√	√						√	√	√	√	√
α-fluorocinnamic acid								√	√			
3-chlorocinnamic acid	√	√						√				
3-chloro-4-methoxycinnamic acid	√			√	√	√		√	√	√	√	√
4-chlorocinnamic acid	√							√				
2-hydroxycinnamic acid											√	
4-hydroxycinnamic acid	√		√	√	√		√	√	√	√	√	√
3-methoxy-4-hydroxycinnamic acid	√		√	√	√		√	√	√	√	√	√
4-methoxycinnamic acid	√			√	√	√	√	√	√	√	√	√
4-methylcinnamic acid	√				√	√						
α-methylcinnamic acid	√		√	√	√			√	√	√	√	√
3-phenylpropanoic acid	√	√	√							√	√	
3-(3'-chloro)phenylpropanoic acid	√	√										
3-(3'-chloro-4'-methoxy)phenylpropanoic acid		√										
3-(3',4'-dihydroxy)phenylpropanoic acid							√					
3-(3'-methoxy)phenylpropanoic acid		√										
3-(4'-methoxy)phenylpropanoic acid		√	√				√	√	√	√		
3-(4'-fluoro)phenylpropanoic acid	√	√					√					
Total	15	10	6	5	7	4	8	12	10	9	10	7

Table A3: Substrate profile of CHS18 involving 12 extender acyl-CoAs with benzoyl-CoA derivatives as starters. 158 out of 240 combinations (65.8%) produced at least one new product. A (√) represents at least one new product is formed. Extender acyl-CoAs are abbreviated as follows: malonyl-CoA (Mal), methylmalonyl-CoA (MeMal), ethylmalonyl-CoA (EtMal), isopropylmalonyl-CoA (IsoMal), butylmalonyl-CoA (ButMal), allylmalonyl-CoA (AlMal), hydroxymalonyl-CoA (OHMal), fluoromalonyl-CoA (Fmal), chloromalonyl-CoA (ClMal), bromomalonyl-CoA (BrMal), phenylmalonyl-CoA (PhMal), and 3-thiophenemalonyl-CoA (3ThMal).

Substrate	Mal	MeMal	EtMal	IsoMal	ButMal	AlMal	OHMal	Fmal	ClMal	BrMal	PhMal	3ThMal
Benzoic acid		√	√		√	√	√	√	√		√	√
2-fluorobenzoic acid	√	√	√	√	√	√	√	√	√	√	√	√
3-fluorobenzoic acid	√	√	√	√		√	√	√	√	√	√	√
4-fluorobenzoic acid	√	√	√	√				√	√	√	√	√
2,6-difluorobenzoic acid			√	√	√	√	√	√	√	√	√	√
2-chlorobenzoic acid		√	√		√	√	√	√	√		√	√
3-chlorobenzoic acid		√	√	√	√	√	√	√	√	√	√	√
4-chlorobenzoic acid	√		√	√	√			√	√	√		√
2-bromobenzoic acid	√		√		√		√	√	√		√	√
3-bromobenzoic acid		√	√		√	√	√	√	√	√		√
4-bromobenzoic acid			√			√		√	√		√	√
2-iodobenzoic acid	√		√		√		√	√	√		√	√
2-hydroxybenzoic acid								√	√		√	√
2,3-dihydroxybenzoic acid								√	√			√
2,4-dihydroxybenzoic acid					√	√		√	√		√	√
2,5-dihydroxybenzoic acid	√							√	√			√
2-methoxybenzoic acid	√		√	√	√	√		√	√		√	√
2-methylbenzoic acid			√		√	√	√	√	√	√	√	√
3-aminobenzoic acid	√				√	√		√	√		√	√
4-aminobenzoic acid			√				√	√	√		√	√
Total	9	7	15	7	13	12	11	20	20	8	16	20

Table A4: Substrate profile of CHS18 involving 12 extender acyl-CoAs with phenylacetyl-CoA and bicyclic aromatic CoA derivatives as starters. For phenylacetyl-CoA derivatives as starters, 37 out of 72 combinations (51.4%) produced at least one new product, while 6 out of 48 combinations (12.5%) produced at least one new product for bicyclic aromatic CoA derivatives as starters. A (√) represents at least one new product is formed. Extender acyl-CoAs are abbreviated as follows: malonyl-CoA (Mal), methylmalonyl-CoA (MeMal), ethylmalonyl-CoA (EtMal), isopropylmalonyl-CoA (IsoMal), butylmalonyl-CoA (ButMal), allylmalonyl-CoA (AlMal), hydroxymalonyl-CoA (OHMal), fluoromalonyl-CoA (FMal), chloromalonyl-CoA (ClMal), bromomalonyl-CoA (BrMal), phenylmalonyl-CoA (PhMal), and 3-thiophenemalonyl-CoA (3ThMal).

Substrate	Mal	MeMal	EtMal	IsoMal	ButMal	AlMal	OHMal	Fmal	ClMal	BrMal	PhMal	3ThMal
Phenylacetic acid	√	√		√	√	√			√	√	√	√
2-hydroxyphenylacetic acid		√					√				√	√
4-hydroxyphenylacetic acid		√	√	√		√		√	√		√	√
4-methoxyphenylacetic acid	√							√		√	√	√
Phenoxyacetic acid		√								√	√	√
Phenylpyruvic acid	√	√						√	√	√	√	√
1-naphthalenecarboxylic acid												√
2-naphthalenecarboxylic acid	√		√								√	√
2-quinolinecarboxylic acid										√		
3-quinolinecarboxylic acid												
Total	4	5	2	2	1	2	1	3	3	5	7	8

Table A5: Substrate profile of CHS18 involving 12 extender acyl-CoAs with saturated and unsaturated aliphatic CoA derivatives as starters. For unsaturated aliphatic CoA derivatives as starters, 74 out of 120 combinations (61.7%) produced at least one new product, while 35 out of 96 combinations (36.5%) produced at least one new product for saturated aliphatic CoA derivatives as starters. A (√) represents at least one new product is formed. Extender acyl-CoAs are abbreviated as follows: malonyl-CoA (Mal), methylmalonyl-CoA (MeMal), ethylmalonyl-CoA (EtMal), isopropylmalonyl-CoA (IsoMal), butylmalonyl-CoA (ButMal), allylmalonyl-CoA (AlMal), hydroxymalonyl-CoA (OHMal), fluoromalonyl-CoA (FMal), chloromalonyl-CoA (ClMal), bromomalonyl-CoA (BrMal), phenylmalonyl-CoA (PhMal), and 3-thiophenemalonyl-CoA (3ThMal).

Substrate	Mal	MeMal	EtMal	IsoMal	ButMal	AlMal	OHMal	Fmal	ClMal	BrMal	PhMal	3ThMal
Propanoic acid			√					√	√		√	√
Butanoic acid	√	√	√	√	√	√	√	√	√	√	√	√
Pentanoic acid		√									√	√
Hexanoic acid	√		√									
Heptanoic acid	√	√	√	√			√	√		√		
Octanoic acid			√			√						
Nonanoic acid			√									√
Decanoic acid			√									√
2-butenic acid		√					√	√	√		√	√
2-methyl-2-butenic acid	√		√	√	√	√	√	√				√
3-methyl-2-butenic acid			√	√	√	√	√	√	√	√	√	√
3-butenic acid	√	√	√	√	√		√	√	√		√	√
2-pentenoic acid	√	√	√	√	√	√	√	√	√	√		√
3-pentenoic acid		√	√								√	√
4-pentenoic acid		√	√	√	√	√	√	√	√	√	√	√
3-methyl-4-pentenoic acid		√	√								√	√
3-hexenoic acid	√	√	√								√	√
5-hexenoic acid		√	√						√		√	√
Total	7	11	16	7	6	6	8	9	8	5	11	15

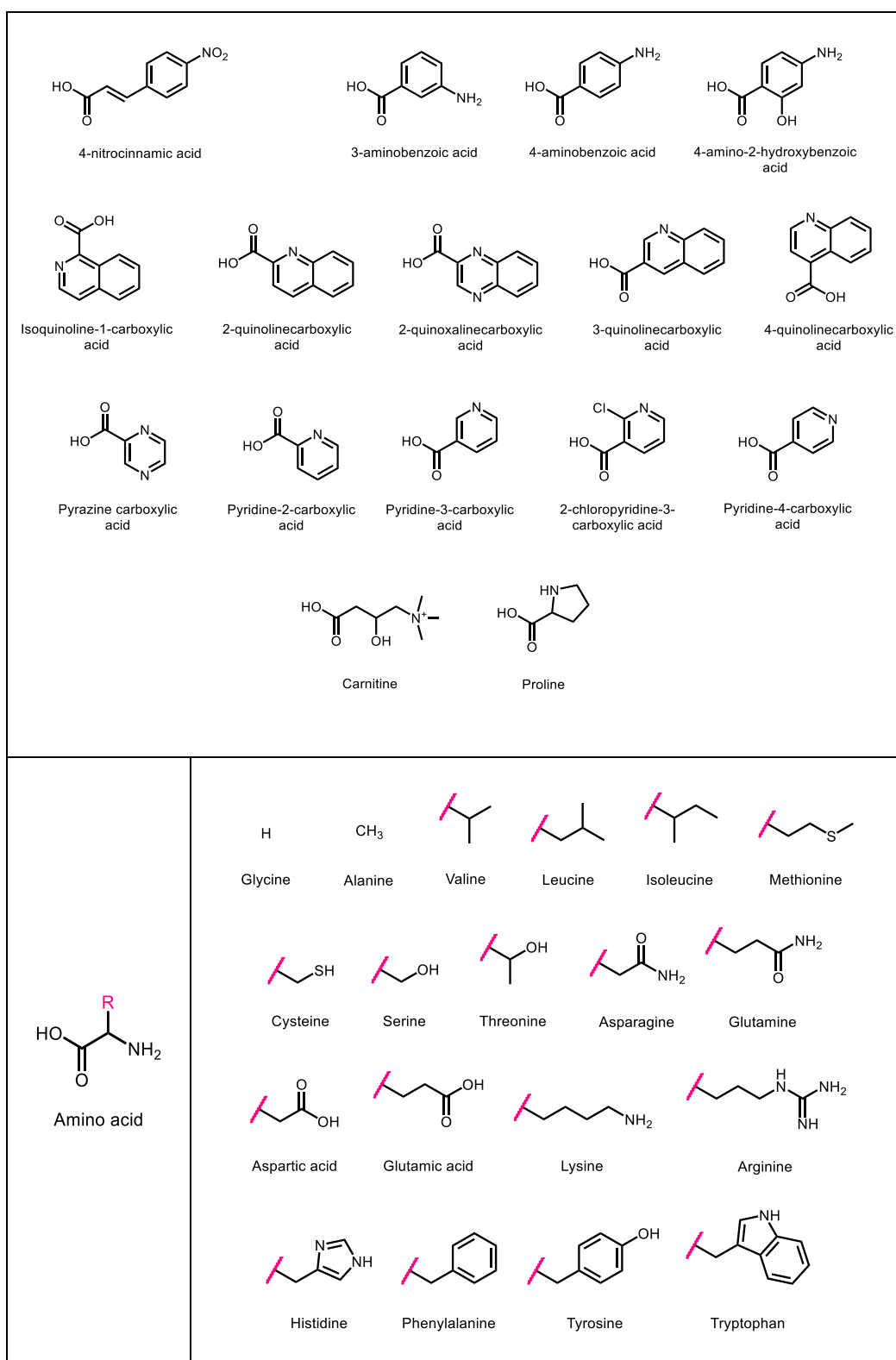


Figure A6: Nitrogen-containing carboxylic acids used for determining substrate profiles of CoA ligases.